

Dissertation
submitted to the
Combined Faculties for the Natural Sciences and for Mathematics
of the Ruperto-Carola University of Heidelberg, Germany
for the degree of
Doctor of Natural Sciences

presented by
M.Sc. Denise Harrach
born in Datteln
oral examination:

CHONDROITINSULFOTRANSFERASES AND THEIR ROLE DURING
DEVELOPMENT – DIFFERENTIATION AND BEHAVIOUR OF NEURAL
STEM CELLS IN THE MAMMALIAN CENTRAL NERVOUS SYSTEM

Referees: Prof. Dr. Thomas Holstein
PD Dr. Alexander von Holst

I. LIST OF FIGURES	III
II. ABBREVIATIONS	IV
III. SUMMARY	VI
IV. ZUSAMMENFASSUNG	VII
1 INTRODUCTION	1
1.1 NEURAL DEVELOPMENT	1
1.1.1 NEUROGENESIS DURING THE DEVELOPMENT OF THE VERTEBRATE CENTRAL NERVOUS SYSTEM	1
1.1.2 NEURAL STEM CELLS AND THEIR NICHE	2
1.2 THE EXTRACELLULAR MATRIX	5
1.2.1 THE EXTRACELLULAR MATRIX IN THE CENTRAL NERVOUS SYSTEM AND ITS COMPLEXITY OF FUNCTIONS	5
1.2.2 PROTEOGLYCANS IN THE EXTRACELLULAR MATRIX	7
1.3 CHONDROITINSULFATE PROTEOGLYCANS	9
1.3.1 CHONDROITINSULFATE PROTEOGLYCAN STRUCTURE AND THEIR MODIFICATION BY CHONDROITINSULFOTRANSFERASES	9
1.3.2 COMPLEXITY AND FUNCTION OF CHONDROITINSULFATES	11
1.3.3 INVOLVEMENT OF CHONDROITINSULFATES IN HEALTH AND DISEASE	13
1.4 AIM OF THE STUDY	15
2 MATERIALS AND METHODS	16
2.1 COMPANIES	16
2.2 MATERIALS	17
2.2.1 EQUIPMENT	17
2.2.2 CHEMICALS	17
2.2.3 MEDIA	18
2.2.4 PLASTIC WARE	18
2.2.5 ENZYMES/GROWTH FACTORS	18
2.2.6 KITS	19
2.2.7 PLASMIDS	19
2.2.8 ANTIBODIES	19
2.2.9 ALL OTHER CONSUMABLES	21
2.3 COMPOSITION OF MEDIA, BUFFERS AND OTHER REAGENTS	21
2.3.1 CELL CULTURE	21
2.3.2 IMMUNOCYTO- AND IMMUNOHISTOCHEMISTRY	21
2.3.3 MOLECULAR BIOLOGY	22
2.3.4 PROTEIN BIOCHEMISTRY	22
2.4 CELL CULTURE	22
2.4.1 CULTIVATION OF MOUSE NEURAL STEM CELLS	22
2.4.2 TRANSFECTION OF THE NSCs	23
2.4.3 DIFFERENTIATION ASSAY	23
2.4.4 CLONAL DENSITY ASSAY	24
2.4.5 PROLIFERATION ASSAY	24
2.5 IMMUNOCYTOCHEMISTRY	24
2.5.1 DIFFERENTIATION	24
2.5.2 PROLIFERATION	24
2.6 IMMUNOHISTOCHEMISTRY	25
2.6.1 DIFFERENTIATION	25
2.6.2 PROLIFERATION	25
2.7 MOLECULAR BIOLOGY	25
2.7.1 RNA ISOLATION AND cDNA SYNTHESIS	25
2.7.2 POLYMERASE CHAIN REACTION (PCR)	25
2.7.3 ISOLATION OF PLASMID DNA	26
2.7.4 RESTRICTION ENZYME DIGESTION	26
2.7.5 SITE-DIRECTED MUTAGENESIS OF UST	26

2.8 OLIGONUCLEOTIDE PRIMERS	26
2.9 PROTEIN BIOCHEMISTRY	27
2.9.1 PROTEIN ISOLATION AND QUANTITATION	27
2.9.2 SDS-PAGE	27
2.9.3 WESTERN BLOT	28
2.10 IN UTERO ELECTROPORATION	28
2.10.1 ANIMALS	28
2.10.2 GLASS CAPILLARIES	28
2.10.3 PLASMID PREPARATION	28
2.10.4 SURGICAL PROCEDURE	28
2.10.5 ANALYSIS	30
2.11 UST CONDITIONAL KNOCKOUT MOUSE STRATEGY	30
2.11.1 ISOLATION OF GENOMIC DNA FROM MOUSE TAILS	30
2.11.2 GENOTYPING OF UST MUTANT MICE	31
2.11.3 STRATEGY	31
2.12 IMAGE ACQUISITION AND STATISTICAL ANALYSIS	33
2.12.1 IMAGEJ (FIJI) AND ADOBE PHOTOSHOP	33
2.12.2 ILASTIK	33
2.12.3 STATISTICAL ANALYSIS	33
3 RESULTS	34
3.1 CHONDROITINSULFOTRANSFERASE UST OVEREXPRESSION AND ITS FUNCTIONALITY	34
3.1.1 OVEREXPRESSION AND FUNCTIONALITY OF UST <i>IN VITRO</i>	34
3.1.2 OVEREXPRESSION AND FUNCTIONALITY OF UST <i>IN VIVO</i>	38
3.2 MODIFICATION OF THE SULFATION PATTERN OF NEURAL STEM CELLS <i>IN VITRO</i>	40
3.2.1 IMPACT OF UST OVEREXPRESSION ON NSC DIFFERENTIATION	40
3.2.2 IMPACT OF UST OVEREXPRESSION ON NSC SELF-RENEWAL AND PROLIFERATION	43
3.3 MODIFICATION OF THE SULFATION PATTERN BY <i>IN UTERO</i> ELECTROPORATION <i>IN VIVO</i>	45
3.3.1 IMPACT OF UST OVEREXPRESSION ON CORTICAL PLATE AND VENTRICULAR ZONE DEVELOPMENT <i>IN VIVO</i>	45
3.3.2 IMPACT OF UST OVEREXPRESSION ON PROLIFERATION <i>IN VIVO</i>	48
3.3.3 IMPACT OF UST OVEREXPRESSION ON NSC DIFFERENTIATION DURING CORTICAL DEVELOPMENT <i>IN VIVO</i>	49
4 DISCUSSION	52
4.1 FUNCTIONALITY OF UST OVEREXPRESSION	52
4.2 IMPACT OF UST OVEREXPRESSION ON NSC DIFFERENTIATION	53
4.2.1 NSC DIFFERENTIATION <i>IN VITRO</i>	53
4.2.2 NSC DIFFERENTIATION <i>IN VIVO</i>	53
4.3 IMPACT OF UST OVEREXPRESSION ON NSC SELF-RENEWAL AND PROLIFERATION	54
4.3.1 NSC SELF-RENEWAL AND PROLIFERATION <i>IN VITRO</i>	54
4.3.2 NSC SELF-RENEWAL AND PROLIFERATION <i>IN VIVO</i>	55
4.4 IMPLICATIONS OF THE SULFATION PATTERN ON NSC BEHAVIOUR AND POSSIBLE MECHANISMS	56
4.5 FUTURE ASPECTS	60
5 ACKNOWLEDGMENTS/DANKSAGUNG	62
5 REFERENCES	63
6 APPENDIX	69

I. LIST OF FIGURES

Figure 1 Schematic overview of neurogenesis in the embryonic vertebrate CNS.....	2
Figure 2 Schematic overview of neural stem cells	3
Figure 3 Schematic overview of neurogenesis with its influencing environmental cues during the embryonic vertebrate CNS development.....	4
Figure 4 Scheme of the major proteoglycan types	8
Figure 5 Schematic overview of proteoglycan structure and the possible CS/DS-unit outcome after sulfation and epimerization.....	11
Figure 6 Differentiation Assay Timescale	23
Figure 7 Clonal Density Assay Timescale	24
Figure 8 Scheme of <i>in utero</i> electroporation procedure	29
Figure 9 Scheme for the analysis of the <i>in utero</i> electroporation data	30
Figure 10 Strategy for conditional Ust knockout mouse line	32
Figure 11 Expression of different Ust constructs <i>in vitro</i> and <i>in vivo</i>	36
Figure 12 Localization of Ust-EGFP fusion protein in the Golgi apparatus.....	36
Figure 13 Modifying the sulfation pattern by Ust overexpression <i>in vitro</i>	37
Figure 14 Modifying the sulfation pattern by Ust overexpression <i>in vivo</i>	39
Figure 15 Impact of a modified sulfation pattern upon Ust overexpression on mouse neural stem cell differentiation: O4 and β III-tubulin.....	41
Figure 16 Impact of a modified sulfation pattern upon Ust overexpression on mouse neural stem cell differentiation: GFAP and Nestin	42
Figure 17 Proliferation of neural stem cells after Ust overexpression.....	43
Figure 18 Self-renewal of neural stem cells after Ust overexpression.....	44
Figure 19 Impact of a modified sulfation pattern after Ust overexpression on the thickness of the cortical plate	46
Figure 20 Impact of a modified sulfation pattern after Ust overexpression on the thickness of the ventricular zone	47
Figure 21 Impact of Ust overexpression on the proliferation: EdU	48
Figure 22 Impact of Ust overexpression on the amount of NeuN ⁺ -cells	50
Figure 23 Impact of Ust overexpression on the amount of Pax6 ⁺ -cells	51
Figure 24 Important functions and possible mechanisms of CSPGs	59

II. ABBREVIATIONS

Ab	antibody
APS	ammoniumperoxodisulfate
AR	antigen retrieval
bp	base pairs
BrdU	5-bromo-2'-deoxyuridine
BSA	bovine serum albumin
cDNA	copyDNA
Chst	chondroitinsulfotransferase
CNS	central nervous system
Cor	cortex
CP	cortical plate
CS	chondroitin sulfate
CSPG	chondroitin sulfate proteoglycan
Cy2	carbocyanine
Cy3	indocarbocyanine
DMEM	Dulbeccos modified MEM
DMSO	dimethyl sulfoxide
DNA	deoxyribonucleic acid
dNTP	deoxyribonucleotide-triphosphate
DS	dermatan sulfate
E	embryonic day
ECL	enhanced chemiluminescence
ECM	extracellular matrix
EDTA	ethylenediaminetetraacetic acid
EdU	5-ethynyl-2'-deoxyuridine
EGF	epidermal growth factor
EGFP	enhanced GFP
EGTA	ethyleneglycoltetraacetic acid
ER	endoplasmic reticulum
ESC(s)	embryonic stem cell(s)
FCS	fetal calf serum
FGF 2	fibroblast growth factor 2
fig.	figure
FITC	fluorescein isothiocyanate
forw	forward
GAG	glycosaminoglycan
GE	ganglionic eminence
GF	growth factor
GFAP	glial fibrillary acidic protein
GFP	green fluorescent protein
GPI	glycosylphosphatidylinositol
h	hour
HRP	horseradish peroxidase
HS	heparin sulfate
HSPG	heparan sulfate proteoglycan
Ig	immunoglobulin
INM	interkinetic nuclear migration
IPC	intermediate progenitor cell
IRES	internal ribosome entry site
kb	kilo base pairs (1000 bp)

kDa	kilodalton
KRH	Krebs Ringer HEPES
LV	lateral ventricle
mA	milli ampere
mAB	monoclonal antibody
MEM	Minimal essential medium
min	minute(s)
mRNA	messenger RNA
NEC	neuroepithelial stem cell
NGS	normal goat serum
NSC(s)	neural stem cell(s)
Nsphs	neurospheres
OPC	oligodendrocyte precursor cell
P-Orn	poly-ornithine
P/S	penicillin/streptomycin
PAGE	polyacrylamide gel electrophoresis
PAPS	3' phosphoadenosine-5'-phosphosulfate
PBS	phosphate-buffered saline
PCR	polymerase chain reaction
PFA	paraformaldehyde
PG	proteoglycan
PMSF	phenylmethanesulfonylfluoride
PVDF	polyvinylidene fluoride
rev	reverse
RNA	ribonucleic acid
RT	room temperature
SD	standard deviation
SDS	sodium dodecyl sulfate
sec	second(s)
shRNA	short hairpin RNA
SVZ	subventricular zone
tab.	table
TAE	tris acetate EDTA
TBS	tris-buffered saline
TBST	TBS with Tween20
TEMED	tetramethylethylenediamine
U	unit
V	volt
VZ	ventricular zone
w/o	without

III. SUMMARY

Chondroitin sulfate proteoglycans (CSPGs) and their specific sulfation pattern by chondroitinsulfotransferases (Chsts) appear to play a crucial role for the behaviour of neural stem cells (NSCs) in the embryonic neural stem cell niche during mouse forebrain development. It has been shown that the inhibition of the sulfation by sodium chlorate or the degradation of the CSPG glycosaminoglycans (GAGs) by chondroitinase ABC leads to less proliferation and altered cell fate decisions of the NSCs (Sirko et al., 2007, Akita et al., 2008, Sirko et al., 2010).

In the present study, the impact of the overexpression of one specific Chst on the behaviour of NSCs was examined. Therefore, Ust was overexpressed in *in vitro* and *in vivo* experiments in order to elucidate the role of disulfated CS-units on NSCs' self-renewal, proliferation as well as differentiation.

The functionality of the Ust fusion proteins (Ust, Ust mut) and their correct location to the Golgi apparatus, where the sulfation of the GAGs takes place, could be confirmed by CS-GAG epitope detection with the monoclonal antibody 473HD and with the Golgi apparatus marker transgolgin-97.

Initially, the effect of Ust overexpression on the differentiation and proliferation behaviour of neurosphere-derived NSCs was examined by the respective *in vitro* assays. Here, I could observe an increase in neurogenesis. The enhanced neuronal differentiation occurred at the expense of oligodendrocyte precursor cell (OPC) generation, while NSC proliferation and self-renewal were not effected. Although, there was a very small but significant increase in the number of neurospheres after Ust overexpression without growth factor supplementation.

To verify, whether Ust overexpression stimulates neurogenesis similarly *in vivo*, I performed *in utero* electroporation experiments. The immunohistochemical analysis of *in utero* electroporated E14.5 mouse cortices two days post-transfection revealed that Ust overexpression caused a thinner cortical plate, which is a consequence of reduced numbers of NeuN⁺-neurons in this area. In contrast, the amount of Pax6⁺ radial glia cells in the ventricular zone was slightly increased. The analysis of NSC proliferation *in vivo* by EdU incorporation did not reveal a significant difference and was consistent with the obtained *in vitro* results.

Moreover, I designed a strategy for an Ust conditional knockout mouse line to enable future examinations of the sulfation pattern impact on CNS development.

In conclusion, I could show an efficient and functional Ust overexpression, which exhibited an effect on NSC behaviour *in vitro* and *in vivo*. The effect is due to the modified sulfation pattern, which could be confirmed by using the negative control Ust mut. Consistent with previous observations, the sulfation of the CSPGs plays a role in the commitment of NSCs within the NSC niche and could function as a possible communication platform between NSCs and their extracellular surrounding in the NSC niche.

IV. ZUSAMMENFASSUNG

Chondroitinsulfatproteoglykane (CSPGs) und deren spezifisches Sulfatierungsmuster durch Chondroitinsulfotransferasen (Chsts) scheinen eine besondere Rolle für das Verhalten von neuronalen Stammzellen (NSCs) in der embryonalen Stammzellnische während der Vorderhirnentwicklung der Maus zu spielen. Durch Inhibierung der Sulfatierung durch Natriumchlorat oder Abverdau der CSPG Glykosaminoglykane (GAGs) durch Chondroitinase ABC konnte gezeigt werden, dass dies zu einer reduzierten Proliferation und veränderten Zellschicksalentscheidungen führte (Sirko et al., 2007, Akita et al., 2008, Sirko et al., 2010).

In der vorliegenden Arbeit wurde der Einfluss einer spezifischen Chst Überexpression auf das Verhalten von NSCs untersucht. Dafür wurde Ust in *in vitro* und *in vivo* Experimenten überexprimiert um die Rolle von disulfatierten CS-Einheiten bezüglich Selbsterhalt, Proliferation und Differenzierung von NSCs zu überprüfen.

Die Funktionalität der Ust Fusionsproteine (Ust, Ust mut) und deren korrekte Lokalisierung im Golgi Apparat, wo die Sulfatierung stattfindet, konnten immunologisch mit dem CS-GAG Epitop erkennenden 473HD Antikörper und dem Golgi Apparat Marker transgolgin-97 bestätigt werden.

Zunächst wurde der Einfluss durch Ust Überexpression auf das Differenzierungs- und Proliferationsverhalten aus Neurosphären generierter NSCs in den jeweiligen *in vitro* Assays untersucht. Dabei konnte ein Anstieg der Neurogenese beobachtet werden. Die verstärkte neuronale Differenzierung trat gegenläufig zur Generation von Oligodendrozyten Vorläuferzellen (OPCs) auf, wobei die Proliferation und der Selbsterhalt der NSCs nicht beeinflusst wurde. Allerdings konnte ein sehr kleiner jedoch signifikanter Anstieg in der Anzahl der Neurosphären nach Ust Überexpression ohne Zusatz von Wachstumsfaktoren beobachtet werden.

Zur Verifizierung, ob Ust Überexpression die Neurogenese *in vivo* ähnlich stimuliert, habe ich *in utero* Elektroporationen durchgeführt. Die immunhistochemische Analyse der E14.5 *in utero* elektroporierter Maus-Cortices zeigten zwei Tage nach der Transfektion, dass die Ust Überexpression eine dünnere kortikale Platte hervorruft, welche durch eine geringere Anzahl an NeuN⁺-Neuronen verursacht wurde. Im Kontrast dazu war die Anzahl Pax6⁺ radialer Gliazellen in der ventrikulären Zone leicht erhöht. Die Proliferationsanalyse der NSCs *in vivo* durch EdU Inkorporation ließ keine signifikanten Unterschiede in der Anzahl der proliferierenden NSCs erkennen und stimmte mit den *in vitro* Ergebnissen überein.

Außerdem habe ich eine Strategie zur Generierung einer konditionalen Ust Knockout-Mauslinie entworfen, um die zukünftige Analyse des Einflusses des Sulfatierungsmusters auf die Entwicklung des ZNS zu ermöglichen.

Zusammenfassend konnte die effiziente und funktionelle Ust Überexpression gezeigt werden, deren Effekte *in vitro* offensichtlicher waren als *in vivo*. Der Effekt beruht auf der modifizierten Sulfatierung, was durch den Einsatz von Ust mut zu sehen war. Übereinstimmend mit früheren Ergebnissen, konnte der Einfluss der Sulfatierung von CSPGs auf das Verhalten von NSCs in der NSC Nische festgestellt werden und es könnte als mögliche Kommunikationsplattform zwischen NSCs und ihrer extrazellulären Umgebung in der Nische fungieren.

1 INTRODUCTION

1.1 NEURAL DEVELOPMENT

1.1.1 NEUROGENESIS DURING THE DEVELOPMENT OF THE VERTEBRATE CENTRAL NERVOUS SYSTEM

During the vertebrate central nervous system (CNS) development a lot of intrinsic and extrinsic cues play a role for the generation of the different cell types and for the establishment of its complex architecture. The vertebrate CNS develops from one single layer of neuroepithelial stem cells (NECs), which are lining the ventricle after neurulation and forming the neural tube. The NECs are undergoing symmetric, proliferative divisions and thereby causing the lateral expansion of the developing brain (Gotz and Huttner, 2005). In symmetric divisions two identical daughter cells are generated, in this case two identical NECs. The NECs exhibit an apical-basal polarity (Huttner and Brand, 1997). They possess two processes, one apical process facing the ventricle and one basal process spanning to the pial basal membrane of the neuroepithelium (Figure 1). Their nucleus is migrating along the apical-basal axis during the cell cycle (interkinetic nuclear migration = INM) and resides at the apical side during mitosis (Taverna and Huttner, 2010). The fact of INM of the NECs creates a stratified appearance and therefore the single layered neuroepithelium is classified as pseudostratified.

The phase of symmetric proliferative divisions is followed by a phase of asymmetric neurogenic divisions (Rakic, 1995), meaning a neural stem cell generates one identical daughter cell and one more differentiated cell. The latter can refer to a pool of intermediate progenitor (IP) cells, that usually undergoes symmetric neurogenic divisions, or to directly generated neurons (Gotz and Huttner, 2005). This process of generating the different neuronal cell types of the CNS is named neurogenesis and the first waves of neurogenesis start in mice at about embryonic day (E) 9-10 (Rowitch and Kriegstein, 2010). Figure 1 gives an overview of neurogenesis depicting the involved types of stem and progenitor cells and their progeny as well as the resulting layers and zones of the developing cortex. With the onset of neurogenesis the NECs transform into radial glia cells (RGCs) and reduce their epithelial properties and hallmarks of astroglial cells appear (Gotz and Huttner, 2005). RGCs still maintain the highly polarized structure, conduct INM and retain their proliferative capacities. They are responsible for the generation of all neurons and at later developmental stages of macroglial cells, astrocytes and oligodendrocytes (Paridaen and Huttner, 2014). That is why they are also often referred as neural stem cells (NSCs), which is further described in the following chapter (1.1.2 Neural Stem Cells and their Niche).

The transition of the NECs to RGCs and the change from symmetric proliferative divisions to asymmetric neurogenic divisions is accompanied by prolongation of the cell cycle length and starts with the onset of neurogenesis (Takahashi et al., 1995, Calegari et al., 2005, Paridaen and Huttner, 2014). Concomitantly, the location of mitosis, cell polarity properties, proliferative capacity and the mode of cell division influence the progeny's cell fate determination and development (Taverna et al., 2014). In the mammalian neocortex, additional progenitor cell types are present as indicated in the box of Figure 1, e.g. basal radial glia cells (bRGs) (Pilz et al., 2013, Taverna et al., 2014). bRGs only have a basal process and seem to be important during the evolutionary expansion of the mammalian cortex (LaMonica et al., 2013). The cells directly lining the ventricle establish the ventricular zone (VZ), whereas the newly generated

progenitors create the adjacent subventricular zone (SVZ) by migrating out of the VZ and detach from the apical membrane (Noctor et al., 2004). The newly born neurons migrate along the RGC processes towards the pial surface to the cortical plate (CP) and generate the six layers of the neocortex in an "inside-out" pattern, with its deep layer neurons born earlier than the upper layer neurons (Rakic, 1972, Marin and Rubenstein, 2003). At around E 18.5 a switch from neurogenesis to gliogenesis occurs, during which most RGCs retract their apical/radial processes and adopt a more astrocytic morphology (Martynoga et al., 2012). This switch from neuro- to gliogenesis is caused by the production of neurons itself: via upregulation of the important factors and crosstalk of the different signalling pathways, the timing signals to end neurogenesis and start producing glial cells are provided (Martynoga et al., 2012). Although, the process of neurogenesis is maintained until adulthood, the RGCs are restricted to a few niches as adult neural stem cells (NSCs) and are drastically reduced in number (Kriegstein and Alvarez-Buylla, 2009, Dimou and Gotz, 2014).

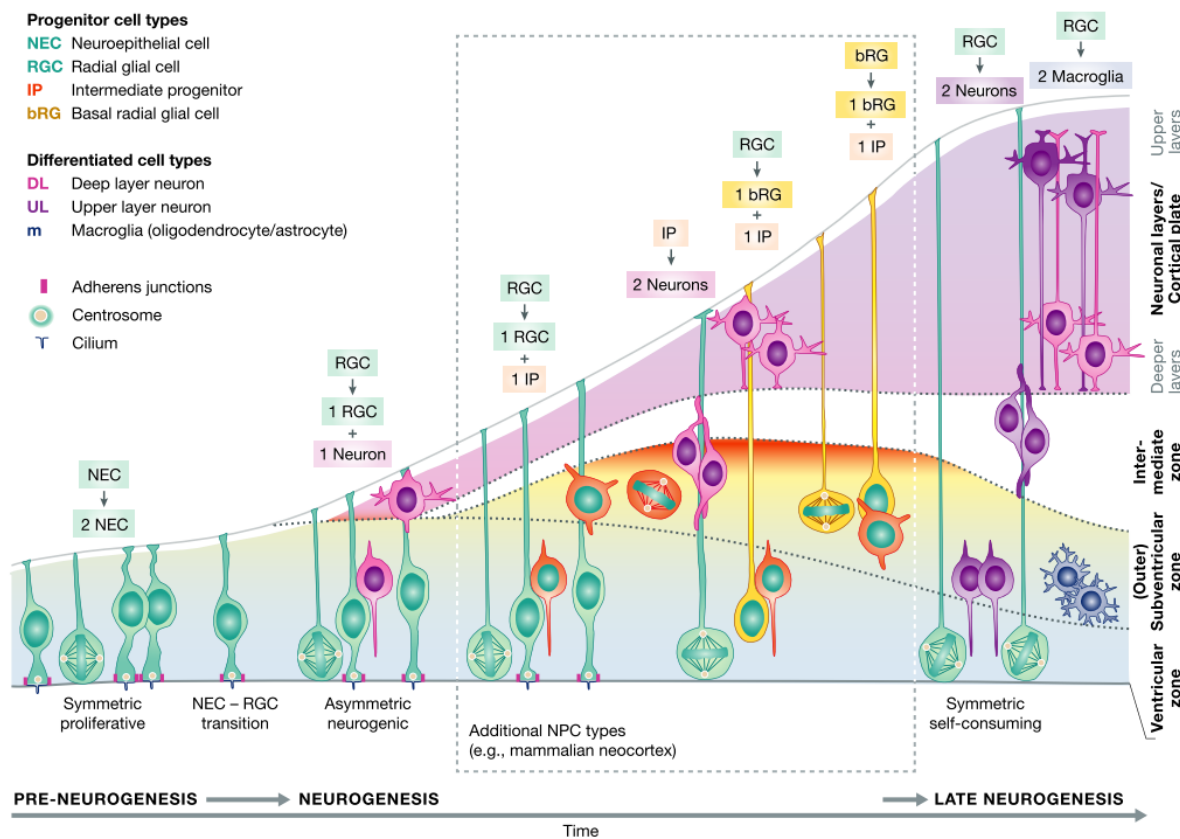


Figure 1 Schematic overview of neurogenesis in the embryonic vertebrate CNS

The different stem/progenitor cell types and their progeny are shown in the indicated colour and the corresponding division mode/lineage outcome is listed beneath/above. In the box are progenitor cell types depicted, that are usually attendant in mammalian species. Note, that not every possible progeny is included here. Modified from Paridaen and Huttner 2014.

1.1.2 NEURAL STEM CELLS AND THEIR NICHE

Stem cells are defined as cells that are capable of self-renewal (for an (un-)limited number of cell divisions) and are multipotent (able to give rise to numerous differentiated cell types of a tissue). In the CNS, these stem cells are called neural stem cells (NSCs), which include NECs and

RGCs as well as the progenitor cells, which are more limited in their proliferation capacity and can be further distinguished by their location of mitosis, their extent of cell polarity and their proliferative capacity (Taverna et al., 2014). They give rise to neurons and macroglial cell types (astrocytes, oligodendrocytes, NG2 glia, ependymal cells) (Taverna et al., 2014). Figure 2 shows a schematic overview of neural stem cells, their self-renewal and potential cell lineage capacities.

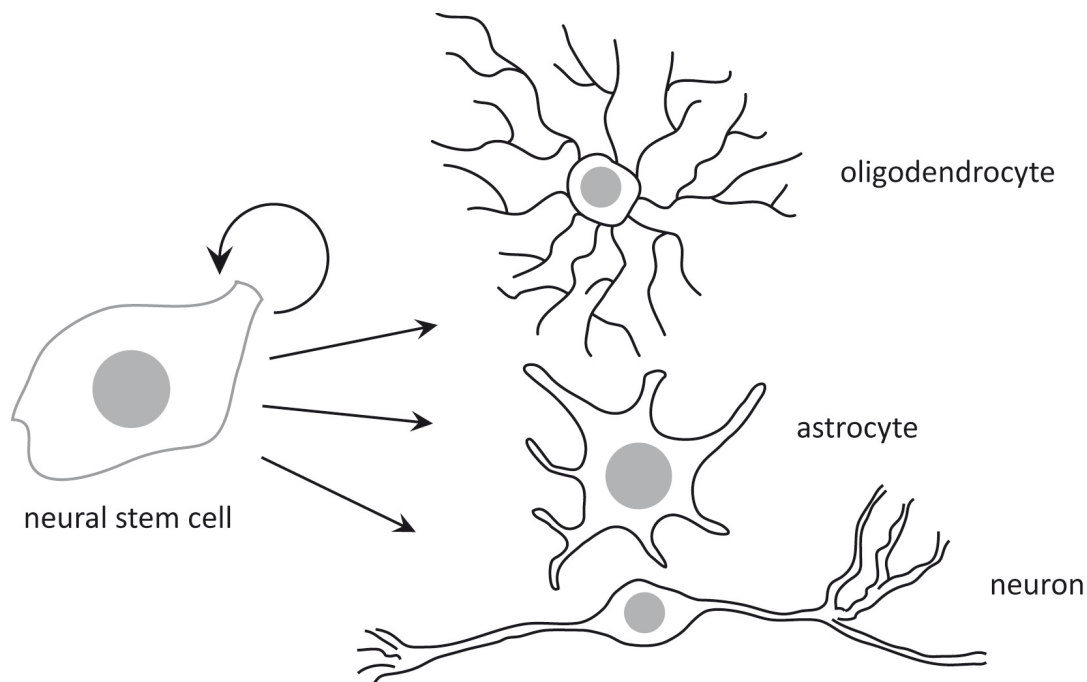


Figure 2 Schematic overview of neural stem cells

The overview shows the capacity of NSCs for self-renewal and their potential progeny lineages. Note: oligodendrocytes and astrocytes are exemplarily depicted for the macroglial lineage.

NSCs are abundant in the embryonic developing brain and also reside in the adult brain of vertebrates, although in a greatly reduced number and in a more regionally restricted manner (Kriegstein and Alvarez-Buylla, 2009, Barry et al., 2014, Ninkovic and Gotz, 2014). The microenvironment, that surrounds NSCs and maintains their stem cell character as well as their proliferation capacity, is called a stem cell niche (Doetsch, 2003, Kriegstein and Alvarez-Buylla, 2009, Ihrie and Alvarez-Buylla, 2011). The stem cell niche usually comprises niche cells, adhesion molecules and a specialised extracellular matrix (ECM) with its corresponding factors (Scadden, 2006, Discher et al., 2009). The distinct microenvironment composition of a stem cell niche will be further described in the following chapter of the ECM. Figure 3 gives an overview of neurogenesis with its involved types of neural stem and progenitor cells and their progeny as well as the influencing environmental factors.

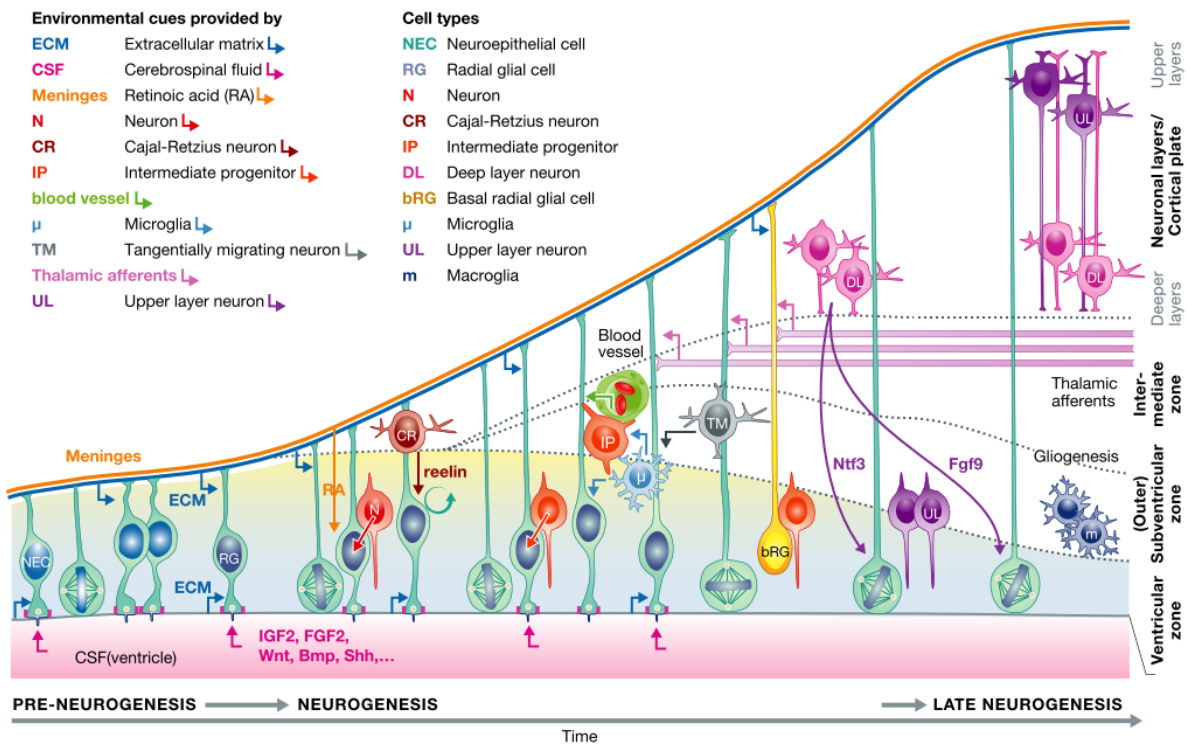


Figure 3 Schematic overview of neurogenesis with its influencing environmental cues during the embryonic vertebrate CNS development

The different cell types present during neurogenesis are indicated in distinct colours. The scheme also depicts influencing cues derived from the surrounding microenvironment, constituted by the present cell types and signals within the extracellular matrix. Modified from Paridaen and Huttner 2014.

During developmental neurogenesis several environmental cues play a role in the commitment of the NSCs. The meninges for example secrete retinoic acid (RA) from the basal side, which promotes asymmetric neurogenic divisions at the onset of neurogenesis (Siegenthaler et al., 2009). Extracellular matrix (ECM) components (e.g. basal lamina of blood vessels) and morphogen gradients, such as Wnts, Shh, FGFs and BMPs, induce by their patterning the expression of homeodomain and bHLH transcription factors and thereby cause the generation of specific cell types (Martynoga et al., 2012). For instance, the FGF signalling pathway is implicated in several ways: among slowing down the RGC to BP progression (Kang et al., 2009), FGF 10 has been shown to increase RGC hallmarks after overexpression and a mutant version of FGF 10 led to the extension of NE expansion and a delayed neurogenesis (Sahara and O'Leary, 2009), whereas a constitutively active form of the FGF 2 receptor (FGFR 2) caused an early transition from NECs to RGCs (Yoon et al., 2004). Additionally, FGF 2 maintains the proliferation of progenitor cells at early stages of neurogenesis (Raballo et al., 2000). Important is the spatial and temporal presence of the various extrinsic cues, which can change over time and thereby modify the NSCs behaviour and properties (Rozario and DeSimone, 2010). Hence, the interaction of various processes regulate cell fate determination: 1) signalling pathways (Notch, Wnt, Shh, FGF, etc.), 2) transcriptional mechanisms (modulation gene expression by transcription factors (TFs) or post-transcriptional/-translational regulations/modifications), 3) epigenetic modifications (DNA-methylation, histone modification), 4) environment (ECM) (Martynoga et al., 2012, Paridaen and Huttner, 2014). The proper construction of the brain's

architecture is a highly organized and complex process, within the orchestration of the balance between self-renewal, proliferation and differentiation (Wang et al., 2012) plays the key role with all its influencing intrinsic and extrinsic cues.

It is a well-known and established method to cultivate NSCs *in vitro* as neurospheres (nsphs) (Reynolds et al., 1992, Reynolds and Weiss, 1992). The NSCs are isolated from embryonic or adult brain and cultured under proliferative conditions as free-floating cells, which then proliferate and generate spherical aggregates, the so-called neurospheres. The NSCs, cultivated with this model system, retain their self-renewal capacity as well as their multipotency over several passages and are able to give rise to neurons, astrocytes and oligodendrocytes under differentiating conditions (Reynolds et al., 1992, Reynolds and Weiss, 1992). Hence, this is an appropriate model system to examine the behaviour of NSCs *in vitro*. For the *in vivo* analysis of NSCs *in utero* electroporation is one of the preferred techniques to manipulate NSC behaviour by overexpression or knockdown of a protein of interest. Further details are mentioned in 2.10 *In Utero* Electroporation.

1.2 THE EXTRACELLULAR MATRIX

1.2.1 THE EXTRACELLULAR MATRIX IN THE CENTRAL NERVOUS SYSTEM AND ITS COMPLEXITY OF FUNCTIONS

The extracellular matrix (ECM) got more into research focus in the last decades, since it is clear that ECM functions exceed being the simple surrounding of cells and only providing structural stability (Rozario and DeSimone, 2010, Burnside and Bradbury, 2014, Levy et al., 2014, Hopkins et al., 2015). Beyond regulating structural properties, the ECM bears biochemical signals as well as physical signals (mechanotransduction), which taken as a whole result in a physical linkage with the cytoskeleton and enable a bidirectional information flow among extra- and intracellular signals (Rozario and DeSimone, 2010).

The ECM is produced and modified by its containing cells and their secreted factors. It mainly consists of glycosaminoglycans (GAGs), proteoglycans (PGs) and glycoproteins (collagens + non-collagenous proteins) (Rozario and DeSimone, 2010). In the CNS ECM, PGs and glycoproteins are abundantly present, whereas collagens and fibronectin are rather present on specific ECM structures (e.g. basement membrane (basal lamina) = BM, perineuronal net = PNN) (Burnside and Bradbury, 2014). Among the diffused composition in the interstitial space, the CNS ECM can be arranged in the already mentioned distinct, condensed ECM forms like PNNs or BMs (Lau et al., 2013). BMs function as boundaries between the meninges or CNS blood vessels and the CNS parenchyma. They predominantly comprise collagens, laminins, fibronectin and play an important role for the maintenance of the blood-brain barrier (BBB) (Lau et al., 2013). The collagens provide for example the physical stability towards tension (Rozario and DeSimone, 2010). PNNs surround cell somas, dendrites or axon segments of distinct neurons and are detectable in later developmental stages as the critical period (Lau et al., 2013, Burnside and Bradbury, 2014). PGs are the major component of PNNs and are also implicated in the PNN functions e.g. to regulate synaptic plasticity (Kwok et al., 2011, Lau et al., 2013). PNN components are mainly CSPGs of the lectican family, hyaluronic acid, link proteins and glycoproteins as tenascin R (Tn-R) (Carulli et al., 2006, Deepa et al., 2006). CSPG rich PNNs

restrict developmental plasticity and in case of elimination of PNN constituents such as CS or link proteins the plasticity can be restored in adult CNS (Carulli et al., 2010, Kwok et al., 2011). Another type of specialized ECM structures are the so-called fractones (Mercier et al., 2002). They are a specialized, extravascular, elongated and highly branched form of BMs with their stem at capillaries in the SVZ of adult brain and are in contact with all cell types of the adult niche (Mercier et al., 2002). The major components of the fractones are similar to normal BMs and comprise laminin, nidogen, collagen and PGs (mainly HSPGs). It is proposed that fractones promote GF (e.g. FGF 2, BMP 7) presentation to NSCs in their niche via the HSPGs and their GAG-chains (Kerever et al., 2007, Douet et al., 2012). The neural interstitial matrix exhibits as key components hyaluronic acid (HA), PGs and glycoproteins such as tenascins (Lau et al., 2013). Altogether, the ECM is serving as adhesive substrate for migration, is providing structure, capable of binding/storing/sequestering signalling molecules (e.g. growth factors = GFs) and sensing/transducing mechanical signals (mechanotransduction) (Rozario and DeSimone, 2010). The modification of the ECM constitution is besides the secretion and generation of the matrix also accomplished via its degradation. This is performed by ECM component degrading enzymes such as matrix metalloproteinases (MMPs) and by family members of a disintegrin and metalloproteinase (ADAMs) (Rozario and DeSimone, 2010). Additionally, the ECM can function as a special microenvironment, called niche, in which stem cells maintain their self-renewal and proliferation capacity even into adulthood (Doetsch, 2003, Kriegstein and Alvarez-Buylla, 2009, Barry et al., 2014). In the CNS, there are few known niches, where NSCs are maintained and retain their neuron generating capacity: the SVZs of the lateral ventricles, the subgranular zone (SGZ) of the hippocampus and in the hypothalamus (Kriegstein and Alvarez-Buylla, 2009, Martynoga et al., 2012, Dimou and Gotz, 2014). The NSCs can be separated in distinct types of NSCs building different pools of NSCs, which differ in their regional identity and properties, thereby causing a distinct capacity to generate specialised and regionalised NSCs in specific regions, respectively (Ninkovic and Gotz, 2014). This effect is provoked by intrinsic signals as well as various signals of the ECM. For instance, NSCs derive key signals (e.g. IGF 2, FGF 2) from the cerebrospinal fluid (CSF) during development and adulthood, which may function as a niche by globally providing secreted factors to the exposed apical, ventricular domains of NSCs (Johansson et al., 2010, Lehtinen et al., 2011, Zappaterra and Lehtinen, 2012, Johansson et al., 2013). Concomitantly, there are also NSCs without contact to the ventricle or the typical apico-basal polarity of RGCs (Kriegstein and Alvarez-Buylla, 2009). These NSCs receive signals from the meninges or blood vessels and their BMs, from other cells like microglia or Cajal-Retzius cells as well as from the neural interstitial matrix (Siegenthaler et al., 2009, Paridaen and Huttner, 2014) (Figure 3). Blood vessels for example have an influence on intermediate progenitor (IP) proliferation during embryonic development similar to the impact on NSCs in the adult NSC niche (Paridaen and Huttner, 2014). Microglia have been identified to regulate the maintenance of RGCs and Cajal-Retzius neurons secrete reelin, which is well known to have an impact on neuronal migration and to promote symmetric proliferative divisions and postpone neurogenesis (Jossin and Cooper, 2011, Paridaen and Huttner, 2014). The signals of the basal BM play a role in self-renewing potential of RGCs and bRGs (Paridaen and Huttner, 2014). RGC apical adhesion and proliferation is for instance influenced by

interstitial matrix components as laminin or syndecan-1 via integrin receptors (Loulrier et al., 2009, Wang et al., 2012).

Thus, the spatially and temporally regulated distinct ECM composition and its 3-dimensional structure surrounding the NSCs imply numerous functions affecting the NSCs behaviour such as cell migration, proliferation and differentiation by, for example, limiting morphogen diffusion or providing signalling molecule binding sites (Rozario and DeSimone, 2010). Only a few of the various functions have already been mentioned, although it would be impossible to introduce all, one last example will be described. The exogenous signalling molecules play an important role in the manifold ECM functions like the establishment of morphogen gradients. A well-studied transcription factor is the paired box containing homeodomain transcription factor Pax6, which is expressed in several CNS regions (e.g. forebrain) (Woodworth et al., 2012, Paridaen and Huttner, 2014). Among its functions concerning the regulation of regional patterning, Pax6 promotes RGC proliferation and also promotes neurogenesis (Osumi et al., 2008, Paridaen and Huttner, 2014). These in some kind opposing functions seem to be enabled by alternative splicing of Pax6 and by interplay with other transcription factors (Paridaen and Huttner, 2014). Pax6 operates upstream of proneural genes, such as neurogenins, and also directly to promote neurogenesis during development (Martynoga et al., 2012). The exogenous signalling molecules and their signalling pathways can modulate each other's mode of operation and exhibit an enormous crosstalk. The spatial and temporal presentation of morphogens (Shh, Wnt, BMP, etc.) and transcription factors (Pax6, neurogenins, etc.) defines progenitor identities, specifies neuronal subtypes by also influencing the sequential generation of distinct neuronal subtypes of the cortical layers (Martynoga et al., 2012).

Altogether, the ECM is implicated during both, CNS development including processes like neuro-/gliogenesis, synaptogenesis, cell migration, axonal outgrowth and guidance (Bandtlow and Zimmermann, 2000, Faissner et al., 2010) as well as during adulthood in the cell survival, plasticity, damage response and regeneration (Soleman et al., 2013).

1.2.2 PROTEOGLYCANS IN THE EXTRACELLULAR MATRIX

Proteoglycans (PGs) and glycosaminoglycans (GAGs) are a major component of the ECM. They are participating in the orchestration of the various signalling pathways and plenty of functions in the complex 3-dimensional ECM meshwork that have already been generally described in the previous section. Below, a focus on the structure and the specific relevance of PG involvement is made.

PGs consist of a core protein and at least one but up to > 100 covalently attached GAG chains at specific sites of the core protein (Esko et al., 2009). GAGs are linear polysaccharides built of repeating disaccharide units. Depending on the disaccharide unit composition, the GAGs can be distinguished into families: heparan sulfate (HS), chondroitin sulfate (CS), dermatan sulfate (DS) and keratan sulfate (KS) (Bandtlow and Zimmermann, 2000). PGs appear as cell surface PGs (transmembrane or glycosylphosphatidylinositol (GPI)-anchored) or become secreted (Figure 4). After the polymerization of the PGs and the GAGs, they can be highly modified by epimerization, sulfation and other modifying enzymes (Habuchi, 2000, Maeda, 2015). These processes will be further explained for CS-GAGs in the following section. The enormous structural complexity of PGs provides a big platform to create the functional diversity of the

ECM, offered by different core proteins, variable number and types of attached GAGs and GAG modifications (length, sulfation pattern) (Esko et al., 2009).



Figure 4 Scheme of the major proteoglycan types

Generally, PGs appear in 3 different forms: they can be transmembrane, GPI-anchored (cell surface PGs) or secreted (ECM PGs). They have a core protein (black) and attached GAG chains (dark green). The GAG chains are able to bind signalling molecules, e.g. growth factors (blue). The number and type of attached GAG chains varies between PG families and are only exemplarily depicted here.

PGs can also be classified into different families by the structure and size of their core proteins: lecticans (aggrecan, neurocan, brevican, versican), syndecans (syndecan 1-4), glypicans (glypican 1-6) and other PGs (e.g. RPTP β , phosphacan, NG2) (Bandtlow and Zimmermann, 2000). One specific and major compound of the ECM is hyaluronic acid (HA), which lacks a core protein and is solely built of a long chain of non-sulfated repeating disaccharide units, which is directly synthesized at the plasma membrane and released into the ECM (Vigetti et al., 2014). HA and PGs belonging to the HSPGs or CSPGs are the key components of the brain's ECM (Zimmermann and Dours-Zimmermann, 2008, Esko et al., 2009, Maeda et al., 2011). Their interaction with the ECM and the surrounded cells can function via the core protein and/or via their GAGs. One well-known function is caused by the GAGs' high density of negative charges, it attracts osmotically active cations and can thereby generate hydrated matrices resistant to mechanical compression or aiding in structural organization (Esko et al., 2009). Another known function of PGs is to localize active molecules to particular places by binding to their GAGs/sulfation motifs and thereby regulating signalling pathways (Deepa et al., 2004, Hacker et al., 2005, Deepa et al., 2006, Alexopoulou et al., 2007, Soleman et al., 2013, Filmus and Capurro, 2014). One example is the binding and storing of TGF β . By capturing TGF β in a

complex in the ECM, it is inaccessible for its receptors and released/secreted by proteolytic cleavage or mechanical inputs (Rozario and DeSimone, 2010).

Neurocan, phosphacan, versican are highly expressed for example in the marginal zone, the SVZ or the subplate and are participating in the regulation of neuronal migration in the cortex during development (Maeda, 2015). Furthermore, syndecans and glypicans participate in morphogen gradient establishment and influence the interaction range of secreted signalling molecules in a passive way (Hacker et al., 2005). Syndecans are also implicated in modulating the responsiveness of NSCs to Wnt ligands and in addition to that, the NSCs for instance highly express syndecan 1 during cortical neurogenesis/development and its knockdown revealed a reduced proliferation as well as a premature differentiation of NSCs (Wang et al., 2012). Moreover, the expression of some transmembrane PGs is regulated in a specific way: for instance, brevican is expressed by oligodendrocyte precursor cells (OPCs) during postnatal development, when the OPCs start ensheathing axon fibers, whereas afterwards OPCs downregulate and astrocytes begin brevican expression in the hippocampus while CNS fiber tract development proceeds (Ogawa et al., 2001). A further PG, NG2, is e.g. highly expressed on OPCs, on which it promotes proliferation as well as migration and also showed high affinity binding sites for GFs such as FGF 2 and thereby acting as reservoir or co-receptor (Wade et al., 2014). Regarding PGs' influence on migration, it is known, that e.g. avian neural crest cells are attracted by versican isoforms and avoid aggrecan containing matrix, whereby these effects are triggered by the PG core and their attached GAG chains (Perissinotto et al., 2000).

1.3 CHONDROITINSULFATE PROTEOGLYCAN

1.3.1 CHONDROITINSULFATE PROTEOGLYCAN STRUCTURE AND THEIR MODIFICATION BY CHONDROITINSULFOTRANSFERASES

Chondroitinsulfate proteoglycans (CSPGs) consist of a protein core which functions as a backbone and can greatly differ in size and contain different family determining domains (Bandtlow and Zimmermann, 2000, Bartus et al., 2012). Covalently linked to the core protein, CSPGs have at least one chondroitinsulfate (CS) glycosaminoglycan (GAG) chain attached via a tetrasaccharide linker to a serine residue of the core protein (Silbert and Sugumaran, 2002, Mikami and Kitagawa, 2013) (Figure 5). The tetrasaccharide linker comprises xylose-galactose-galactose-glucuronic acid and becomes subsequently elongated into a mature CS-GAG, whereas the synthesis of the CS core protein and the linker assembly starts in the endoplasmic reticulum (ER), the maturation continues in the Golgi apparatus compartments with the polymerization of the CS-GAG chains and their sulfation by chondroitinsulfotransferases (Chsts) (Kitagawa et al., 2001, Kwok et al., 2012). The CSPGs comprise several families/groups, which are not consistently categorized, but always include the following members: lectican family (neurocan, brevican, versican, aggrecan; mainly secreted, GPI-anchored) (Bandtlow and Zimmermann, 2000), RPTP β /phosphacan (transmembrane, secreted), small leucine-rich PGs (decorin, biglycan; secreted) (Galtrey and Fawcett, 2007), testicans (secreted) (Schnepp et al., 2005, Maeda, 2015) and others (neuroglycan C, NG2, etc.; transmembrane) (Galtrey and Fawcett, 2007). Each group includes different isoforms or alternative splice variants, as well as posttranslational modifications, e.g. cleaving/shedding of cell surface compartment of the PG

protein core and thereby releasing soluble, active GAG-containing ectodomains, which was reported for syndecans and hypothesized for NG2 (Manon-Jensen et al., 2010, Burnside and Bradbury, 2014).

CS-GAGs are linear, unbranched chains of repeating disaccharide units built of alternating N-acetylgalactosamine (GalNAc) and glucuronic acid (GlcA) sugars (Iozzo and Murdoch, 1996, Mikami and Kitagawa, 2013). The number of attached CS-GAGs can vary from 1 to 100 (Dyck and Karimi-Abdolrezaee, 2015). The length of a CS-GAG is variable as well and can possess over 100 repeating disaccharide units (Galtrey and Fawcett, 2007, Dyck and Karimi-Abdolrezaee, 2015). Another step to create the great heterogeneity is the modification by epimerization and sulfation. After epimerization of the GlcA to iduronic acid (IdoA) by C5-epimerases, the disaccharide unit is converted to dermatan sulfate (DS) (Sugahara, 2003, Mikami and Kitagawa, 2013). The creation of the complex sulfation pattern of CS/DS-GAGs is enabled by seven chondroitinsulfotransferases (Chsts), which are expressed in the neurogenic regions of the embryonic and adult CNS (Kusche-Gullberg, 2003, Akita et al., 2008). Chsts catalyze the transfer of a sulfate group from 3'-phosphoadenosine 5'-phosphosulfate (PAPS) to a specific carbon atom of the CS-GAG sugars (Mikami and Kitagawa, 2013). The specific sulfation by Chsts generates five different units in principle, which can be mono- (CS-A, CS-C) and disulfated (iB, CS-D, CS-E), including the epimerized DS units (iA, iB, iE) (Sugahara and Mikami, 2007, Mikami and Kitagawa, 2013, Dyck and Karimi-Abdolrezaee, 2015) (Figure 5). The Chsts differ in their sulfating position and are grouped according to the position where the sulfate is added to the sugar molecule: the 6th carbon atom of GalNAc can be sulfated by the Chst 3 or Chst 7 (Uchimura et al., 1998, Kitagawa et al., 2000) and thereby generates the monosulfated CS-C unit. The second monosulfated CS-unit CS-A is sulfated by Chst 11, Chst 12 or in the case of iA by Chst 14 at the 4th carbon atom of GalNAc (Hiraoka et al., 2000, Yamauchi et al., 2000, Evers et al., 2001). These monosulfated CS-units are the basis for the disulfated CS-units. The synthesis of CS-D and iB is performed by the Chst Ust, which transfers a sulfate group to the 2nd carbon atom of the GlcA or IdoA of the corresponding monosulfated disaccharide units CS-C and iA (Kobayashi et al., 1999, Mikami and Kitagawa, 2013). The last member of the Chsts is the Chst GalNAc, which generates CS-E or iE out of CS-A or iA by adding a sulfate group to the 4th carbon atom of the GalNAc sugar (Ohtake et al., 2001). The Chsts are transmembrane type II proteins, that are localized to the Golgi apparatus with the major and catalytically active part positioned in the lumen of the Golgi cisterns (Kusche-Gullberg, 2003).

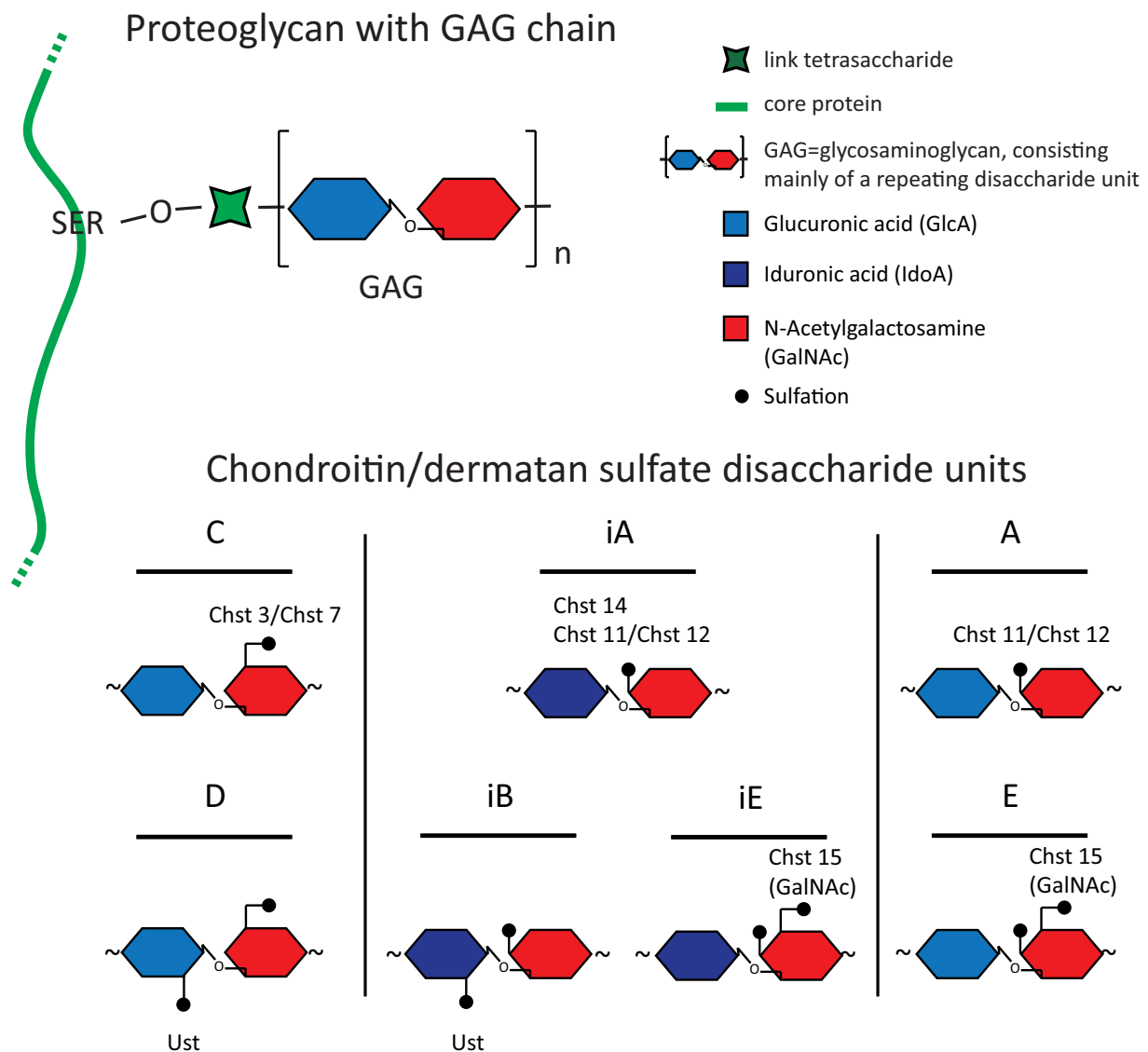


Figure 5 Schematic overview of proteoglycan structure and the possible CS/DS-unit outcome after sulfation and epimerization

Chondroitin sulfate proteoglycans (CSPGs) consist of a core protein (green) and attached glycosaminoglycan (GAG) chains. They are linked via a tetrasaccharide to specific serine residues of the core protein. Chondroitin sulfate (CS) GAGs are built of repeating disaccharide units, namely glucuronic acid (GlcA) and N-acetylgalactosamine (GalNAc). GlcA can be epimerized to iduronic acid (IdoA) and the generated CS-unit is then named dermatan sulfate. Specific chondroitinsulfotransferases (Chsts) transfer sulfate groups to distinct carbon atoms at specific sites and thereby generate distinguishable CS-units: monosulfated (C, A and iA) and disulfated (D, E, iB and iE).

1.3.2 COMPLEXITY AND FUNCTION OF CHONDROITINSULFATES

PGs and their attached GAG chains are an important factor in a lot of cellular processes such as for example neuronal migration, proliferation and differentiation of NSCs, axon pathfinding, myelination, axon regeneration as well as maturation and plasticity of synapses (Maeda et al., 2011, Soleman et al., 2013, Silver and Silver, 2014, Theocharidis et al., 2014). In contrast to the former understanding of CSs as simple repellents, the idea consolidates that the operating mode of CS seems to be much more complex and works rather in a context-dependent manner by the structural PG/GAG chain diversity (Lindahl, 2014, Maeda, 2015). In the case of cellular

migration it depends on the factors that are bound to the GAG chains, which causes CS to operate either as a repellent or attractant in a sulfation pattern dependent manner (Shipp and Hsieh-Wilson, 2007, Maeda, 2015).

The sulfation pattern of PG GAG chains, including CS-GAGs, with its manifold heterogeneity are implicated in a lot already mentioned cellular processes. Isolated CS-units show for instance different binding affinities to distinct axon guidance molecules (e.g. CS-E high affinity, CS-A weak binding (Shipp and Hsieh-Wilson, 2007)) or GFs (e.g. CS-E high affinity to NGF, BDNF (Rogers et al., 2011)). Syndecans, for example, bind various GFs (FGF, PDGF, EGF, HGF, VEGF, etc.) through their HS- and CS-chains (Carey, 1997, Deepa et al., 2004). Syndecans are actually belonging to the HSPG family, although also CS chains can be attached to their core protein (Maeda, 2015). Besides providing distinct functions for distinct tissues or providing niche specificity by HS/CS complexity (length, sulfation pattern) (Haupt et al., 2009), also the temporal and spatial regulation of HSPG/CSPG expression or their affinity to bind signalling molecules changes during development and adulthood (Nurcombe et al., 1993, Akita et al., 2008, Ishii and Maeda, 2008b, Mizumoto et al., 2013). Loss of function studies of distinct CSPG members of the lectican family (versican, aggrecan, neurocan, brevican) exhibited defects in neural crest cell migration, synaptic plasticity, long-term potentiation and also cartilage defects (Rozario and DeSimone, 2010). CSPGs interact with GFs, chemokines and guidance molecules (Hirose et al., 2001, Kwok et al., 2012, Mizumoto et al., 2013). Highly sulfated (disulfated) CS bind to FGFs (e.g. FGF 2) or to guidance molecules as for instance slit, netrin, semaphorins in a sulfation-dependent manner (Maeda, 2010, Mizumoto et al., 2013). The CSPGs expression profiles possess distinct roles at distinct developmental time periods, although there is kind of redundancy, shown by specific CSPG knockout experiments (e.g. neurocan, brevican) (Rauch et al., 2005). It seems that the orchestration of CSPGs is important and the missing CSPGs are supplemented by others of the at least 16 CSPGs, known so far (Herndon and Lander, 1990).

Lecticans are mainly secreted PGs and the major constituents of the brain matrix (Carulli et al., 2005, Maeda, 2015). They interact with the ECM molecules in two ways: protein-protein and protein-carbohydrate interaction. An example for protein-protein interaction is the cooperation of lecticans with tenascins (Tn-C, Tn-R), which are oligomeric glycoproteins. Together with HA and link proteins they create the network surrounding the cells and thus form the basic framework for the CNS ECM (Maeda, 2015). Besides the secreted CSPGs, the lecticans, the CNS comprises transmembrane CSPGs as for example several isoforms of receptor-type protein tyrosine phosphatase β (RPTP β) or neuroglycan C (Maeda et al., 1994, Maurel et al., 1994, Maeda, 2015). One alternative splice variant of RPTP β is a secreted CSPG, phosphacan (Maurel et al., 1994). Phosphacan is known to bind several proteins, midkine, pleiotrophin, tenascins, contactin, NCAM (Peles et al., 1998), whereas it is shown, that pleiotrophin and midkine interact via the HS- and CS-chains (Maeda et al., 2003, Muramatsu, 2014). Especially a higher amount of Ust generated CS-D on phosphacan increased the binding affinity to pleiotrophin (Maeda et al., 2003). Other studies indicated opposing effects of phosphacan on neurite outgrowth, dorsal root ganglion (DRG) neurons were inhibited in contrast to the promoting effect on hippocampal neuron growth *in vitro* (Faissner et al., 1994, Garwood et al., 1999). In this case CS-D seemed to act growth-promoting (Clement et al., 1998).

RPTP β /phosphacan bears a specific CS epitope, which can be recognized by the monoclonal antibody (mAb) 473HD (Faissner et al., 1994). Corresponding to the presence of 473HD on actively cycling RGCs/NSCs in neurogenic niches of the developing as well as in the adult brain, the addition of the mAb 473HD caused a decrease in the number of nsphs *in vitro* (von Holst et al., 2006). The 473HD motif contains at least one CS-D unit and recognizes hexasaccharide sequences, e.g. D-A-D, D-A-A (Ito et al., 2005, Sugahara and Mikami, 2007). It could be shown, that in the nsphs culture system CS-B, CS-D and CS-E have the potential to support FGF-mediated cell proliferation of NSCs (Ida et al., 2006). Additionally, cell surface Ust sulfation exhibited a high binding capacity and thereby promoted the FGF 2 responsiveness in cell migration (Nikolovska et al., 2015). Another mAb, which detects CS-D units, is MO-225 (Ito et al., 2005). In western blot analysis MO-225 exhibits distinct bands in NSC, neurons and astrocytes, varying in size and amount (Yamauchi et al., 2011) referring to the specific regulation of sulfation and the structural heterogeneity during development. NSCs reveal a lower expression of Ust and the C5 epimerase than more differentiated cells like astrocytes or neurons (Yamauchi et al., 2011). Furthermore, Ust expression increases e.g. during cerebellar development and concomitantly the amount of CS-B and CS-D (Ishii and Maeda, 2008b). More and more focus on the GAG research emerges and unravelled their involvement in a lot of signalling pathways and establishing the brain's architecture. For instance, CS-E and CS-D are important for the correct neuronal positioning during developmental migration in the cerebral cortex (Ishii and Maeda, 2008a).

Chondroitinase ABC (ChABC) is a bacterial enzyme, which specifically cleaves CS-GAGs from the core protein and is often used to investigate the impact of missing sulfation and CS-GAGs. ChABC treatment of NSCs *in vitro* and *in vivo* resulted in decreased proliferation and neurogenesis, whereas the number of astrocytes was increased *in vitro*, which means, that CS-sulfation plays a role in lineage decision of NSCs towards a neuronal or glial fate (Sirko et al., 2007). Additionally, further ChABC studies with NSC revealed, that CS-GAGs are essential for FGF 2-mediated proliferation and maintenance of embryonic, cortical NSCs (Sirko et al., 2010). Furthermore, in experiments, in which sulfation was blocked by addition of sodium chlorate to neurosphere cultures, the expression of the 473HD epitope was inhibited and the number of nsphs was decreased (Akita et al., 2008). It was also shown, that changes in the CSPG environment of hippocampal neurons by either ChABC or hyaluronidase, an HA degradation enzyme, the synaptic plasticity was increased (Pyka et al., 2011).

ChABC is frequently mentioned in relation to CNS injury by enabling an increased plasticity, regeneration and promoting structural and functional recovery after ChABC treatment (Galtrey and Fawcett, 2007, Soleman et al., 2013).

1.3.3 INVOLVEMENT OF CHONDROITINSULFATES IN HEALTH AND DISEASE

Because of the vast distribution of PGs in more or less every ECM a big variety of implicated diseases occur by mutations or by imbalance of PG expression/PG-related genes. As already mentioned before, HSPGs and CSPGs are closely related and similar in structure, although they have similar functions in development, they are involved in distinct types of diseases. For instance, HSPGs play a role in Alzheimer's disease, PNNs are associated with epilepsy and

several ECM components are upregulated in malignant glioma (Lau et al., 2013, Soleman et al., 2013). Additionally, specific CSPG containing PNNs might have a neuroprotective function in Alzheimer's disease, by isolating the neurons via HA and CS-GAGs from external stress factors or stimulating anti-apoptotic signalling pathways (Soleman et al., 2013). After traumatic CNS injury or demyelination, CSPG expression is increased and limits axonal regeneration/remyelination by formation of the glial scar, which generally restricts CNS repair (Bradbury et al., 2002, Morgenstern et al., 2002, Lau et al., 2012). Glial scars formed after CNS injury are especially rich in CSPGs and so far supposed to be the key reason for the regeneration failure, because the CSPGs in the glial scar inhibit the axon growth and restrict the plasticity (Silver and Miller, 2004, Silver and Silver, 2014). The specific CSPG upregulation and modification of their sulfation pattern can mediate the regulation of the effect on axonal regeneration after CNS injury (Properzi et al., 2005). The upregulation of CSPGs in glial scars also plays a role in ischemic stroke pathology and exhibits a specific regulation of the CSPGs: direct at the lesion site CSPGs are upregulated, whereas more distant CSPGs are downregulated in PNNs and thereby enabling kind of regeneration, namely axonal sprouting (Soleman et al., 2013). But the implicated diseases concomitant with CS and CS-related protein mutations range from mood/mental disorders (e.g. schizophrenia, bipolar disorder) through autosomal recessive short stature syndrome, intellectual disability to hydrops fetalis or cancer with wide spectra of severity, respectively (Freeze, 2009, Wade et al., 2013, Maeda, 2015). Also an involvement of PGs or specifically sulfated GAGs in physiological and pathological cellular processes by their capacity to regulate GF signalling pathways, affecting for instance cancer, angiogenesis, fibrosis, immunity and infectious diseases, has been described (Uyama et al., 2006, Iozzo and Karamanos, 2010).

Changes in the protein cores of PGs appear in cancer associated with the thereby caused modifications of cell signalling pathways (Wade et al., 2013). A differentially regulated expression of CS- and HS-related enzymes (biosynthesis, sulfation, desulfation) occurs in glioblastoma and might be relevant as putative therapeutic target or function as biomarker in disease classification (Wade et al., 2013).

Thus, for a healthy brain the correct spatiotemporal expression pattern of the various PGs and their GAGs has to be orchestrated and kept in homeostasis. Therefore, ECM modification is an important therapeutic target referring to the wide implication of the surrounding ECM e.g. CSPGs and interaction with cytokines, GFs and receptors (Burnside and Bradbury, 2014). A lot of research is already going on in this field by using enzymes as for instance ChABC together with cell transplantation, manipulating CSPG synthesis and expression of MMPs/ADAMTSs after CNS injury or demyelinating/neurodegenerative diseases (Lau et al., 2013, Burnside and Bradbury, 2014).

1.4 AIM OF THE STUDY

The aim of this study was to investigate the involvement of the sulfation pattern modified by the chondroitinsulfotransferase (Chst) Ust on the behaviour of neural stem cells (NSCs) *in vitro* and *in vivo* during the development of the mouse central nervous system.

Since there is growing evidence, that the neural extracellular matrix (ECM) is participating in various cellular processes and also chondroitin sulfate proteoglycans (CSPGs) are involved in regulating cell behaviour and plasticity, I wanted to elucidate the role of a modified sulfation pattern by the enzyme Ust on the self-renewal capacity, differentiation and proliferation of NSCs. It was shown, that inhibition of the sulfation by sodium chlorate or the degradation of the CSPG glycosaminoglycan chains by chondroitinase ABC led to a decreased proliferation and altered cell fate decisions of NSCs (Sirko et al., 2007, Akita et al., 2008, Sirko et al., 2010). Additionally, first investigations of the impact of distinct Chst overexpression, in combination or single transfected, revealed a tendency to promote neurogenesis after oversulfation *in vitro* (Harrach, 2010). Because the preliminary data exhibited only tendencies towards an increased neurogenesis, I further elucidated the impact of a manipulated chondroitin sulfate (CS) sulfation pattern on NSCs derived from E 13.5 mouse cortices by Ust overexpression concerning NSCs self-renewal, proliferation and cell fate decisions. Furthermore, the analysis of Ust overexpression *in vivo* by *in utero* electroporation should reveal the impact of a modified sulfation pattern on NSCs' behaviour. To enable future examinations of sulfation pattern manipulations during development as well as during later developmental stages, I designed a strategy for a conditional Ust knockout mouse line, including the design and cloning of the targeting plasmid.

2 MATERIALS AND METHODS

2.1 COMPANIES

Amersham pharmacia, Freiburg, Germany

AMS Biotechnology (Europe) Ltd (Amsbio),
Frankfurt, Germany

AppliChem, Darmstadt, Germany

Beckman Coulter, Krefeld, Germany

Becton Dickinson (BD Biosciences), Heidelberg,
Germany

bela-pharm, Vechta, Germany

Bio-Rad, Munich, Germany

Biochrom, Berlin, Germany

Charles River, Sulzfeld, Germany

Clontech, Saint-Germain-en-Laye, France

Dianova, Hamburg, Germany

Enzo Life Sciences GmbH, Lörrach, Germany

Eppendorf, Hamburg, Germany

Fermentas (Thermo Scientific), Schwerte,
Germany

FineScienceTools (FST), Heidelberg, Germany

Fisher Scientific (Thermo Fisher), Nidderau,
Germany

GATC Biotech AG, Konstanz, Germany

GE Healthcare, Freiburg, Germany

GERBU, Heidelberg, Germany

Gibco (Invitrogen), Darmstadt, Germany

Gilson, Limburg-Offheim, Germany

Greiner Bio-One, Frickenhausen, Germany

Grüssing, Filsum, Germany

Harvard Apparatus (Hugo Sachs), March-
Hugstetten, Germany

Heraeus, Hanau, Germany

Hirschmann Laborgeräte, Eberstadt, Germany

ibidi, Martinsried, Germany

Invitrogen, Karlsruhe, Germany

J.T. Baker, Deventer, Netherlands

Kisker Biotech, Steinfurt, Germany

Labnet International, Edison, NJ, USA

Leica Microsystems, Solms, Germany

LMS, Brigachtal, Germany

Lonza, Cologne, Germany

Macherey-Nagel, Düren, Germany

Marienfeld, Lauda-Koenigshofen, Germany

Medical Developments International (Cegla),
Montabaur, Germany

Menzel, Braunschweig, Germany

Merck/Merck Millipore, Darmstadt, Germany

Mo Bi Tec, Göttingen, Germany

NeoLab Migge, Heidelberg, Germany

Nepagene, Ichikawa-City, Japan

New England Biolabs (NEB), Frankfurt, Germany

Novus Biologicals, Cambridge, United Kingdom

Nuaire (ibs tecnomara), Fernwald, Germany

Nunc (Thermo Scientific), Wiesbaden, Germany

Pan Biotech, Aidenbach, Germany

PeproTech, Hamburg, Germany

Peqlab, Erlangen, Germany

Polysciences Europe, Eppelheim, Germany

Qiagen, Hilden, Germany

Roche Diagnostics, Mannheim, Germany

Roth, Karlsruhe, Germany

Santa Cruz Biotechnology, Heidelberg, Germany

Sarstedt, Nümbrecht, Germany

SERVA, Heidelberg, Germany

Sicgen, Cantanhede, Portugal

Siemens Healthcare, Erlangen, Germany

Sigma-Aldrich Chemie, Taufkirchen, Germany

Starlab, Hamburg, Germany

Sutter Instrument, Lambrecht, Germany

Tecan, Mainz, Germany

Th. Geyer, Renningen, Germany

Thermo Fisher Scientific Biosciences, St. Leon-
Rot, Germany

VWR International, Bruchsal, Germany

Worthington (CellSystems), Troisdorf, Germany

Zeiss, Oberkochen, Germany

2.2 MATERIALS

2.2.1 EQUIPMENT

AGFA Curix 60, Siemens Healthcare	Microplate Reader Mode 550, BioRad
Amersham Hyperfilm ECL, GE Healthcare	Mini Centrifuge, LMS
Axiophot, Zeiss	Mini-Protean Tetra Cell, BioRad
Centrifuge 5415R, Eppendorf	NanoDrop, Peqlab
Centrifuge 584R, Eppendorf	PerfectBlue Gel System Mini S, M, Peqlab
CO ₂ incubator, Nuaire	Pipetman M, Gilson
Komesaroff Anaesthetic Machine, Medical Developments International	Pipetus, Hirschmann
Leica CM 3050S cryostat, Leica	Power Station 300, Labnet International
Leica DM 6000, Leica	Sunrise Microplate Reader, Tecan
Micropipette Puller Model P-97, Sutter Instrument	Thermomixer Compact, Eppendorf
	Trans-Blot SD Semi-Dry Transfer Cell, BioRad

2.2.2 CHEMICALS

0,25 % Trypsin-EDTA (T/E), phenol red, Invitrogen	Ethanol, Sigma
Acrylamide, Merck	Fast Green FCF, Sigma
Agar, Invitrogen	Fetal calf serum (FCS), Biochrom
Agarose, AppliChem	GeneRuler 100bp Plus DNA Ladder, Fermentas
Albumin, Bovine, Fraction V, Sigma	GeneRuler 1kb Plus DNA Ladder, Fermentas
Ampicillin sodium salt, Roth	Glycerol, J.T. Baker
APS, J.T. Baker	Glycine, Roth
B27 Serum-Free Supplement, Invitrogen	Heparin sodium salt, Sigma
Bactotryptone, BD	HEPES 1M, Invitrogen
Betaine solution, 5 M PCR reagent, Sigma	Hoechst 33258, Sigma
BrdU (5-Bromo-2'-deoxyuridine), Sigma	Horse serum, Biochrom
Bromophenol blue, SERVA	Isopropanol, Sigma
CaCl ₂ x 2 H ₂ O, Sigma	Kanamycin Sulfate, Invitrogen
Citric acid, Grüssing	KCl, Sigma
Complete Mini; Protease Inhibitor Cocktail, Roche	KH ₂ PO ₄ , AppliChem/GERBU
D-Glucose, Sigma	L-Cystein hydrochloride, Sigma
DMSO (Dimethyl sulfoxide), Sigma	L-Glutamin, Sigma
Donkey serum, Millipore	Laminin-1 (EHS cells), Invitrogen
EDTA, Merck/Roth	Methanol, Sigma
EdU (5-ethynyl-2'-deoxyuridine), Invitrogen	MgCl ₂ , J.T. Baker
EGTA, AppliChem	MgSO ₄ x 7 H ₂ O, J.T. Baker
	Milk Powder, Roth
	Na-carbonate, AppliChem/Grüssing

Na-citrate, AppliChem	SDS, SERVA
Na-deoxycholate, AppliChem	Shandon Immu-Mount, Fisher Scientific
Na ₂ HPO ₄ x 2 H ₂ O, AppliChem	Sodium chlorate, Sigma
NaCl, Sigma	Sucrose, Roth
Normal Goat Serum (NGS), Invitrogen	TEMED, Roth
Novaminsulfon, bela-pharm	Tissue freezing medium (Jung), Leica
PageRuler Plus Prestained Protein Ladder, Fisher Scientific	Tris, Roth
Paraformaldehyde (PFA), J.T. Baker	Tris-HCl, Roth
Pen/Strep (P/S), Gibco	Triton X 100, AppliChem
PMSF, Roth/Sigma	Trypsin Inhibitor, Sigma
Poly-L-Ornithine Hydrobromide, Sigma	Tween20, AppliChem
	Yeast Extract, Roth

2.2.3 MEDIA

BME (Basal Medium Eagle)	Sigma
DMEM	Invitrogen
L15 Leibovitz Medium	Sigma
MEM HEPES Modification	Sigma
Nutrient Mixture F12-Ham	Sigma
PBS	Sigma

2.2.4 PLASTIC WARE

100 cm ² culture flask (T100)	Nunc
100 mm petri dish	Sarstedt
15 ml tube	Greiner Bio-One
25 cm ² culture flask (T25)	Nunc
35 mm petri dish	Nunc
4-well multiwell dish (35 mm)	Greiner Bio-One
50 ml tube	Greiner Bio-One
6-well plate	Greiner Bio-One
60 mm petri dish	Nunc
75 cm ² culture flask (T75)	Nunc
Cell Cultureware 24-Well	Becton Dickinson
flexiPerm slides	Sarstedt
Microloader	Fisher Scientific
Microplate 96 Well	Greiner Bio-One
μ-Chamber 12 well	ibidi
μ-Slide 8 well	ibidi

2.2.5 ENZYMES/GROWTH FACTORS

Chondroitinase ABC	Amsbio
Deoxyribonuclease I	Worthington
DNaseI (RNase free)	Mo Bi Tec

Epidermal growth factor (EGF)	PeproTech
Fast Digest AleI (OliI)	Fermentas
Fibroblast growth factor-2 (FGF 2)	PeproTech
FseI	New England Biolabs
Kapa Hifi Polymerase	Peqlab
Papain	Worthington/Sigma
Proteinase K	Roth
RNase-Free DNase Set	Qiagen
T4 Ligase	Fermentas

2.2.6 KITS

Bromo-2-deoxy-uridine Labeling and Detection Kit I	Roche
Click-iT EdU Alexa Fluor 488 Imaging Kit	Invitrogen
Click-iT EdU Alexa Fluor 647 Imaging Kit	Invitrogen
DC Protein Assay Kit II	BioRad
dNTP Set	Fermentas
First Strand cDNA Synthesis Kit	Fermentas
NucleoBond Xtra Maxi Plus EF	Macherey-Nagel
P3 Primary Cell 4D Nucleofector X Kit L	Lonza
P3 Primary Cell 4D Nucleofector X Kit S	Lonza
PARIS-Kit	Invitrogen
QIAprep Spin Miniprep Kit	Qiagen
QIAquick PCR Purification Kit	Qiagen
RNeasy Mini Kit	Qiagen
SuperSignal West Pico	Fisher Scientific

2.2.7 PLASMIDS

pCR®II-TOPO®	Invitrogen
pEasyflox	AG Müller, University of Heidelberg
pEGFP N1	Clontech
pXL201-3xFLAG	AG Alvarez-Bolado, University of Heidelberg
pUst-EGFP N1 (Ust)	AG von Holst, Richard Sturm, University of Heidelberg
pUst-EGFP N1 mutated (Ust mut)	AG von Holst, Denise Harrach, University of Heidelberg
pXL-Ust	AG von Holst, Valentin Evsyukov, University of Heidelberg

2.2.8 ANTIBODIES

Primary Antibodies							
Antigen	Clone	Produced in	Specificity	Isotype	Dilution	Company	Order Nr
473HD		rat		IgM	1:100-1:300	Faissner et al., 1994	
Bassoon	SAP7F407	mouse	ms, rat	IgG2a	1:1000	Enzo Life Sciences	ADI-VAM-PS003-F

Primary Antibodies							
Antigen	Clone	Produced in	Specificity	Isotype	Dilution	Company	Order Nr
Ctip2	25B6	rat	ms, GP, h, zf	IgG2a	1:1000	abcam	ab18465
GFAP	G-A-5	mouse		IgG1	1:300	Sigma	G 3893
GFP		rabbit			1:300	Millipore	AB3080
GFP-FITC		goat	wt, rGFP, eGFP		1:500	Biomol (Rockland)	600-102-215
Ki67		rabbit			1:100-1000	Millipore	AB9260
mCherry (tdTomato)		goat		IgG	1:250	Sicgen	AB0081-200
Nestin	rat-301	mouse	ms, rat	IgG1	1:500	Millipore	MAB353
NeuN	EPR12763	rabbit	ms, rt, h, zf	IgG	1:500-1000	abcam	ab177487
O4	O4	mouse		IgM	1:50	Sigma	O7139
O4		mouse		IgM	1:30	(Sommer and Schachner, 1981)	
Pax6		mouse		IgG	1:100	Stoykova et al	
tGFP	2H8	mouse		IgG2b	1:2000	VWR	ORIGTA150041
Ust		rabbit		IgG	1:300	abcam	Ab137624
VGlut1		guinea pig	rat	IgG	1:1000	Millipore	AB5905
α -Tubulin	DM1A	mouse		IgG1	1:5000-10000	Sigma	T6199
Transgolgin-97		mouse		IgG1	1:250	Dr. C. Hartmann-Fatu, ZMB Uni Duisburg-Essen	
β III-Tubulin	2G10	mouse		IgG2a	1:300	Sigma	T8578

Secondary Antibodies					
Species Reactivity	Produced in	Conjugation	Specificity	Dilution	Company
α goat	donkey	Cy3	IgG (H+L)	1:500	Dianova
α goat	donkey	Cy2		1:250	Dianova
α goat	donkey	HRP	IgG	1:10000	Santa Cruz
α guinea pig	goat	633 Alexa	IgG (H+L)	1:500	Invitrogen
α mouse	goat	Cy3	IgG + IgM (H+L)	1:500	Dianova
α mouse	goat	HRP	IgG + IgM (H+L)	1:5000	Dianova
α mouse	goat	Cy3	IgG (H+L)	1:500	Dianova
α mouse	donkey	Cy2	IgM (μ chain)	1:250	Dianova
α mouse	sheep	Cy2	IgG (H+L)	1:250	Dianova
α mouse	goat	647 Alexa	IgG + IgM (H+L)	1:500	Dianova
α mouse	goat	Cy5	IgM (μ chain)	1:500	Dianova
α mouse	donkey	Cy2	IgG	1:250	Dianova
α mouse	donkey	Cy3	IgM (μ chain)	1:500	Dianova

Secondary Antibodies					
Species Reactivity	Produced in	Conjugation	Specificity	Dilution	Company
α mouse	goat	647 Alexa	IgG (H+L)	1:500	Invitrogen
α rabbit	goat	Cy3	IgG (H+L)	1:500	Dianova
α rabbit	goat	HRP	IgG (H+L)	1:5000	Dianova
α rabbit	goat	Cy2	IgG (H+L)	1:300	Dianova
α rabbit	donkey	Cy5	IgG (H+L)	1:500	Dianova
α rabbit	goat	647 Alexa	IgG	1:300	Dianova
α rat	goat	Cy3	IgM (μ chain)	1:500	Dianova
α rat	goat	HRP	IgM (μ chain)	1:5000	Dianova
α rat	goat	647 Alexa	IgM (μ chain)	1:500	Dianova
α rat	donkey	Cy3	IgG	1:500	Dianova

2.2.9 ALL OTHER CONSUMABLES

0,22 μm sterile filters	Millipore
0,4 μm sterile filters	Millipore
Borosilicate Capillaries, thin wall with filament (OD 1.2 mm, ID 0.94 mm, length 100 mm)	Harvard Apparatus
Cover Slip circles, 9 mm	Menzel
dNTP mix	Fermentas
ECL	GE Healthcare
Menzel Adhesion slides SuperFrostPlus	Menzel/Fisher Scientific
Parafilm M	Roth
PVDF membrane (Immobilon® P)	Millipore
Roti-Free Stripping buffer	Roth
Whatman paper (3 mm Chr)	Fisher Scientific

2.3 COMPOSITION OF MEDIA, BUFFERS AND OTHER REAGENTS

2.3.1 CELL CULTURE

Digestion buffer	30 U/ml Papain, 40 μg/ml DNase, 0,24 mg/ml L-Cysteine in MEM
Neurosphere differentiation medium	Neurosphere medium, 1 % (v/v) FCS
Neurosphere medium	DMEM/F12 (1:1), 0,2 mg/ml L-Glutamin, 2 % (v/v) B27, 100 U/100 μg/ml Pen/Strep
Ovomucoid	L-15 Medium, 1 mg/ml Trypsin Inhibitor, 50 μg/ml BSA, 40 μg/ml DNase
Phosphate-buffered-Saline (PBS)	137 mM NaCl, 3 mM KCl, 6,5 mM Na ₂ HPO ₄ *2H ₂ O, 1,5 mM KH ₂ PO ₄

2.3.2 IMMUNOCYTO- AND IMMUNOHISTOCHEMISTRY

4 % (w/v) PFA	4 % (w/v) Paraformaldehyde, 1xPBS; pH 7,3
Citrate buffer	2 mM Citric acid, 8 mM Na-citrate
Krebs-Ringer-HEPES (KRH)	125 mM NaCl, 4,8 mM KCl, 1,3 mM CaCl ₂ *2H ₂ O, 1,2 mM MgSO ₄ *7H ₂ O, 1,2 mM KH ₂ PO ₄ , 5,6 mM D-Glucose, 25 mM HEPES; pH 7,3

KRH/A	KRH, 0,1 % (w/v) BSA
PBS/A	PBS, 0,1 % (w/v) BSA
PBS/Glycerol	PBS + Glycerol (1:1)
PBT 1	PBS, 1 % (w/v) BSA, 0,1 % (v/v) Triton X-100
Phosphate-buffered-Saline (PBS)	137 mM NaCl, 3 mM KCl, 6,5 mM Na ₂ HPO ₄ *2H ₂ O, 1,5 mM KH ₂ PO ₄

2.3.3 MOLECULAR BIOLOGY

DNA loading buffer (6x)	0,25 % Bromophenol blue, 30 % Glycerol in H ₂ O
LB-Medium	10 g NaCl, 10 g Bactotryptone, 5 g Yeast extract in 1 l H ₂ O
LB-Medium with Agar	LB-Medium with 15 g Agar
Tail buffer for genomic DNA	100 mM TrisHCl pH 8,5, 5 mM EDTA, 0,2 % SDS, 200 mM NaCl
Tris-acetate-EDTA Electrophoreses buffer (TAE)	40 mM Tris-acetate, 1 mM EDTA

2.3.4 PROTEIN BIOCHEMISTRY

Blocking buffer	5 % (w/v) Milkpowder in TBST
Cell lysis buffer	50 mM Tris-Cl pH 7,5, 150 mM NaCl, 5 mM EDTA, 5 mM EGTA, 1 % (v/v) Triton X-100, 0,1 % (v/v) Na-deoxycholate, 0,1 % (v/v) SDS
Laemmli sample buffer (SDS) 5x	156 mM Tris-HCl pH 7,4, 5 % (w/v) SDS, 0,25 % (w/v) Bromophenol blue, 25 % Glycerol, 12,5 % (v/v) β-mercaptoEtOH, H ₂ O
Running buffer (SDS-PAGE)	25 mM Tris, 192 mM Glycine, 0,1 % (v/v) SDS
TBS	19 mM Tris-Cl, 137 mM NaCl; pH 7,4
TBST	TBS, 0,05 % (v/v) Tween 20
Transfer buffer (Semi Dry Blot)	25 mM Tris pH 8,2-8,4, 0,1 % (v/v) SDS, 192 mM Glycine, 20 % (v/v) Methanol
Transfer buffer (Tank Blot; Fairbanks)	40 mM Tris, 20 mM Sodium acetate, 2 mM EDTA, pH 7,4; 10 % (v/v) Methanol, 0,05 % (v/v) SDS

2.4 CELL CULTURE

2.4.1 CULTIVATION OF MOUSE NEURAL STEM CELLS

Mouse neural stem cells (NSCs) were obtained by dissecting the cortices of E13-E14.5 mouse embryos to generate cultures of free-floating neurospheres. The embryos were derived from timed pregnancies of NMRI mice obtained from Charles River. The age of the embryos was determined by Theiler stages (Theiler (1989)). Embryos of stages from E12.5 (Theiler 20) to E14.5 (Theiler 22) were used. The cortical hemispheres were dissected in MEM and the meninges were removed. The cortices were collected in 1 ml MEM and then digested for 25 min at 37°C by adding 1 ml filter-sterilized MEM with Papain (30 U/ml), L-Cysteine (240 µg/ml) and DNase (40 µg/ml). The tissue was gently triturated to a single cell suspension. The digestion was stopped by an equal volume of ovomucoid. The cells were pelleted for 5 min at 180 x g and afterwards resuspended in neurosphere (Nsph) growth medium. The cells were plated (100.000 cells/ml) in T25 flasks in 4 ml Nsph growth medium with the growth factors EGF (10 ng/ml), FGF 2 (10 ng/ml) and the cofactor Heparin (0,5 U/ml) and incubated at 37°C and 5 %

CO₂. After 5 days of cultivation the cells were passaged to generate secondary neurospheres. Therefore, the primary neurospheres were pelleted for 5 min at 80 x g and digested with 450 µl T/E for 3 min at 37°C. By adding the same volume of ovomucoid the digestion was stopped. In order to generate a single cell suspension, the cells were gently triturated and again pelleted for 5 min at 120 x g. Afterwards, the cells were plated (50.000 cells/ml) in T25 flasks in 4 ml Nsph growth medium and the above mentioned growth factors. After 4 days of cultivation the secondary neurospheres were treated as described before to generate tertiary neurospheres. Thereby, 10⁶ cells were plated in T75 flasks in 12 ml nsph growth medium and growth factors were added at the same concentration as listed above. After another 3 days of incubation the Nsphs were used for transfection and following procedures.

2.4.2 TRANSFECTION OF THE NSCs

Isolated NSCs from mouse tissue were expanded in cell culture under proliferative conditions. For the transfection of the NSCs a single cell suspension was prepared by digestion with T/E for 2-3' at 37°C. The addition of an equal volume of Ovomuroid stopped the digestion. The appropriate amount of cells was transfected with Lonza's P3 Primary Cell 4D Nucleofector X Kit S (5 x 10⁵) or L (5 x 10⁶) according to the manufacturer's instructions. 0,5 µg Plasmid was used for Kit S and 5 µg Plasmid for Kit L with the transfection pulse DS 113. For an improved regeneration the cells have been transferred into Nsphs-medium to recover for 1 d in the incubator.

2.4.3 DIFFERENTIATION ASSAY

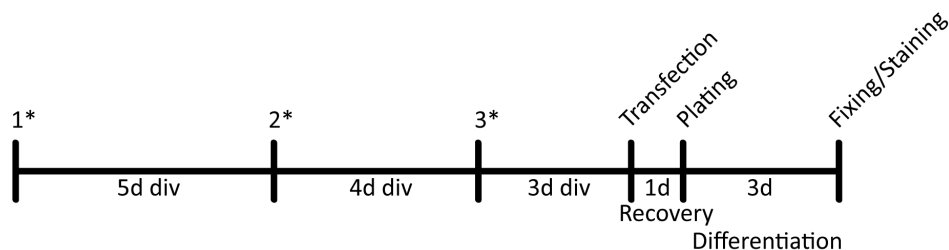


Figure 6 Differentiation Assay Timescale

For the differentiation of NSCs 4-well multiwell dishes, flexiPERM slides, µ-Slide 8 well or µ-Chamber 12 well have been prepared. They were sequentially coated for 1 h with P-Orn [10 µg/ml in H₂O] followed by Laminin [10 µg/ml in PBS]. The transfected NSCs could rest for 24 h after transfection in the incubator with Nsph growth medium. Afterwards, a single cell suspension was prepared as described in the cultivation conditions of NSCs and 20.000 cells/well (4-well, flexiPERM, 8 well) or 10.000 cells/well (12 well) have been plated in differentiation medium. As soon as the cells attached to the bottom of the wells, the dish was floated with 1,6 ml differentiation medium and left for 3 d in the incubator to differentiate (4 well). The following analysis of the differentiation of NSC-derived cell types and the expression of the used constructs were performed by immunocytochemical stainings.

2.4.4 CLONAL DENSITY ASSAY

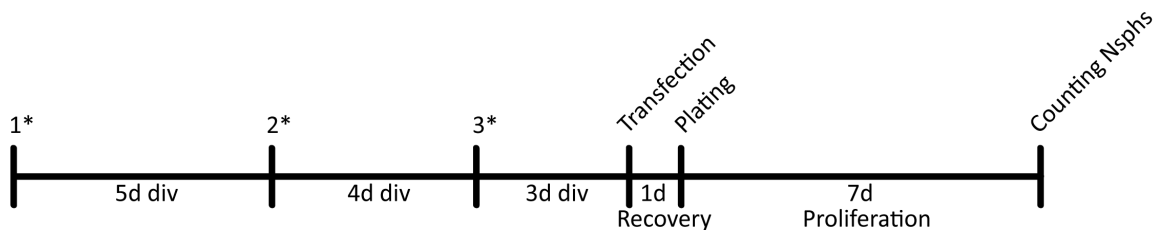


Figure 7 Clonal Density Assay Timescale

To define the amount of Nsph forming cells within the transfected NSCs a Clonal Density Assay was performed. After the recovery from the transfection, 2500 cells/T25 flask have been plated in 2 ml Nsph growth medium with distinct concentrations of the growth factors FGF 2 [2 ng/ml], EGF [2 ng/ml] and Heparin [0,0625 U/ml]. After one week the number of Nsphs was evaluated under a light microscope and documented.

2.4.5 PROLIFERATION ASSAY

The proliferative capacity of the transfected NSCs was checked by the EdU proliferation assay. Therefore, the transfected cells have been plated following the same procedure as in the differentiation assay, but before fixing the cells with PFA, the cells were pulsed for 2-3 h with EdU. In one case the addition of 2 ng/ml FGF 2 was used to increase the proliferation rate in general.

2.5 IMMUNOCYTOCHEMISTRY

2.5.1 DIFFERENTIATION

For the immunological antigen detection of cultured NSCs after the differentiation assay, the medium of the NSCs has been removed and for a staining of cell surface molecules the cells were washed with KRH/A. The primary antibodies for the cell surface molecules were incubated for 25 min in KRH/A at RT. Afterwards the cells were fixed with 4 % PFA for 10 min at RT. Two washing steps with PBS/A were followed by a permeabilization with PBT 1 for 30 min at RT. After another two washing steps with PBS/A, the cells have been incubated overnight with primary antibodies in PBS/A at 4°C. The next day, the cells were washed twice with PBS/A and secondary antibodies were incubated for 1 h in PBS/A at RT. The cells were washed with PBS twice and mounted with PBS/Glycerol for subsequent immunofluorescence microscopy analysis.

2.5.2 PROLIFERATION

The proliferation of the NSCs after transfection was examined by using the EdU assay. Here, the base analogue EdU was added to the cultures for 2-3 h before fixing the cells after the differentiation assay. The pulse and the EdU staining were performed as described in the manufacturer's instructions. For additional antigen detection the procedure was expanded in the following way: After the fixation for 10 min with 4 % PFA at RT the cells have been incubated for 20 min with PBT 1 and then washed twice with the washing buffer. The EdU

reaction cocktail incubation was followed by another two washing steps with PBS/A and incubation of the primary antibodies in PBS/A overnight at 4°C. The next day the cells were washed with PBS/A twice and the secondary antibodies were incubated for 1 h at RT in PBS/A. To finish the staining, the cells were washed twice with PBS and mounted with PBS/Glycerol.

2.6 IMMUNOHISTOCHEMISTRY

2.6.1 DIFFERENTIATION

The cryo sections were thawed at RT and rehydrated in PBS for 10 min. For permeabilization, the slides have been incubated in PBS with 0,5 % Triton X-100 for 20 min. The slides have been washed for another 10 min in PBS and afterwards incubated for 1 h at RT with blocking solution (PBS + 10 % serum + 3 % BSA). Primary antibodies have been incubated overnight at 4°C in PBS with 3 % BSA. On the next day the slides have been washed with PBS/A twice for 5 min, before the slides have been incubated with the secondary antibodies for 1 h at RT in PBS/A. After another two washing steps with PBS the slides have been mounted.

For the primary antibodies that need an antigen retrieval treatment the following steps came ahead of the rest of the procedure: The thawed slides have been boiled in citrate buffer until the temperature reached 90°C, then put aside until the temperature reached about 60°C and subsequently washed in PBS.

2.6.2 PROLIFERATION

The cryo sections were thawed at RT and washed in PBS + 3 % BSA twice for 5 min. After permeabilization for 20 min in PBS with 0,5 % Triton X-100, the slides were incubated again twice for 5 min with PBS + 3 % BSA. Then, the EdU cocktail incubated for 30 min as described in the manual of the kit. After another two washing steps with PBS + 3 % BSA, the sections incubated with the primary antibodies overnight at 4°C in the washing buffer. On the next day the secondary antibodies incubated for 1 h at RT in PBS/A after washing the slides twice with the same buffer. The slides were washed twice in PBS, followed by mounting them in Imm-Mount.

2.7 MOLECULAR BIOLOGY

2.7.1 RNA ISOLATION AND cDNA SYNTHESIS

Total RNA was isolated from pelleted NSCs or Nsphs. Therefore, the RNeasy Mini Kit including QIAshredder columns were used according to the manufacturer's instructions. Depending on the used cell amount a volume of 30-50 µl was used for elution.

cDNA was transcribed from isolated RNA with the First Strand cDNA Synthesis Kit as described in the instructions.

2.7.2 POLYMERASE CHAIN REACTION (PCR)

The polymerase chain reaction was always performed with a PCR reaction mix mentioned in the table below with distinct conditions for PCR reaction program depending on the used primers (see also 2.8 Oligonucleotide Primers). The optimal conditions were tested for each primer pair separately.

PCR reaction mix	
template DNA	0,5-1 μ l
dNTPs (5 nmol)	0,5 μ l
forward primer (5 pmol)	0,5 μ l
reverse primer (5 pmol)	0,5 μ l
10x buffer	2,5 μ l
Taq polymerase	0,5-1 μ l
(Betaine solution	5 μ l)
H ₂ O	x μ l
Total volume	25 μ l

PCR reaction program			
1. denaturation	94°C	5 min	25-45 cycles
2. denaturation	94°C	30 sec	
3. annealing	see 2.8	30-60 sec	
4. elongation	72°C	30-90 sec	
5. elongation	72°C	5 min	
6. cooling	4°C	∞	

2.7.3 ISOLATION OF PLASMID DNA

Plasmid DNA was isolated from 3 ml bacterial cultures with the QIAprep Spin Miniprep Kit and from 500 ml cultures with the NucleoBond Xtra Maxi Plus EF Kit according to the manufacturers' instructions. The DNA was eluted with H₂O and stored at -20°C.

2.7.4 RESTRICTION ENZYME DIGESTION

Plasmid DNA or PCR products were cut with specific restriction enzymes as described in the manufacturers' instructions and with the following standard procedure: A distinct amount of DNA was mixed with the specific restriction enzyme, the appropriate restriction buffer and H₂O in a volume of 10-20 μ l and was digested for the recommended time at 37°C. The reaction was usually stopped by inactivating the enzymes at 70-80°C for 10-20 min.

2.7.5 SITE-DIRECTED MUTAGENESIS OF UST

For inactivation of the catalytic active lysine of Ust, a site-directed mutagenesis of Ust on the pEGFP-N1 plasmid was performed. The lysine was mutated with special primers (Ust mut K->A forw/rev) into a catalytically inactive alanine. For the PCR Pfu polymerase was used and 100 ng of the plasmid DNA. The PCR product was digested with DpnI for 1 h at 37°C. After the digested PCR product was checked, a transformation was performed, clones were picked, plasmid DNA isolated and sequenced by Sanger sequencing.

2.8 OLIGONUCLEOTIDE PRIMERS

All primers were synthesized by Sigma and are listed in the following table (inserted restriction sites are highlighted in red).

Primer	Sequence 5'-3'	Annealing Temp
3'arm full forw	CGCTAAGCTTGTCAACTGTGCCGCTTCG	
3'arm full rev	CAGCCTCGAGAGCCTATCTCTACTGAAGATCAATCC	
3'arm seq rev'	GCAGAATGGCAGAGAATGAAGAGG	57-65°C
5'arm full forw	GCAGATCGATGCTTGGCAACTCCCATCTCC	60-62°C
5'arm full rev	ATCGGCCGCTATCCGAGAACAGGGCTGC	60-62°C
5'arm seq forw	CCTGACCACTGACCTCACTTCC	55-59°C
A	CCAGGACCAGATTGTCAGAAGAGG	61-65°C
B'	ATGTGGAATGTGTGCGAGGC	59-65°C
C	CGATTAAGTGTGTTTGATAGAGCAGC	59-65°C
D	CCTCCCTCGTCTTACAAGCACTCC	57-65°C
E	CCTTCTGAGTTGTGTGGGCTGG	60-65°C
F'	GGAATTTACACCCTCCCTCAGC	61-65°C
KO element full forw	CCTGTTCTCGGATAGGTCTCTGG	60-62°C
KO element full rev	CGAAGTCGACGCACAGTTGACTGGCACC	60-62°C
KO seq forw	GTCAAGGAGGTGGAGCGAGAGG	65°C
KO seq rev	CGTGGTGGCCGTGACAGC	65°C
Ust mut K->A forw	GTACAACAGAGTTGGCGCGTGTGGCAGTCGTACC	60°C
Ust mut K->A rev	GGTACGACTGCCACACGCGCAACTCTGTTGTAC	60°C
Ust Sonde forw	GCAACTTTGGCGGTCAGAGG	64°C
Ust Sonde rev	GGTCCTGGAGCAGAGCCTGG	64°C
GFP forw	ATGGTGAGCAAGGGCGAGG	63°C
GFP rev	TTACTTGTACAGCTCGTCCATGCC	63°C
tdTomato forw	CATGGCACCGGCAGCAC	60°C
tdTomato rev	TCACTTGTTCATCGTCATCCTTG	60°C

2.9 PROTEIN BIOCHEMISTRY

2.9.1 PROTEIN ISOLATION AND QUANTITATION

For cell lysis, Nsphs or single cell suspension were pelleted and directly put on ice for protein isolation or frozen for storage. Depending on the cell amount, distinct amounts of lysis buffer with 1 % protease inhibitor (40-140 μ l) were added and incubated for 1 h on ice. The lysate was cleared by centrifugation at 16.000 x g for 30 min at 4°C. The supernatant was transferred into a fresh tube on ice.

Protein concentration was determined using the BioRad DC Protein Assay Kit II according to the manufacturer's instructions.

2.9.2 SDS-PAGE

SDS-PAGEs were performed with BioRad's Mini-Protean Tetra Cell electrophoresis system. Therefore, the samples have been heated in Laemmlis sample buffer at 95°C for 5 min. After loading the gel (8 % or 10 % gels), the protein separation was accomplished by a constant power of 15 mA per gel for 1 h 15 min. The composition of the SDS gels is listed in the following table:

For 2 gels:	8 % separation gel	10 % separation gel	5 % stacking gel
H ₂ O	4,66 ml	4 ml	2,7 ml
Acrylamide	2,64 ml	3,3 ml	670 µl
1,5 M Tris pH 8,8	2,5 ml	2,5 ml	–
1 M Tris pH 6,8	–	–	500 µl
10 % SDS	100 µl	100 µl	40 µl
10 % APS	100 µl	100 µl	40 µl
TEMED	4 µl	4 µl	4 µl

2.9.3 WESTERN BLOT

For blotting the proteins onto a methanol-activated PVDF membrane, the SDS gel, Whatman paper and the membrane were collected in transfer buffer. Depending on the method (Semi Dry or Tank Blot), the gel, the PVDF membrane and the Whatman paper were stratified or the Tank Blot sandwich was prepared. For the Semi Dry blotting a constant current of 75 mA per gel 1 h 15 min was used to transfer the proteins to the membrane. The Tank Blot was performed overnight at 4°C with a constant voltage of 9 V.

After the transfer, the membrane was incubated with 5 % blocking buffer for 1 h at RT. Primary antibodies were incubated overnight at 4°C after a short washing step with TBST. The membrane was washed 3 times for 20 min with TBST before incubating the HRP conjugated secondary antibodies for 1 h in blocking buffer at RT. After another 3x15 min washing steps with TBST, the membrane was incubated with ECL reagent and Amersham Hyperfilms of different exposure times were developed in a developing machine.

2.10 IN UTERO ELECTROPORATION

2.10.1 ANIMALS

For the *in utero* experiments timed pregnant C57BL/6 mice were used. They were purchased either from Charles River Laboratories or Janvier.

2.10.2 GLASS CAPILLARIES

Injection capillaries were pulled with a micropipette puller from Sutter Instrument. Therefore, borosilicate capillaries were used and pulled as thin and long as possible to minimize any injury to the embryo.

2.10.3 PLASMID PREPARATION

For the plasmid DNA injection into the lateral ventricle, the plasmid was isolated as described in 2.7.3 and eluted in water. The plasmid was diluted in PBS to a concentration of 1-2 µg/µl and the dye fast green FCF was added to enable the visualization of the injected DNA in the ventricle system.

2.10.4 SURGICAL PROCEDURE

The anaesthesia of the pregnant mice at embryonic day E12.5 was initiated by isoflurane inhalation, as recommended by the Institut für Labortierkunde der Universität Zürich

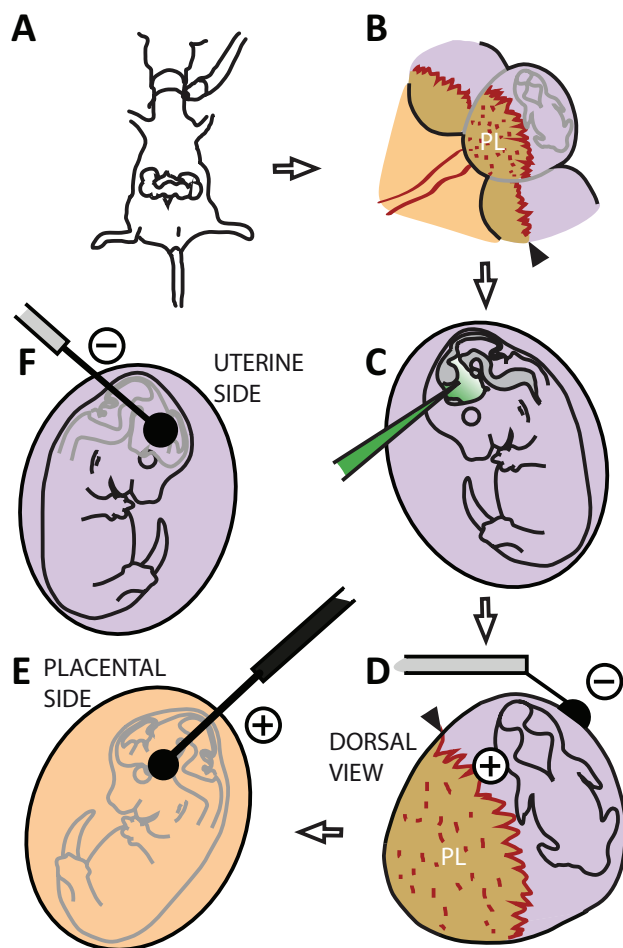
(<http://www.ltk.uzh.ch/de>). Anaesthesia was maintained by isoflurane inhalation via an anaesthetic machine with a face mask.

The next step was to open the abdomen, take and hold the uterus with a forceps. After visualizing the ventricle system of the embryo, one injected the plasmid DNA into the lateral or third ventricle of the embryo. The correct injection could be controlled by the distribution of the green dyed DNA.

To transfer the injected DNA into the neuroepithelial cells of the central nervous system one needed to generate an electric field. The electroporation took place after injecting the embryos by using tweezer electrodes. Thereby, the positive pole of the electrode was placed on the area, that should be targeted, whereas the negative electrode was placed somewhere on the opposite site of the embryo.

The given pulse was the following:
50 Volt/ 50 msec(on)/ 950 msec(off)/ 5 pulse.

After the electroporation, the uterus was placed back as accurately as possible into the peritoneal cavity as it had been situated before. To finish the surgery, first the muscle layer and then the skin were sewed with absorbing yarn and a strong analgesic (Metamizol) was injected into the peritoneal cavity. The whole procedure is depicted in the scheme in Figure 8.



modified from Haddad-Tovolli, R et al 2013

Figure 8 Scheme of *in utero* electroporation procedure

2.10.5 ANALYSIS

Analysis group 1: The mice were injected with EdU (100 mg/1 kg bodyweight) one day after the *in utero* electroporation at E13.5. Two days after the surgery at E14.5 the mice were injected with the base analogue BrdU (100 mg/kg bodyweight) two hours before they were sacrificed.

Analysis group 2/3: Since the pregnant mice in this analysis groups directly ate or expelled the newborn pups, no examination of changes in the cortical development of transfected mice was possible at postnatal stages.

The brains of the embryos were fixed with 4 % PFA for 2-4 h at 4°C. After incubating the brains first in 15 % sucrose and then in 30 % sucrose solution overnight at 4°C, the brains were frozen and cut using a cryostat for the following immunohistochemical stainings (see 2.6.1 and 2.6.2).

Figure 9 shows the classification criteria for further analysis of the *in utero* electroporation data. It was distinguished between cortex electroporated and not electroporated as well as midline electroporated and not electroporated. In addition to the total analysis of the whole hemispheres, the analysis was divided along the rostrocaudal axis. The criteria to split into either rostral or caudal slices are shown in Figure 9 B, where the appearance of the ganglionic eminence was important.

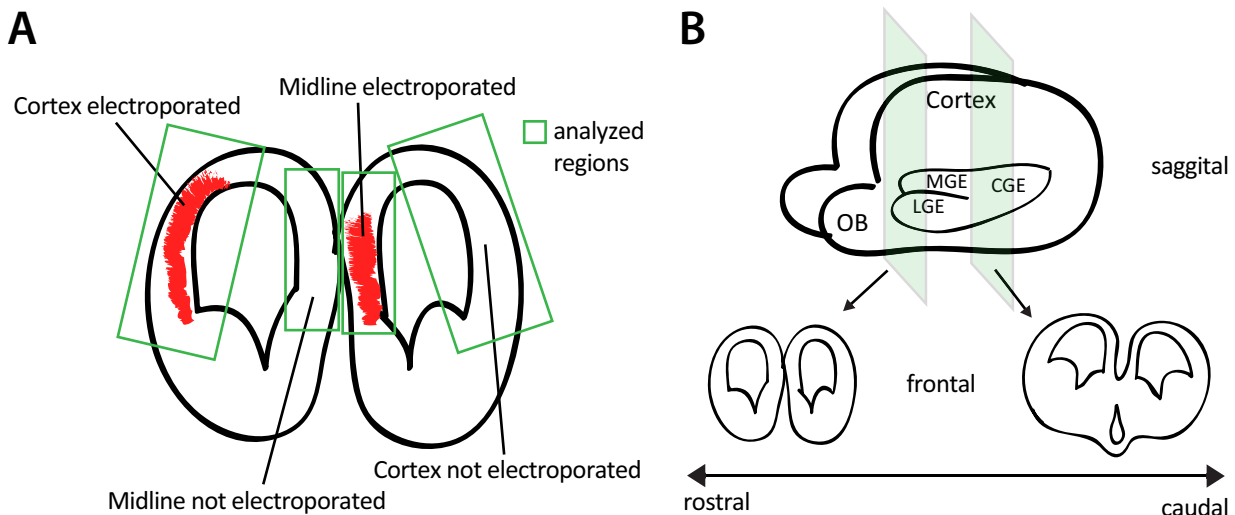


Figure 9 Scheme for the analysis of the *in utero* electroporation data

A: Schematic frontal view of an *in utero* electroporated mouse brain E 14.5. Areas in red are the target areas for electroporation. Areas included in the analysis are marked with green rectangles. **B:** Schematic overview for the classification of the slices into rostral and caudal by the appearance of the ganglionic eminence. The green areas are cross sections through the brain and are shown in frontal below with the according ganglionic eminence appearance. OB=olfactory bulb, MGE=medial ganglionic eminence, LGE=lateral ganglionic eminence, CGE=caudal ganglionic eminence.

2.11 UST CONDITIONAL KNOCKOUT MOUSE STRATEGY

2.11.1 ISOLATION OF GENOMIC DNA FROM MOUSE TAILS

For isolation of genomic DNA, the tips of mouse tails were cut and incubated in 500 μ l lysis buffer (tail buffer + proteinase K [50 μ g/ml]) overnight at 55°C, 400 rpm in an Eppendorf Thermomixer. The next day, 500 μ l Isopropanol were added and the tube was inverted to mix thoroughly. For 30 min the mixture was cooled down to -80°C and then centrifuged at full speed (16.000 x g) at 4°C for 30 min. The supernatant was carefully removed and the pellet

washed with 300 μ l 70 % EtOH. The tube was centrifuged again for 15 min with full speed at 4°C and the supernatant carefully removed. The pellet was air-dried at RT and was resuspended in 60-80 μ l of 10 mM TrisHCl pH 8,0. To resolve the pellet, the tube was incubated overnight at 55°C and 400 rpm in the Thermomixer. The isolated genomic DNA was stored at -20°C.

2.11.2 GENOTYPING OF UST MUTANT MICE

The conditions for genotyping of Ust mutant mice were established with genomic DNA of embryonic stem cells (ESCs) kindly provided by Simone Reimer (AG Müller, University of Heidelberg). Therefore 20 ng of genomic DNA were used as template for genotyping PCR and for cloning the knockout plasmid inserts. The different primer combinations and sizes are shown in Figure 10 and the following table.

2.11.3 STRATEGY

Ust is encoded by an enormously large gene with a size of about 314.000 kb (Figure 10). The first line in the figure shows the whole gene with its 8 exons and very large introns in between. In the second line the introns are shortened for a better visualization of the Ust exons. The complete deletion of the Ust gene is because of the enormous size not feasible. Besides being the start of transcription, exon 1 is encoding the transmembrane region (red rectangle), which is naturally localized to the Golgi apparatus cisterns. Exon 3 and exon 5 contain the catalytic domain (blue circle) and the binding sites for the sulfate donor PAPS (yellow rectangle). So far, no splice variants of Ust are known. Hence, the deletion of the first exon should be sufficient to stop the transcription of Ust. Even for the case there would be a splice variant of Ust, the deletion of the first exon abolishes the transmembrane region of the protein, thereby no localization to its normal occurrence in the Golgi apparatus could take place. The knockout of exon 3 or exon 5 might produce a truncated protein variant, which would still be localized to the Golgi apparatus with an unknown effect on sulfation. For this reason I designed a knockout strategy to conditionally delete the first exon of Ust as depicted in the following figure (Figure 10).

To generate the targeting plasmid I used the pEasyflox plasmid, which was kindly provided by AG Ulrike Müller in Heidelberg. For the integration of the floxed exon into the genomic DNA via homolog recombination, two recombination arms are necessary. One arm is flanking the first exon at the 5'end (5'arm: 1,7 kb) and the other arm at the 3'end (3'arm: 4,4 kb). These recombination arms flank the KO element (2 kb), which is composed of the first exon, the beginning of the first intron and about 600 bp upstream of the first exon to include possible promoter regions. The correct homolog recombination can be controlled by positive selection (neomycin resistance) as well as by negative selection (HSV-TK=herpes simplex virus-thymidine kinase). The selected clones can be further analysed by genotyping PCR and/or southern blotting (probe) with the respective fragment sizes listed in the table underneath the figure and the corresponding primers (2.8 Oligonucleotide Primers). In the correctly targeted locus the neomycin cassette will be removed by Cre recombination. This can also be screened by PCR and reveals the correct recombination events. The finally selected, correct ESC clone (Ustflox) can be used for the injection into the blastocyst to generate the future Ust conditional KO mouse line.

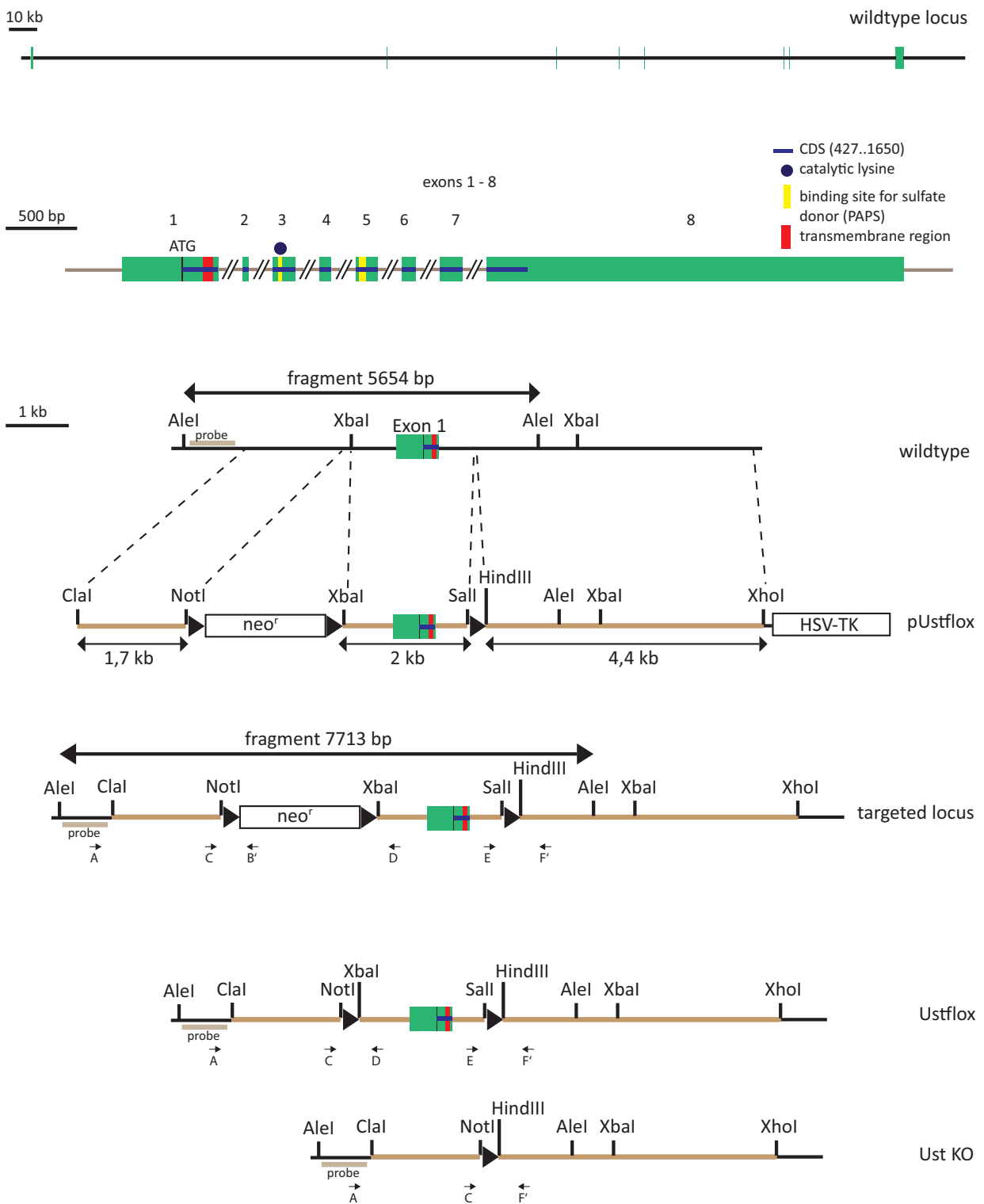


Figure 10 Strategy for conditional Ust knockout mouse line

Fragment size (bp)				
	WT	targeted	Ustflox	Ust KO
AB'	--	1934	--	--
AD	1946	3941	1950	--
CB'	--	207	--	--
CD	219	2214	223	--
CF'	2282	4341	2350	318
EF'	437	501	501	--

2.12 IMAGE ACQUISITION AND STATISTICAL ANALYSIS

2.12.1 IMAGEJ (FIJI) AND ADOBE PHOTOSHOP

In vitro experiments:

- Quantification of immunopositive cells was performed with the ImageJ Cell Counter by counting 4 images per experiment for each condition.
- Quantification of band intensity of western blots or PCRs was performed by using the ImageJ software (Analyze->Gels->Select/Plot Lanes). Therefore, equally sized rectangles (Rectangular Selection Tool; Select First/Next Lane) were set to surround the bands to measure, afterwards plotted and then the area of the peak was destined with the Wand (tracing) Tool. All values were normalized to actin or α -tubulin.

IUE experiments:

- Thickness measurements for the ventricular zone and the cortical plate were performed with ImageJ (Fiji). Therefore 5 different measurements were made per cortex or midline for each image and then the average was calculated. Besides, the different slices of one hemisphere were grouped to 1 n.
- The overview pictures were stitched together with Adobe Photoshop (File->Scripts->Load Files into Stack...).

2.12.2 ILASTIK

Ilastik: Interactive Learning and Segmentation Toolkit (Kreshuk et al., 2011)

The quantification of the different immunohistochemically detected cell amounts of the IUE slices was performed with the Ilastik software version 1.1.5 (www.ilastik.org). Therefore, for each staining a teach file was generated, within which the program was taught how to distinguish background from signal. After this training was successfully accomplished, the images were loaded into the program and the total cell density per image was obtained. All obtained values were normalized to the corresponding total cell amount (Hoechst).

2.12.3 STATISTICAL ANALYSIS

The statistical analysis was done with GraphPad Prism 5 by using the appropriate statistical test as mentioned in the corresponding figure legend (either t-test or 1way ANOVA and Bonferroni's Multiple Comparison Test). 1way ANOVA or one sample t-test were used for statistical analysis of normalized data. In each case at least 3 independent experiments had been performed, otherwise it is indicated in the figure or the legend. All data are expressed as mean \pm SD and the p-value is given as the following: *P < 0,05; **P < 0,01; ***P < 0,001.

3 RESULTS

3.1 CHONDROITINSULFOTRANSFERASE UST OVEREXPRESSION AND ITS FUNCTIONALITY

The chondroitinsulfotransferase (Chst) Ust (uronyl-2-sulfotransferase) belongs to a group of enzymes that determines the sulfation pattern of chondroitin and dermatan sulfates (CS/DS) in the extracellular matrix (ECM). These sulfation-modifying enzymes are endogenously localized in the Golgi apparatus, where they transfer sulfate groups to the sugar chains of proteoglycans (Kobayashi et al., 1999, Kusche-Gullberg, 2003). The functional principle and the influence of the sulfation pattern on cells and their behaviour are not well understood yet. To get a better insight into the effect of the sulfation pattern on cell-behaviour, I investigated the influence of Ust overexpression on neural stem cell (NSC) behaviour *in vitro* and *in vivo*. For this purpose I generated in our research group several constructs to induce a forced expression of Ust and thereby modify the sulfation rate of CS-glycosaminoglycans (GAGs).

3.1.1 OVEREXPRESSION AND FUNCTIONALITY OF UST *IN VITRO*

For the analysis of Ust overexpression, two different types of constructs were used. One type induces the expression of a functional wild type protein of Ust. The other construct generates a mutated version of Ust (Ust mut). Ust mut's catalytically active domain is mutated and not able to transfer sulfate groups to the glycosaminoglycan (GAG) chains anymore. Two different types of plasmids were used to insert the coding DNA sequence (CDS) of Ust: pEGFP N1 (N1) and pXL201-3xFLAG (XL). N1 Ust and N1 Ust mut were cloned as fusion proteins with EGFP and for this reason the EGFP signal is localized in the Golgi apparatus. The empty vectors (N1 or XL) served as controls, whereas Ust mut was used as a negative control to see whether the effects of Ust overexpression originate from a clogged Golgi apparatus or from the modified sulfation pattern. The localization of the EGFP signals after overexpressing the different constructs is exemplarily depicted in Figure 11. Panel A displays transfected NSCs 3 d after differentiation and panel B frontal sections of E14.5 mouse brains 2 d after *in utero* electroporation. Figure 11 A shows representative images of transfected NSCs after an immunocytochemical staining against the oligodendrocyte precursor cell marker O4. The EGFP signal of the N1 plasmid is cytoplasmatic in the control situation (N1), while the dotted GFP staining close to the nucleus indicates the localization of the Ust and Ust mut fusion proteins in the Golgi apparatus. As it is shown in the upper part of Figure 11 C, EGFP is the fluorescent protein of the N1 plasmid, whereas the XL plasmid contains tdTomato as fluorescent marker (lower part of Figure 11 C). tdTomato is localized in the cytoplasm for the empty vector (XL) as well as for Ust (XL Ust) (lower panel of Figure 11 A and in B), because of an inserted internal ribosome entry site (IRES) in the vector (Figure 11 C). XL Ust also exhibits a dotted EGFP signal in the Golgi apparatus, because the Ust-EGFP fusion protein of the N1 plasmid was subcloned into the XL plasmid (Figure 11 A, C). The EGFP signal of the fusion proteins from the N1-based constructs was poorly visible in the *in vivo* experiments. In the end, the constructs based on N1 were only used for the *in vitro* analysis, whereas the XL-based constructs were used for *in vitro* and *in vivo* experiments to have a better overview of the electroporated areas. For the successive analysis steps of the *in vivo* experiments, the poorly visible EGFP signal of XL Ust was neglected to gain an additional colour channel for expanded staining opportunities.

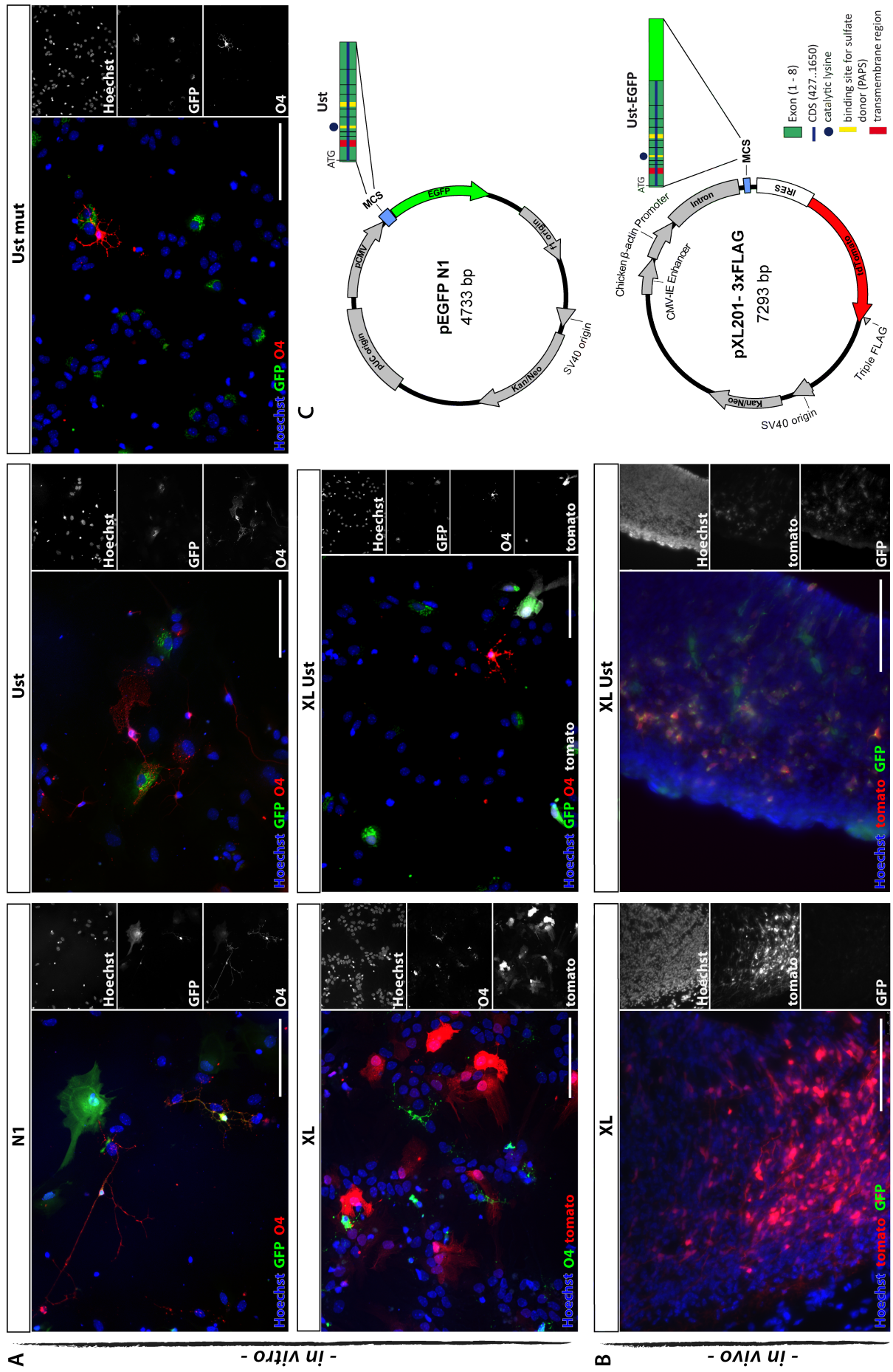
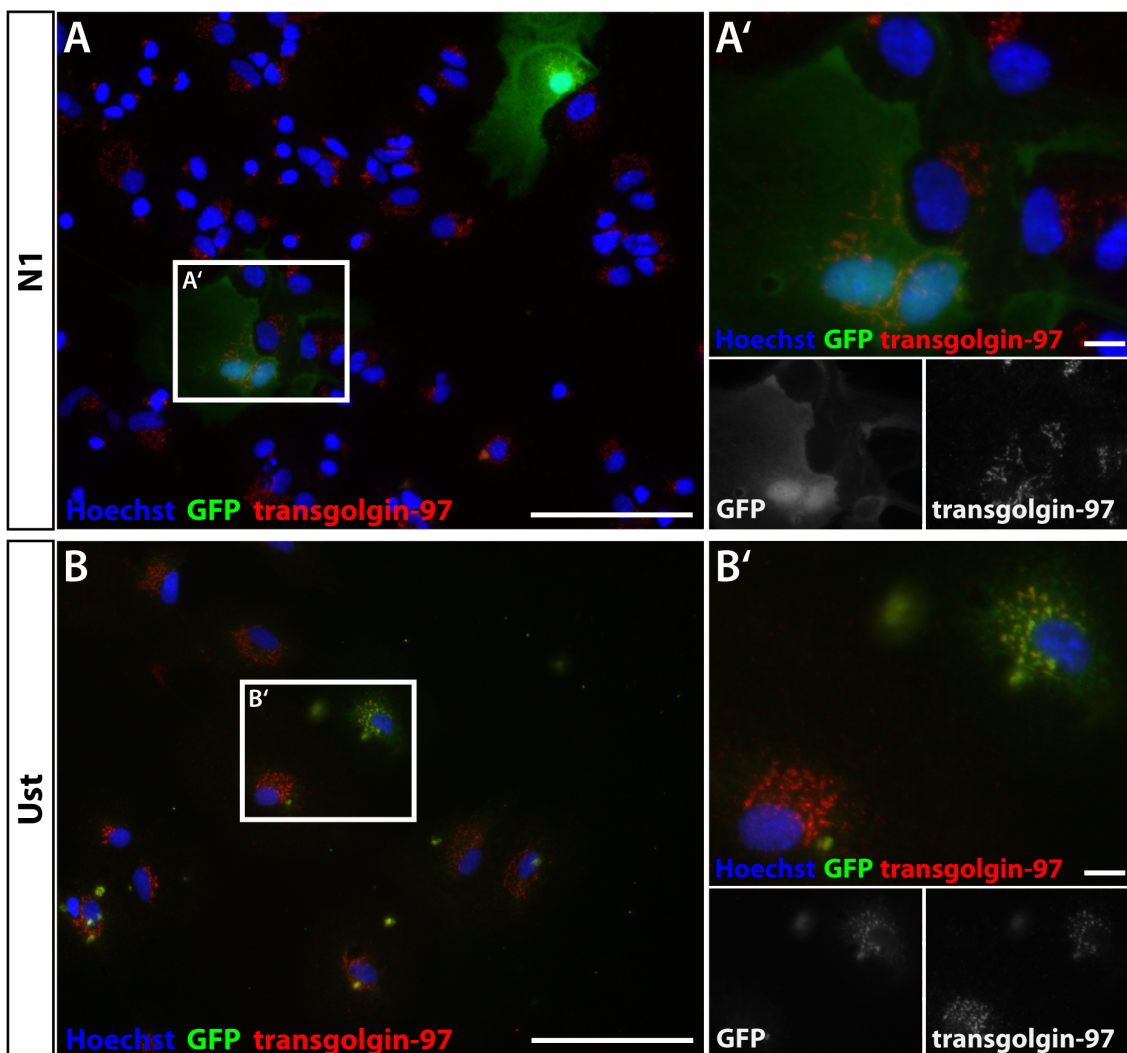


Figure 11 Expression of different Ust constructs *in vitro* and *in vivo* (see description on next page)

Figure 11 Expression of different Ust constructs *in vitro* and *in vivo*

A: Immunocytochemical stainings for oligodendrocyte precursor cells ($O4^+$) and GFP. For *in vitro* experiments pEGFP N1 and pXL constructs were used. The images display the intracellular distribution of the EGFP signal in neural stem cells 3 d after their transfection with the denoted constructs. EGFP of the control plasmid N1 and tdTomato of the XL constructs are cytoplasmically localized. Ust and Ust mut plasmids express a fusion protein, which is localized in the Golgi apparatus. Ust mut functions as negative control, which is not functional because of a mutated catalytic domain. **B:** Immunohistochemical staining for GFP. *In vivo* experiments were performed with the XL plasmid constructs. XL control only has a tdTomato signal, whereas XL Ust also exhibits the Ust-EGFP fusion protein. **C:** Plasmid maps of the used constructs are depicted. Scale bar = 100 μm .

**Figure 12 Localization of Ust-EGFP fusion protein in the Golgi apparatus**

A + B: Immunocytochemical staining for transgolgin-97 and GFP of transfected NSCs after 3 d of differentiation. **A:** The EGFP in the control plasmid N1 is cytoplasmically localized and thus does not co-localize with the Golgi apparatus as shown in the inset in **A'**. **B:** The Ust-EGFP fusion proteins are localized in the Golgi apparatus which is identified by the co-localization with the Golgi marker transgolgin-97 in the inset **B'**. A + B scale bar = 100 μm , A' + B' scale bar = 10 μm .

The correct targeting of the fusion protein to the Golgi apparatus was confirmed by a transgolgin-97 co-localization staining that is exemplarily shown for N1 and Ust in Figure 12. In

the control (N1), no co-localization with the Golgi marker transgolgin-97 is visible because of the cytoplasmatic distribution of the GFP signal (Figure 12 A). Whereas Ust shows a co-localized signal with transgolgin-97 in the Golgi apparatus of the transfected cells (Figure 12 B).

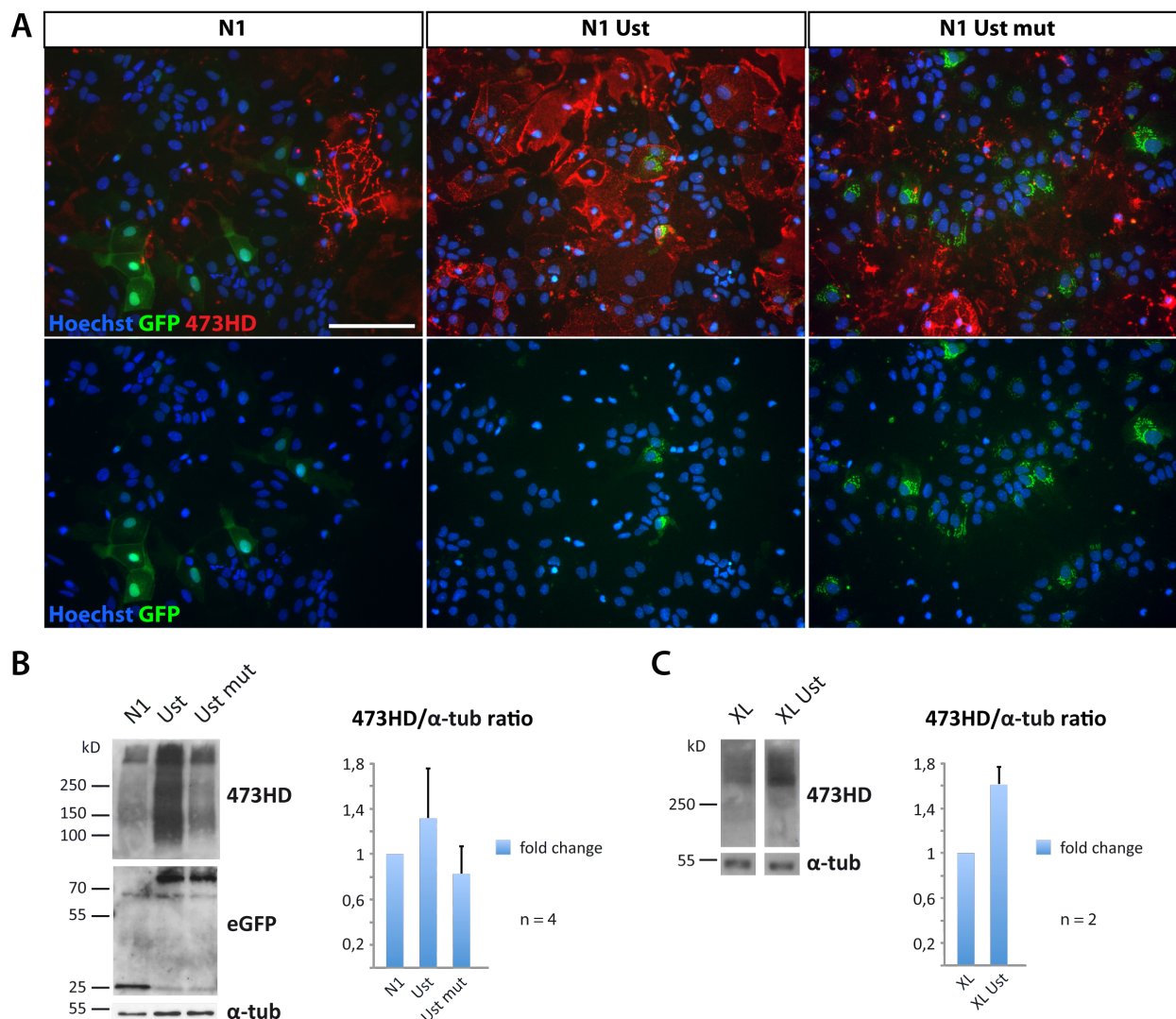


Figure 13 Modifying the sulfation pattern by Ust overexpression *in vitro*

A: Immunocytochemical staining for 473HD and GFP of transfected NSCs after 3 d of differentiation. The GFP signal is located in the Golgi apparatus for Ust and Ust mut. N1 shows a cytoplasmatic GFP signal. The overexpression of Ust leads to an increase in 473HD reactivity, which is an antibody that recognizes a specific sequence of sulfated CS-GAGs, including the D-unit. The overexpression of the mutated version of Ust shows that the 473HD reactivity is not altered in comparison to the control. Scale bar = 100 μm. **B/C:** The increased CS-GAGs' sulfation upon forced Ust-EGFP expression was detected by western blot analysis. Blots and corresponding quantifications are shown. Data are expressed as mean values ± SD, statistics were performed by 1way ANOVA (N1 constructs) or one sample t-test (XL constructs) with the data normalized to the control (N1 or XL).

The directed modification of the sulfation pattern by Ust overexpression was confirmed by CS-GAG epitope detection. The overexpression of Ust led to an increase in 473HD reactivity, which recognizes a specific sequence of sulfated CS-GAGs, including the D-unit. The D-unit is a sulfated CS-unit that is generated by the enzymatic activity of Ust and the 473HD antibody can

therefore be used as readout of Ust functionality and for a quantitative readout. Figure 13 exemplarily shows the directed modification of the sulfation pattern by overexpression of Ust in panel A. It displays an immunocytochemical staining of transfected NSCs after 3 d of differentiation with the N1 based constructs. The 473HD reactivity was strongly increased after Ust overexpression in comparison to the control N1 and Ust mut. The quantification of construct functionality revealed a 1,4-fold for N1 Ust (Figure 13 B) and a 1,6-fold for XL Ust (Figure 13 C) higher 473HD reactivity in comparison to the control (N1 or XL). This was determined by 473HD western blot analysis. The 473HD reactivity was normalized to the expression of the housekeeping gene α -tubulin (α -tub). Additionally, the GFP signal could be detected in the western blot analysis for N1 (25 kD) and the fusion proteins (47 kD + 25 kD) (Figure 13 B).

3.1.2 OVEREXPRESSION AND FUNCTIONALITY OF UST *IN VIVO*

The functionality of the used constructs was also analysed after *in utero* electroporation. Figure 14 shows frontal overviews of *in utero* electroporated brain sections (E14.5) of XL (A) and Ust (B) 2 d after electroporation. The boxed areas are shown at higher magnifications in A', A'', B' and B''. The tdTomato signal can be seen in the cortex (A' and B') and the midline (A'' and B''), whereas the 473HD signal was just weakly visible. But in comparison to the control, the 473HD signal was slightly more visible in the electroporated midline area after Ust overexpression (Figure 14 B''). However, the altered 473HD expression *in vivo* was not as conclusive as obtained in the *in vitro* experiments and was therefore neglected for a quantitative analysis. There was no obvious local increase of the 473HD signal, where transfected cells overexpressed Ust. The endogenous 473HD expression in the control seemed to be predominantly in the pial basal membrane, distributed generally in the ganglionic eminence, cortex and in the midline, although the signal appeared less dominant in the cortical plate. The tdTomato signal in the cortex was mainly localized in the growing cortical plate and to a lesser extent in the adjacent intermediate zone 2 d after *in utero* electroporation, whereas in the ventricular zone almost no transfected cells resided. In the electroporated midlines was the tdTomato signal localized closer to the cortical surface than to the ventricular cavity and the transfected cells exhibit a rather neuronal-like morphology. Anyway, the tdTomato signal intensity was more prominent in the control situation than after Ust overexpression.

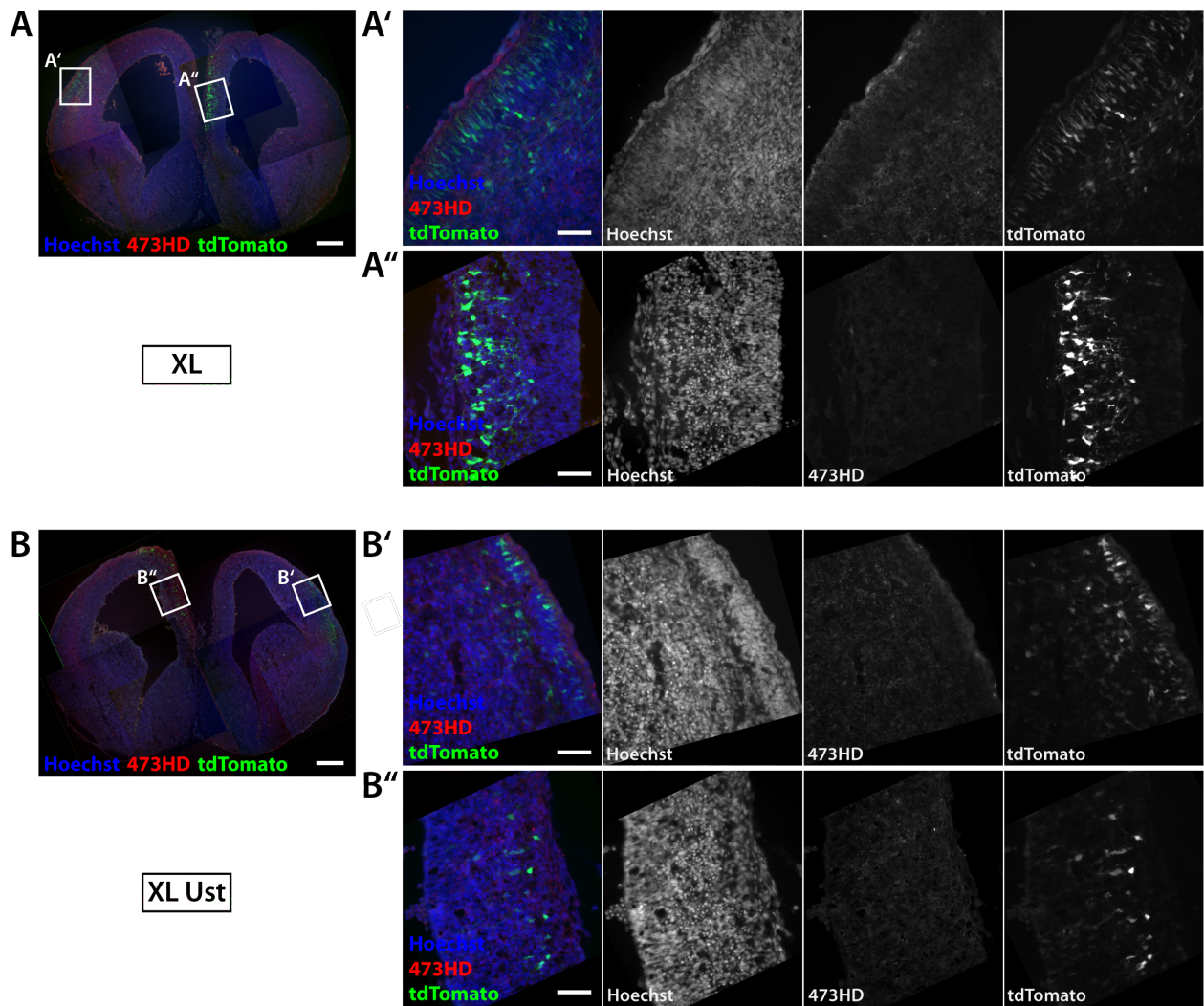


Figure 14 Modifying the sulfation pattern by Ust overexpression *in vivo*

A + B: Immunohistochemical staining for 473HD of E14.5 mouse frontal sections 2 d after electroporation. **A:** The electroporation with the control plasmid XL shows tdTomato signal in the cortex and the midline. The boxed areas show higher magnifications of the cortex (**A'**) and the midline (**A''**). 473HD immunoreactivity is poorly visible in both areas. **B:** After electroporation with Ust, tdTomato signal can be seen in the expected areas, cortex (**B'**) and midline (**B''**). The overexpression of Ust might slightly increase 473HD reactivity, most visible in the area of the midline (**B''**). A, B scale bar = 250 μm , A', A'', B', B'' scale bar = 50 μm .

3.2 MODIFICATION OF THE SULFATION PATTERN OF NEURAL STEM CELLS *IN VITRO*

3.2.1 IMPACT OF UST OVEREXPRESSION ON NSC DIFFERENTIATION

For the analysis of the impact of the modified sulfation pattern on NSC differentiation a differentiation assay was performed. The timeline of the differentiation assay is shown in Figure 15 A. NSCs were obtained from mouse cortices at E13.5 and cultivated until the 3rd passage. The neurosphere-derived NSCs were electroporated with the corresponding construct and after one day of recovery cultured under differentiating conditions for 3 d. The subsequent immunocytochemical staining revealed the differentiation into distinct NSC-derived cell types. Figure 15 B shows exemplarily the differentiation of NSCs into oligodendrocyte precursor cells (O4⁺) and neurons (β III-tubulin⁺), which were electroporated with N1-based constructs, and the respective quantification of N1 and also of the XL experiments (Figure 15 C). Figure 16 gives an insight into the amount of astrocytes (GFAP⁺) and progenitor cells (Nestin⁺) present in the transfected cell cultures. Ust overexpression induced a significantly reduced differentiation into oligodendrocytes (N1 = 1, Ust = $0,53 \pm 0,06$, Ust mut = $0,78 \pm 0,31$; n = 4) and a significant increase in the generation of neurons compared to the controls (N1 = 1, Ust = $1,27 \pm 0,18$, Ust mut = $1,06 \pm 0,09$; n = 4) (Figure 15 C). The XL construct experiments exhibited the same trends regarding the decreased differentiation into oligodendrocytes (XL = 1, Ust = $0,93 \pm 0,79$; n = 4) and the increased neurogenesis (XL = 1, Ust = $1,34 \pm 0,44$; n = 4). For the generation of astrocytes and neural progenitors no difference could be observed after modifying the sulfation pattern by overexpressing Ust (Figure 16).

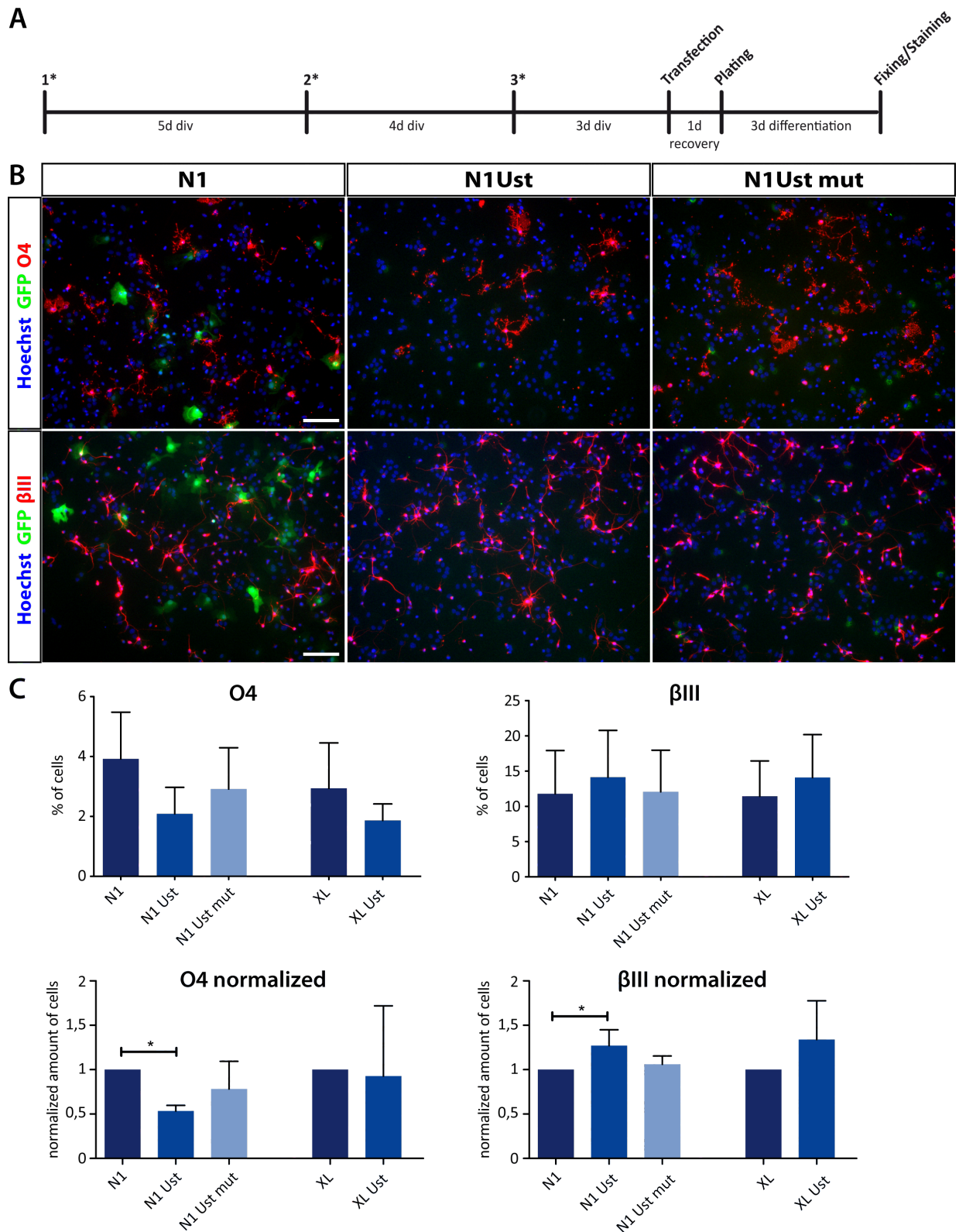


Figure 15 Impact of a modified sulfation pattern upon Ust overexpression on mouse neural stem cell differentiation: O4 and β III-tubulin

A: Experimental timeline of the differentiation assay. **B:** Transfected NSCs are shown after 3 d of differentiation as exemplarily shown for the N1 constructs. The cells were stained with cell type-specific antibodies against O4 (oligodendrocyte precursor cells) and β III-tubulin (neurons). The GFP signal is located in the Golgi apparatus for Ust and Ust mut. N1 shows a cytoplasmatic expression of GFP. Scale bar = 100 μ m. **C:** Quantification of the different cell types. Data are expressed as (normalized) mean

values \pm SD, statistics were performed by 1way ANOVA, (N1 constructs) or t-test/one sample t-test (XL constructs) with * $p \leq 0,05$ and ** $p \leq 0,01$, $n = 4$.

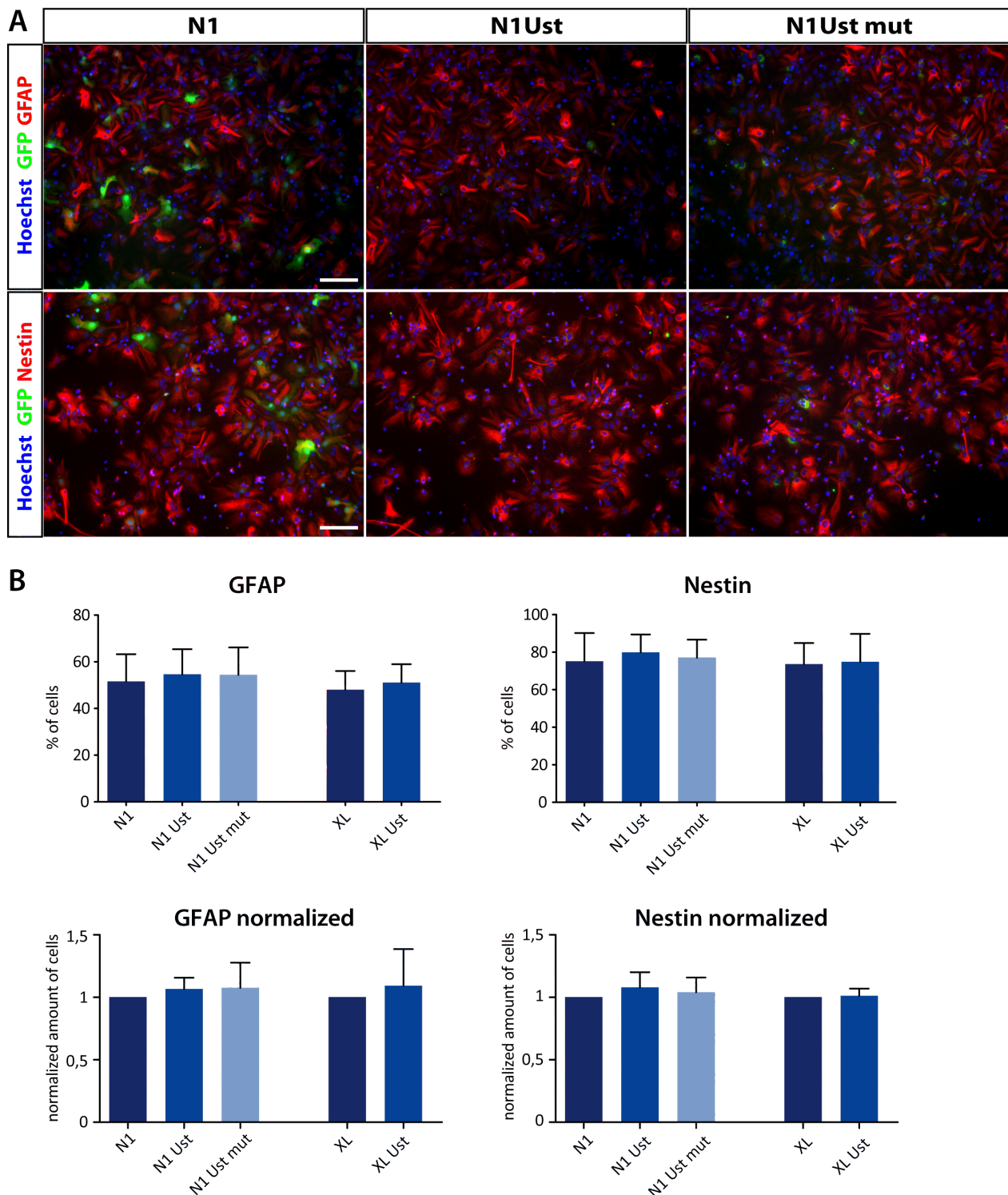


Figure 16 Impact of a modified sulfation pattern upon Ust overexpression on mouse neural stem cell differentiation: GFAP and Nestin

A: Transfected NSCs are shown after 3 d of differentiation as exemplarily shown for the N1 constructs. The cells were stained with cell type-specific antibodies against GFAP (astrocytes) and Nestin (neural progenitors). The GFP signal is located in the Golgi apparatus for Ust and Ust mut. N1 shows a cytoplasmic GFP signal. Scale bar = 100 μ m. **B:** Quantification of the different cell types. Data are

expressed as (normalized) mean values \pm SD, statistics were performed by 1way ANOVA (N1 constructs, $n = 4$) or t-test/one sample t-test (XL constructs, $n = 4$).

3.2.2 IMPACT OF UST OVEREXPRESSION ON NSC SELF-RENEWAL AND PROLIFERATION

To assess the NSC proliferation capacities after modifying the sulfation pattern I performed several experiments. At first, the transfected NSCs were pulsed with EdU for 2-3 h after plating to check, whether there is a change in EdU incorporation. Afterwards, the cells that incorporated EdU were counted (Figure 17). The statistical analysis revealed, that there was no significant difference in the number of EdU⁺, proliferating NSCs upon Ust overexpression, in comparison to the control situations. These results are in agreement with the data obtained from the differentiation assay, where no significant change in the number of neural progenitor cells (Nestin⁺) was reported. The additional control Ust mut exhibited, that the obtained effects were specifically due to the modified sulfation pattern upon Ust overexpression and not caused by clogging the Golgi apparatus with a mass of overexpressed fusion proteins. Therefore, Ust mut was not further included in the subsequent analysis procedures.

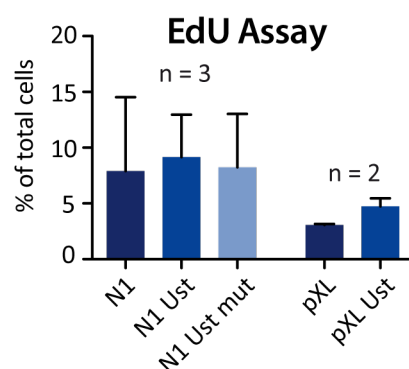


Figure 17 Proliferation of neural stem cells after Ust overexpression

The EdU proliferation assay was performed by giving an EdU pulse 2-3 h before fixing the cells. The quantification shows no significant difference between control and Ust overexpression. Data are expressed as mean values \pm SD, statistics were performed by 1way ANOVA (N1 constructs) or t-test (XL constructs).

Subsequently, NSC self-renewal capacity was analysed by clonal density assay experiments. Figure 18 A depicts the timeline of the clonal density assay. The experimental timeline of the clonal density assay is the same procedure as the differentiation assay until the electroporation, followed by 1 d recovery. Then, for the proliferation assay the cells are plated under proliferative conditions for 7 d with the listed growth factors (Figure 18 B). There was no significant change in the responsiveness to the added growth factors, although there might be a trend towards a higher responsiveness to FGF 2 and heparin after Ust overexpression (N1 = $6,9 \pm 3,2$ %, $n = 4$; Ust = $9,5 \pm 2,6$ %, $n = 2$). Besides, a very small but significant increase for the generation of nsphs without supplemented growth factors could be observed, whether this represents a biological relevance needs to be discussed.

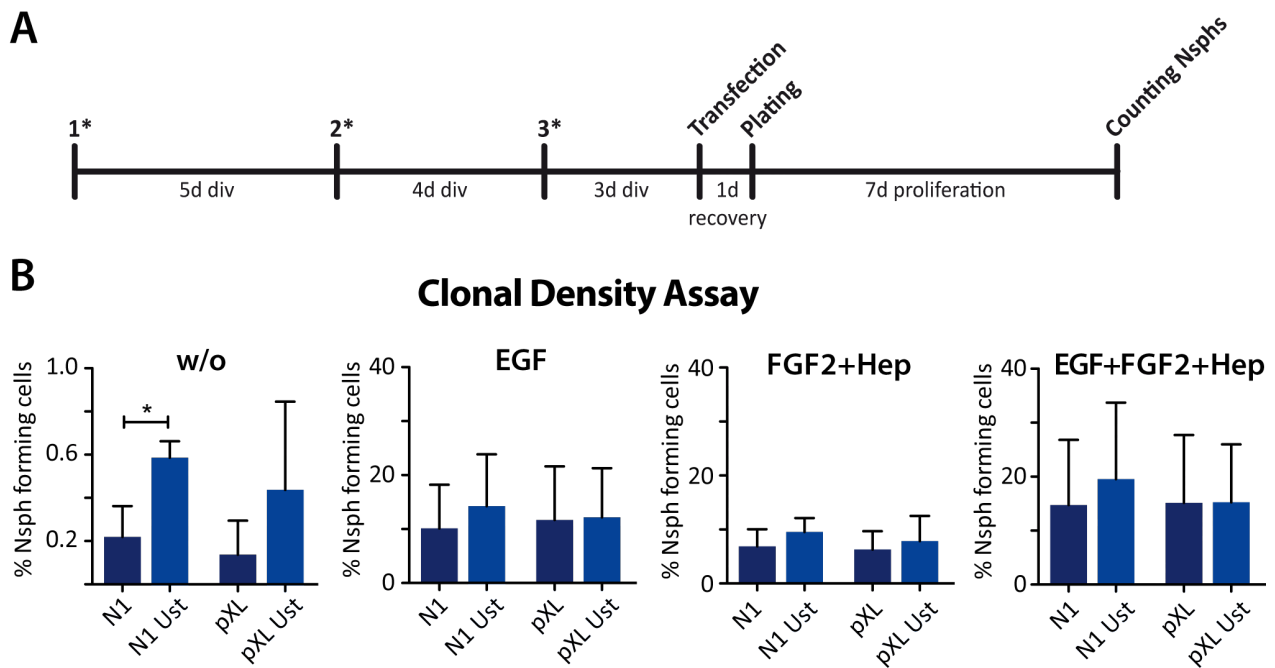


Figure 18 Self-renewal of neural stem cells after Ust overexpression

A: Experimental timeline of the clonal density assay (CDA). **B:** For the CDA transfected cells were plated and cultured under proliferating conditions with the listed growth factors (EGF, FGF 2, Hep = heparin) at a concentration of 2 ng/ml for 7 d. No difference was observed for the distinct conditions. Data are expressed as mean values \pm SD, statistics were performed by t-test (N1 constructs, N1 n = 4, Ust n = 2; XL constructs, n = 4).

3.3 MODIFICATION OF THE SULFATION PATTERN BY *IN UTERO* ELECTROPORATION *IN VIVO*

3.3.1 IMPACT OF UST OVEREXPRESSION ON CORTICAL PLATE AND VENTRICULAR ZONE DEVELOPMENT *IN VIVO*

To confirm the promising *in vitro* results I pursued the idea of an Ust overexpression *in vivo* analysis. The effect of Ust overexpression on *in vivo* cortical development was investigated by *in utero* electroporation of the Ust construct into the embryonic cortex and the analysis of the influence of the subsequently modified sulfation pattern on the anatomy of the developing cortex and its neuronal and NSC numbers. The *in utero* electroporation was analysed 2 d after the procedure. Figure 19 A depicts a schematic drawing of an *in utero* electroporated E14.5 mouse brain. Usually two areas were hit by the electric pulse that was given during the electroporation procedure: the cortex on the one side and the midline in the other hemisphere (red). The thickness of the cortical plate was analysed by measuring the thickness of the region of NeuN⁺-cells from the lateral to the medial side (white lines). For each region, the thickness was measured at 5 different spots in an apical to pial direction and the average was calculated for the cortex and the midline, respectively. In the quantification for the cortex (Figure 19 B) a trend towards a radially thinner cortical plate was revealed for Ust electroporated mice in comparison to the control. The effect was visible for the electroporated side of the cortex as well as for the contralateral non-electroporated side, but it was only significantly different in the more rostral brain (XL = 206,3 ± 27,6 µm, n = 4; Ust = 161,8 ± 22,1 µm, n = 5) (Figure 19 C). Figure 19 D depicts the quantification of the effect on the midline. The same trend towards a shorter cortical plate can be observed after Ust overexpression. This effect was significant in the more caudal brain sections for the electroporated midline (XL = 114,4 ± 12,5 µm, n = 6; Ust = 96,7 ± 12,9 µm, n = 5). At first glance, this effect appears counterintuitive concerning the increased neurogenesis obtained in the differentiation assay and will be further discussed in the following discussion section.

The ventricular zone contains mainly Pax6⁺ radial glia cells during early developmental stages (Martynoga et al., 2012). In order to explore the impact of the altered sulfation pattern upon Ust overexpression on radial glia cell fate, I analysed the thickness of the ventricular zone by measuring the Pax6⁺-cells containing area in the cortex and the midline after *in utero* electroporation. Figure 20 A shows a schematic overview of a frontal section after *in utero* electroporation. The electroporated areas are indicated in red. The measured area for the thickness of the ventricular zone is depicted in Figure 20 B with white lines. Pax6⁺-area was determined similarly to the thickness of the cortical plate. Cortex and midline, each with 5 measurements, were analysed and average values were calculated. The quantification is shown for the cortex in Figure 20 C and for the midline in Figure 20 D. The results do not indicate a change in the thickness of the ventricular zone after Ust overexpression in comparison to the control for the cortex and midline on the electroporated sides as well as on the contralateral sides and were somewhat expected regarding the unmodified proliferation/self-renewal capacities *in vitro*.

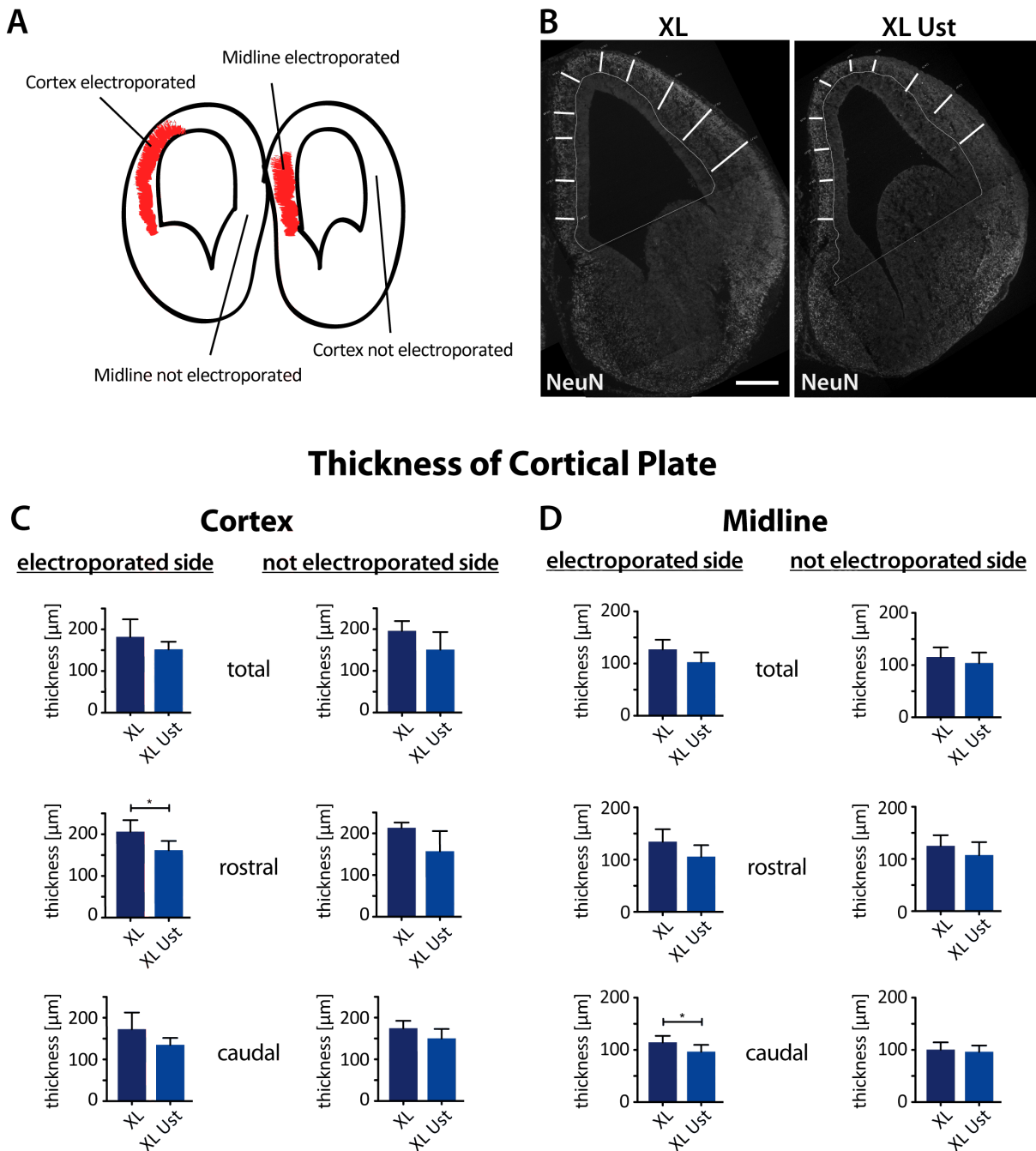
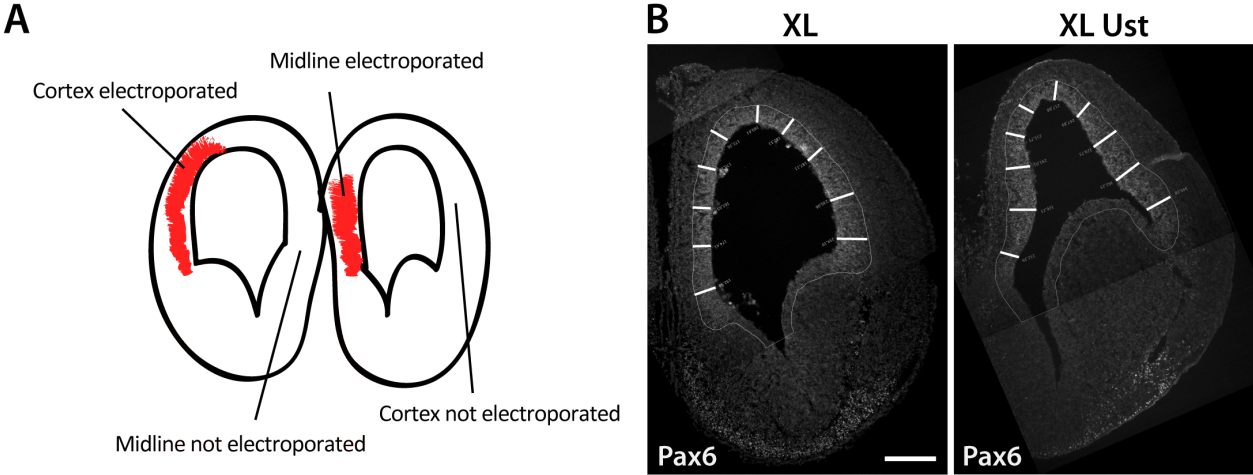


Figure 19 Impact of a modified sulfation pattern after Ust overexpression on the thickness of the cortical plate

A: A schematic frontal view of an *in utero* electroporated mouse brain at E14.5 is shown. Areas in red are the targeted areas of the electroporation. **B:** Frontal view of hemispheres after *in utero* electroporation is depicted. The thickness of the cortical plate (white lines) was calculated as average of 5 for each region, cortex and midline. Afterwards average values were calculated. Different slices of one brain were grouped as one experiment and calculated as total or divided into rostral and caudal regions (see also Figure 9). Scale bar = 250 μm. **C/D:** Quantification of cortical plate thickness in cortex and midline, respectively. Data are expressed as mean values ± SD, statistics were performed by t-test with * $p \leq 0,05$, $n = 4-6$ embryos, 1-6 slices per embryo.



Thickness of Ventricular Zone

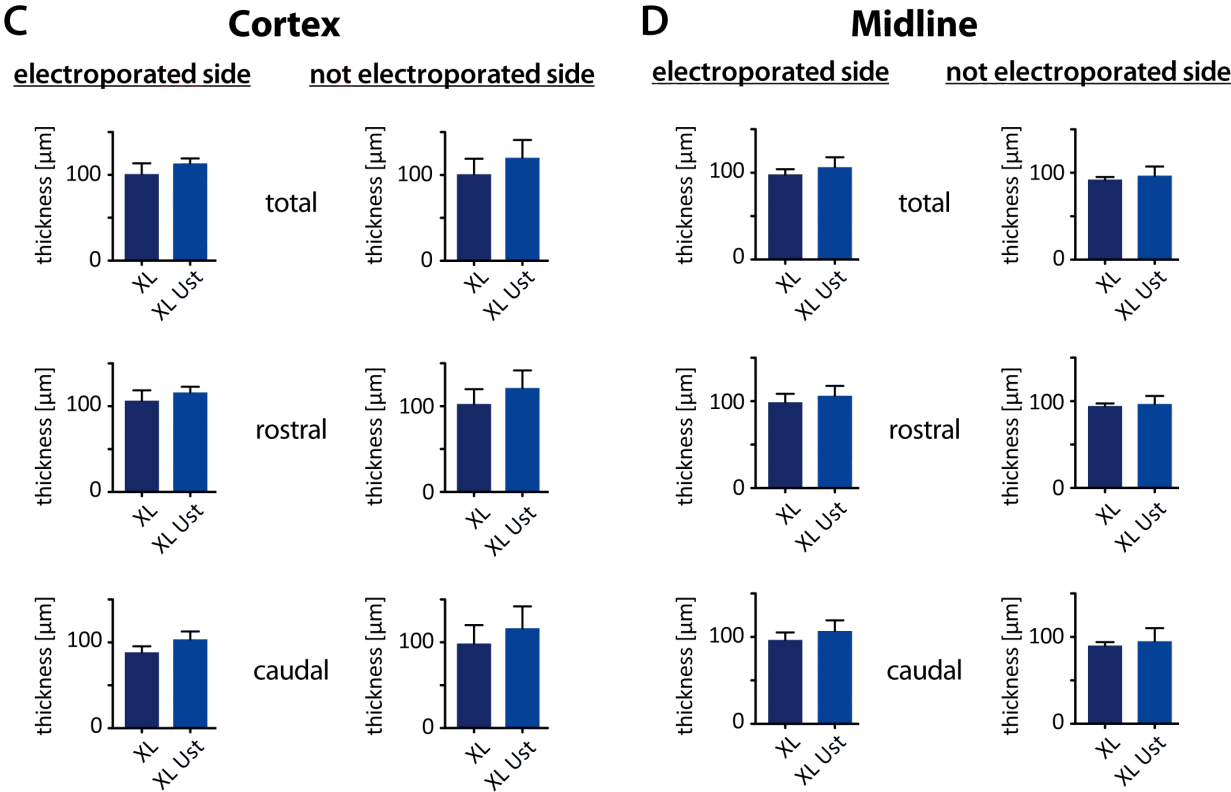


Figure 20 Impact of a modified sulfation pattern after Ust overexpression on the thickness of the ventricular zone

A: A schematic frontal view of an *in utero* electroporated mouse brain (E 14.5) is shown. Areas in red are the targeted areas of the electroporation. **B:** Frontal view of hemispheres after *in utero* electroporation is depicted. The thickness of the ventricular zone was calculated by measuring 5 times for each region, cortex and midline, the thickness of the ventricular zone (white lines). Scale bar = 250 μm. **C/D:** Quantification of ventricular zone thickness in cortex and midline, respectively. Data are expressed as mean values ± SD, statistics were performed by t-test, n = 3-4 embryos, 5-6 slices per embryo.

3.3.2 IMPACT OF UST OVEREXPRESSION ON PROLIFERATION *IN VIVO*

To explore whether altered proliferation was the cause of the reduced cortical plate thickness, proliferation was analysed by using the EdU-incorporating method *in vivo*. The *in vitro* results showed no significant effect on the numbers of proliferating, EdU-incorporating cells after Ust overexpression (Figure 17 D). EdU was injected 1 d before sacrificing the mice and its incorporation was analysed afterwards (Figure 21). The immunohistochemical staining was quantified (Figure 21 C). As expected, there was no significant difference between the two experimental conditions. Thus, proliferation did not induce the reduced cortical plate thickness. Additionally, proliferative capacity was not influenced by the modification of the sulfation pattern upon Ust overexpression and *in vitro* proliferation data was confirmed.

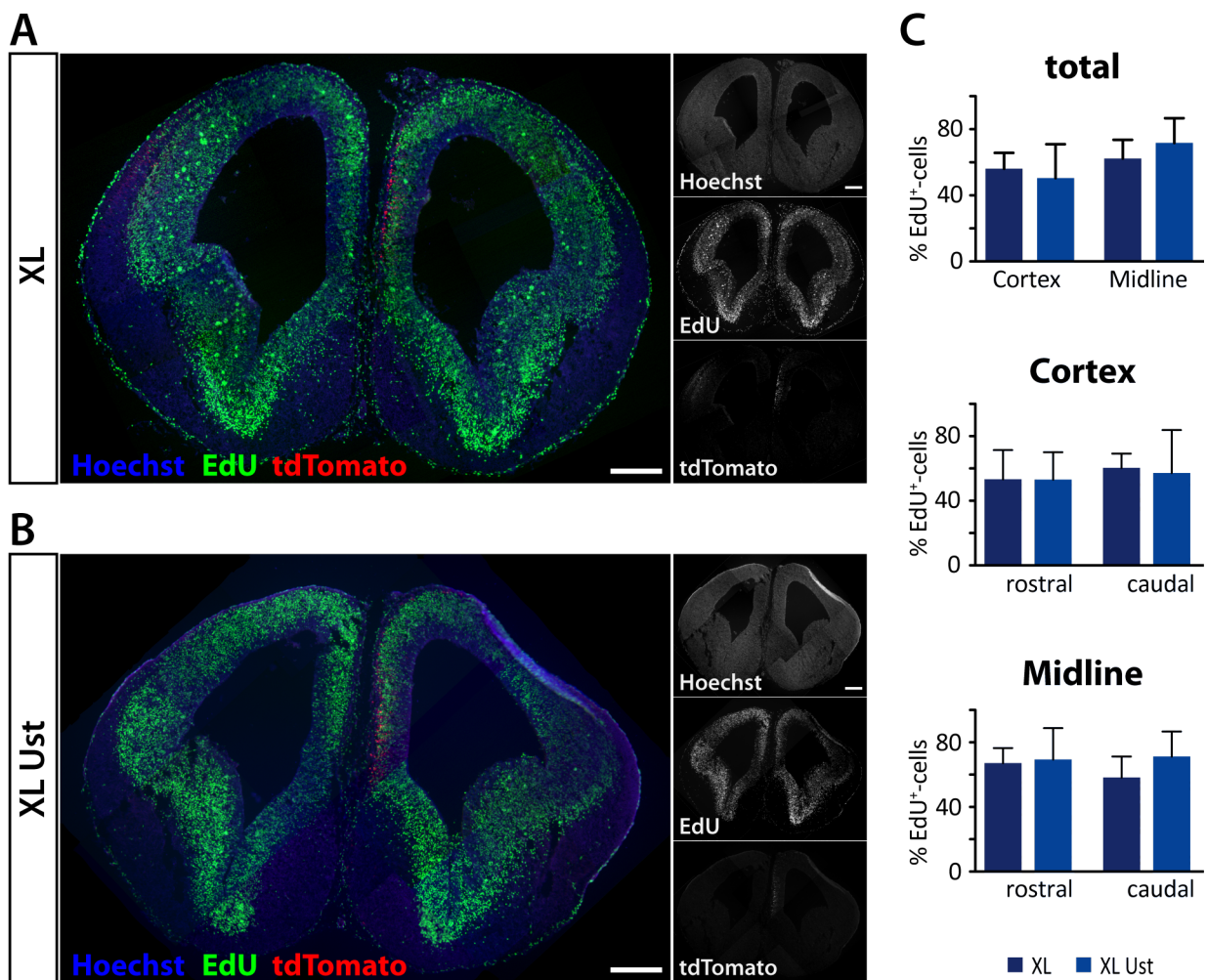


Figure 21 Impact of Ust overexpression on the proliferation: EdU

A: Overview of a frontal brain section of a XL *in utero* electroporated brain (E14.5) is shown. Proliferating cells are detected by EdU staining and the percentage of EdU⁺-cells in the cortex or the midline area was determined. The EdU pulse was given 1 d before sacrificing the mice. **B:** Frontal brain section of an Ust *in utero* electroporated brain at E14.5. Scale bar = 250 μ m. **C:** Quantification of the amount of EdU⁺-cells. Data are expressed as mean values \pm SD, statistics were performed by t-test with * $p \leq 0,05$ and ** $p \leq 0,01$, $n = 4-6$ embryos, 2-12 slices per embryo.

3.3.3 IMPACT OF UST OVEREXPRESSION ON NSC DIFFERENTIATION DURING CORTICAL DEVELOPMENT *IN VIVO*

The overexpression of Ust caused a modified CSPG sulfation pattern, which ultimately diminished the size of the cortical plate in a radial dimension. The effect may be either due to a reduced number of NeuN⁺-neurons in the cortical plate or a consequence of more densely packed cells in this area. The amount of neurons was detected by an immunohistochemical staining for NeuN. Afterwards, the number of NeuN⁺-cells was calculated with the program ilastik (compare 2.10.5 Analysis and 2.12.2 Ilastik) and depicted as percent of the total cell amount (Hoechst). Panel A and B of Figure 22 show representative frontal sections of E14.5 mice brain and their corresponding insets of the electroporated areas, cortex (A' + B') and midline (A'' + B''). The quantification of the sections along the total brain revealed a significantly decreased number of neurons in the midline (XL = 24,9 ± 6,9 %, Ust = 16,8 ± 4,7 %; n = 6) and showed the same trend for the cortex area (Figure 22 C). After a subsequent division along the rostrocaudal axis, the effect of a decreased number of neurons became more pronounced for the more caudal cortex sections (XL = 25,9 ± 11,0 %, n = 6; Ust = 16,5 ± 5,3 %, n = 4), while it even significantly decreased with respect to the more rostral midline sections (XL = 25,0 ± 6,3 %, Ust = 16,2 ± 4,7 %; n = 6). The results obtained from the thickness measurements match the numbers of NeuN⁺-cells and still appear counterintuitive (see Discussion).

The most abundant cell types during cortical development at around E14 are radial glia cells and the newly generated neurons. For this reason, also the amount of radial glia cells was determined in the *in utero* electroporated sections, whereas astrocytic cell analysis was excluded, because no differences in the amount of GFAP⁺ astrocytes were obtained in the differentiation assay *in vitro*. Oligodendrocyte precursor cells (O4⁺) were not analysed as well, justified by their incidental occurrence during neurogenesis peak time.

Accordingly, I also wanted to clarify if there is a change in the number of radial glia cells. Therefore, the number of Pax6⁺-cells using the ilastik software (compare 2.10.5 Analysis and 2.12.2 Ilastik) was determined. Figure 23 shows immunohistochemical stainings of XL-electroporated (A) and Ust-electroporated (B) sections of mice brains at E14.5. The higher magnifications depict the electroporated midline areas. The quantification of the Pax6⁺-cells revealed a higher number of radial glia cells after Ust overexpression, especially visible in the more caudal midline sections (XL = 26,0 ± 4,1 %, n = 4; Ust = 34,4 ± 2,3 %, n = 3). These results were unexpected, although this minor effect somehow coincides with the very small but significant higher generation of nsphs without supplemented growth factors and might therefore correspond to a promoted self-renewal capacity of Pax6⁺ radial glia cells after Ust overexpression and might have led to an enlarged ventricular zone.

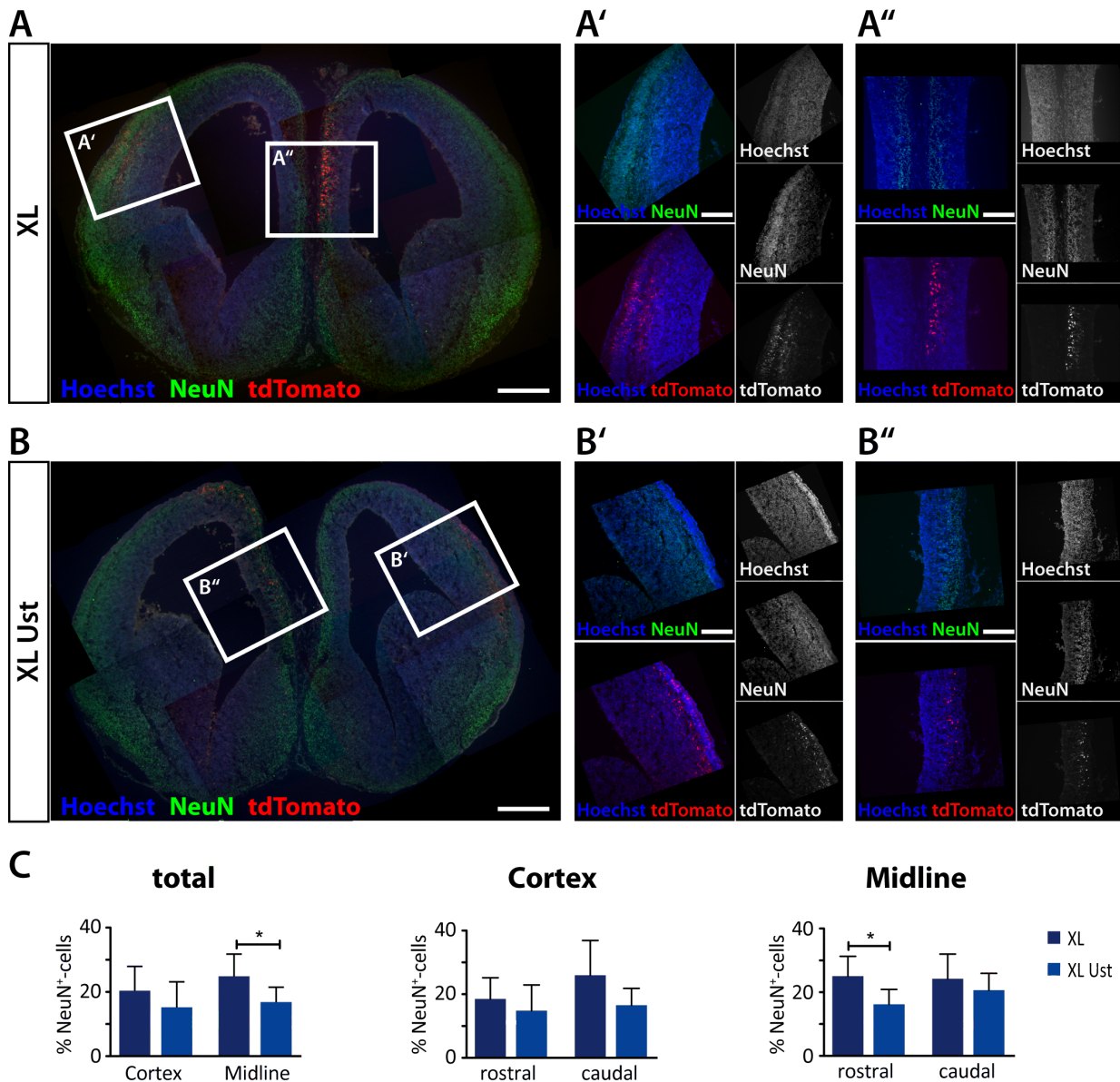


Figure 22 Impact of Ust overexpression on the amount of NeuN⁺-cells

A: Frontal brain section of XL *in utero* electroporated brain (E14.5) with higher magnifications of the electroporated cortex (**A'**) and the midline (**A''**). Neurons are detected by NeuN staining and the amount of NeuN⁺-cells in the cortex or the midline area was obtained by using the program ilastik (compare: 2.10.5 Analysis and 2.12.2 Ilastik). **B:** Frontal brain section of Ust *in utero* electroporated brain E14.5 with magnifications of the electroporated cortex (**B'**) and the midline (**B''**). A, B scale bar = 250 μ m; A', A'', B', B'' scale bar = 150 μ m. **C:** Quantification of the amount of NeuN⁺-cells. Data are expressed as mean values \pm SD, statistics were performed by t-test with * $p \leq 0,05$ and ** $p \leq 0,01$, $n = 6-8$ embryos, 2-12 slices per embryo.

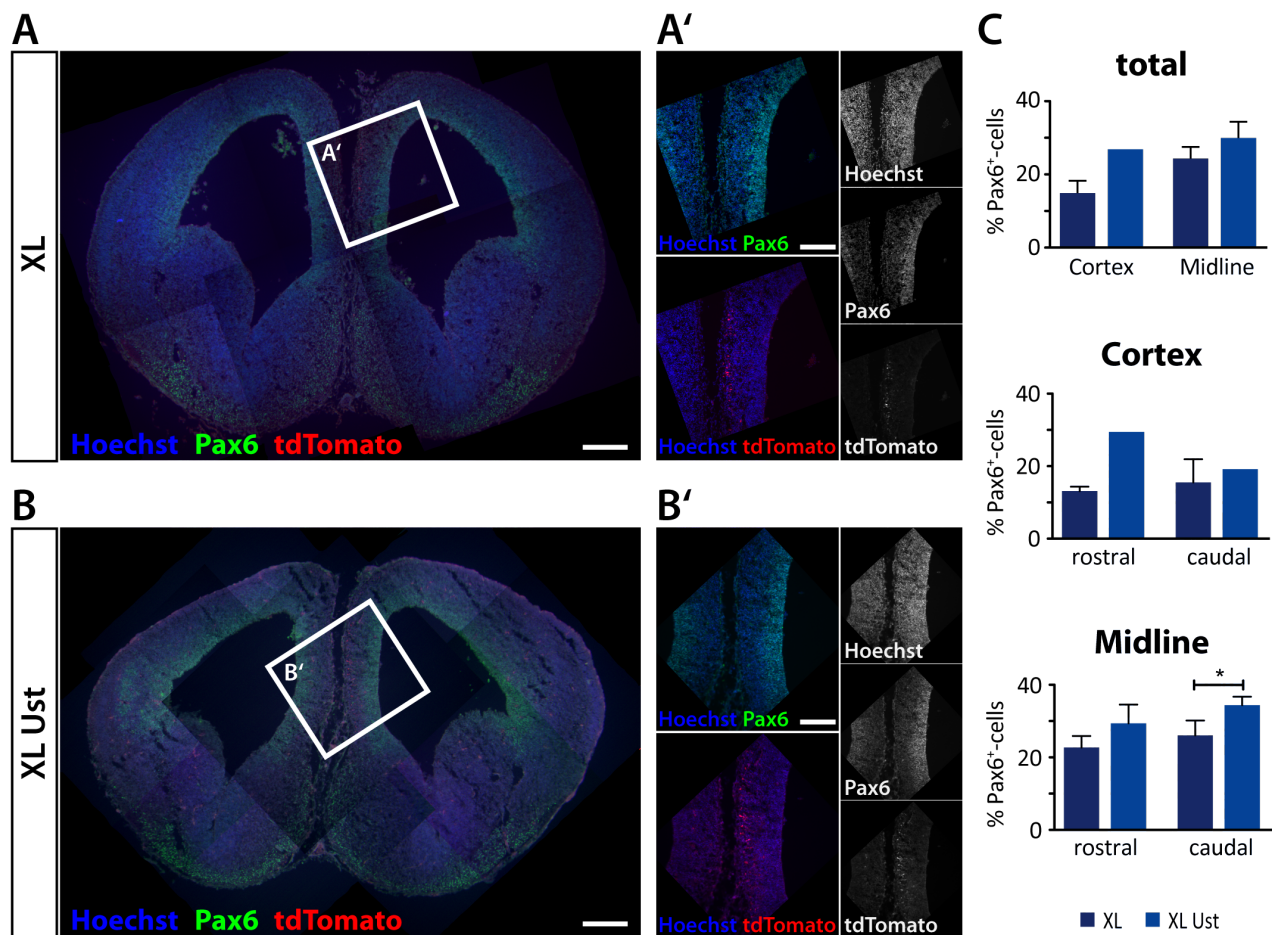


Figure 23 Impact of Ust overexpression on the amount of Pax6⁺-cells

A: Frontal brain section of XL *in utero* electroporated brain (E14.5) with a higher magnification of the electroporated midline (**A'**). Radial glia cells are detected by Pax6 staining and the amount of Pax6⁺-cells in the cortex or the midline area was calculated by using the ilastik software (compare: 2.10.5 Analysis and 2.12.2 Ilastik). **B:** Frontal brain section of Ust *in utero* electroporated brain (E14.5) with magnifications of the electroporated midline (**B'**). **A, B** scale bar = 250 μ m; **A', B'** scale bar = 150 μ m. **C:** Quantification of the amount of Pax6⁺-cells in the cortex and the midline. Data are expressed as mean values \pm SD, statistics were performed by t-test with * $p \leq 0,05$ and ** $p \leq 0,01$, cortex $n = 1-2$ embryos, 3-6 slices per embryo, midline $n = 3-5$ embryos, 3-6 slices per embryo.

4 DISCUSSION

In the present study, the impact of a modified CSPG sulfation pattern upon Ust overexpression on NSC behaviour was investigated. Therefore, a wild type protein form and a sulfation inactive form of Ust were used for cortical E13.5 NSC electroporation experiments. The differentiation assay revealed an increase of β III⁺-neurons (19 %) and a decrease of O4⁺-oligodendrocytic precursor cells (46 %) after Ust overexpression, whereas the amount of neural precursor cells (Nestin⁺) and astrocytes (GFAP⁺) remained constant. The analyses of NSC proliferation and self-renewal unfortunately exhibited, besides a very small but significant increased self-renewal without the addition of GFs, no obvious changes in the present study.

To confirm the obtained *in vitro* results, an *in vivo* analysis by using *in utero* electroporation was performed. Initially, the analysis of the mainly appearing layers of the developing cortex revealed a thinner cortical plate, while the ventricular zone thickness remained stable. This difference in CP thickness was not caused by altered proliferation rates. Afterwards, the analysis of the NeuN⁺-neurons confirmed the thinner CP by a decreased amount of neurons. In contrast to the stable VZ thickness, there was a slight increase in the number of Pax6⁺-RGCs.

I focused on the analysis of Ust because of several reasons. Ust overexpression has not yet been analysed in neural stem cells referring to their differentiation and proliferation during development. Ust is not redundant and has only one variant generating two distinct disulfated CS-units (CS-D and iB). So far, it seems that disulfated sugar units have a greater impact on the regulation of signalling molecule binding capacities and therefore exhibit a potentially higher biological relevance than monosulfated sugar units (Maeda et al., 2003, Bao et al., 2005, Ida et al., 2006, Ishii and Maeda, 2008a).

4.1 FUNCTIONALITY OF UST OVEREXPRESSION

The expression of the Ust fusion proteins was localized to the Golgi apparatus and corresponds to the endogenous localization of Chsts (Kusche-Gullberg, 2003). The transfection efficiency for Ust was always lower than for the empty control vectors and even for the negative control Ust mut. So, the overexpression of a relatively big fusion protein in the Golgi apparatus does not seem to be the general reason for the reduced transfection efficiency. It is not clear, if the lower transfection efficiency is due to a lower expression level or if the modified sulfation pattern after Ust overexpression caused more cells to undergo apoptosis and thereby the amount of transfected cells was reduced. If cell death is the reason, then a potentially disturbed homeostasis of Chsts expression and compensatory regulations of Ust and other Chsts should be analysed to unfold possible implications in cell survival signalling pathways. Yet, a role for specific CSPG sulfation in cell death commitment remains to be determined, although the implication of CSPGs e.g. versican already has been shown (LaPierre et al., 2007, Wight et al., 2014).

The functionality of Ust overexpression was confirmed by the 473HD epitope detection. This analysis is feasible because the 473HD antibody recognizes specific sulfation pattern sequences (Ito et al., 2005), which contain CS-D units and is therefore an appropriate marker for sulfation pattern modification concerning changes involving CS-D units.

4.2 IMPACT OF UST OVEREXPRESSION ON NSC DIFFERENTIATION

4.2.1 NSC DIFFERENTIATION *IN VITRO*

Ust overexpression led to an increased neurogenesis (β III⁺) and a decreased oligodendrogenesis ($O4^+$) in NSC differentiation at E13.5. Accordingly, ChABC treatment *in vitro* studies revealed an impaired neurogenesis and a favoured gliogenesis (GFAP⁺): 1) ChABC treatment of nsphs reduced the amount of about 13 % neurons (β III⁺) to 4 %, whereas the number of GFAP⁺-astrocytes increased from 4 % to 11 %, 2) even more pronounced was the effect of ChABC treatment on nsphs generated from 473HD-immunoselected NSCs: 80 % neurons were reduced to 20 % and 10 % astrocytes were increased to 40 % (Sirko et al., 2007). The very high amount of about 80 % neurons generated by 473HD-selected precursor cells had already been shown (von Holst et al., 2006). Especially the data obtained from 473HD-selected precursor cells imply a role of the sulfation pattern on NSC differentiation and supports the reported results concerning neurogenesis of the present study. It appears, that Ust overexpression suffices to modulate the increased generation of neurons and if Ust generated CS-units are missing less neurons are generated. Interestingly, the amounts of GFAP⁺ astrocytes and neural progenitor cells (Nestin⁺) were not altered upon Ust overexpression in the present study, in contrast to the reported favoured astrocytogenesis (Sirko et al., 2007). Moreover, Chst knockout (KO) studies reported impaired neuronal differentiation upon Chst 14 deficiency (Bian et al., 2011). Chst 14 generates the iA-unit and is thereby probably part of the 473HD epitope, which resulted in a significant decrease of 473HD expression after Chst 14 KO, confirming the 473HD sulfation pattern implication in the regulation of NSC differentiation processes.

Regarding gliogenesis, there was no change observed in the amount of GFAP⁺-astrocytes upon Ust overexpression and therefore an involvement of increased CS-D and CS-B units in the sulfation pattern can be excluded as an astrocytogenesis promoting factor. There was no analysis of oligodendrocytogenesis in the mentioned studies, whereas it appears plausible, that Ust overexpression can modulate the generation of oligodendrocytes as it reduced the $O4^+$ -precursor cell amount about 46 %. Additionally, the endogenous expression level of Ust raises from E14 to P7 and declines afterwards again (Ishii and Maeda, 2008a), leading to the assumption that Ust is involved during the peak of neurogenesis going along with the switch when the transition to gliogenesis appears. Other studies revealed an increased Ust expression level in more differentiated cells (neurons and astrocytes) than in NSCs (Yamauchi et al., 2011). The additional control Ust mut exhibited, that the obtained effects were specifically due to the modified sulfation pattern upon Ust overexpression and not caused by for example clogging the Golgi apparatus with a mass of overexpressed fusion proteins. Therefore, Ust mut was not further included in the subsequent analysis procedures.

4.2.2 NSC DIFFERENTIATION *IN VIVO*

To support the obtained *in vitro* results concerning the increased neurogenesis, NSC differentiation was also analysed *in vivo*, whereas gliogenesis analyses by detecting GFAP⁺ and $O4^+$ cells were excluded for the following reasons: 1) there was no difference in the numbers of GFAP⁺ astrocytes revealed *in vitro*, 2) gliogenesis starts at later stages at around E18 and $O4^+$ oligodendrocyte precursor cells are only sparsely present at the examined time point (E14.5)

and therefore the minor change of cell numbers exhibits probably no biological relevant effect. So, I restricted the analysis to the most abundant cell types during neurogenesis, RGCs and the generated neurons (Martynoga et al., 2012, Paridaen and Huttner, 2014).

The analysis of NeuN⁺ cell numbers revealed that the thinner CP is caused by a reduced neuronal cell amount in this area. This result appears counterintuitive to the reported increase in the number of β III-neurons in the differentiation assay *in vitro*. Corresponding to the concomitant increase in Pax6⁺ RGCs *in vivo* it seems plausible, that Ust overexpression keeps RGCs in their self-renewing state and thereby less neurons are generated. The Ust overexpression effect might be caused by prolonged cell cycle length, as it is known to occur during the transition of NECs to RGCs with the start of neurogenesis *in vivo* and under proliferative conditions in the clonal density assay *in vitro* (Takahashi et al., 1995, Calegari et al., 2005, Paridaen and Huttner, 2014). Furthermore, it promotes the generation of neuronal lineage restricted cells under differentiating conditions in the differentiation assay *in vitro*. The contradictory results from the *in vitro* and *in vivo* experiments might be caused by the differences in the ECM structure and composition. The *in vitro* ECM lacks the 3D characteristics and differs in the composition compared to *in vivo* conditions because of 2D culture dishes and the selected NSC pool used for the experiments. Hence, the *in vitro* ECM is less complex in its structure and molecular composition. However, this issue might be solved by using 3D matrix scaffolds in culture dishes. Additionally, the analysed time points were time-delayed and might be a reason for the altered experimental outcome. The *in vitro* experiments comprised a longer analysis time period of 3 d as well as a later developmental stage of the used NSCs from E13.5 to E16.5, when neurogenesis already proceeded. The localization of Ust expression at E14 in the developing cerebral cortex was detected mainly in the ventricular zone and in the cortical plate (Ishii and Maeda, 2008a), where the obtained effects in the present study were located. The analysis of the Pax6⁺ RGCs is further described in the discussion part on NSC self-renewal and proliferation *in vivo*.

4.3 IMPACT OF UST OVEREXPRESSION ON NSC SELF-RENEWAL AND PROLIFERATION

4.3.1 NSC SELF-RENEWAL AND PROLIFERATION *IN VITRO*

Self-renewal of NSCs was examined by clonal density assay (CDA). This assay determines the amount of NSCs that are capable of generating new neurospheres under proliferative conditions, meaning by self-renewing and thereby generating more NSCs. In the present study, there was no effect on self-renewal with supplemented growth factors, although there was a small but significant effect without any GFs (w/o). If this effect has any potential biological role remains to be elucidated.

In former experiments I could show that the overexpression of a combination of Chsts, here Chst 3, Chst 7 and Ust led to a significantly increased number of neurospheres (nsphs) in the presence of FGF 2 and heparin compared to the control (N1 = 114 ± 43, Chsts = 156 ± 46; n = 3) (Harrach, 2010). It was also revealed that a growth factor concentration higher than 5 ng/ml seems to induce a rather saturated situation, where the effect of the modified sulfation pattern was diminished. Chst 3 and Chst 7 generate the CS-C unit, which is the monosulfated basis for Ust to generate the CS-D unit. Thus, an influence of the single Ust overexpression on NSC self-

renewal was probable, but could maybe not reach a significant level, because not enough required CS-C was present to enable the overexpressed Ust the proper CS-D sulfation. However, the increased CS-D detection via 473HD antibody in the immunocytochemical stainings and western blot analysis appear inconsistent with this hypothesis. When sulfation is inhibited by sodium chlorate, the number of generated nsphs was reduced and even adding defined CS-units, randomly patterned, did not rescue the nsphs formation (Akita et al., 2008). So an impact of the endogenously sulfated CS-GAGs has already been shown, although a random supplementation with CS-units or a singular overexpression of one Chst, here Ust, is not sufficient to clearly change self-renewal capacities.

Further studies reported the 473HD epitope expression on RGCs and its implementation in self-renewal capacity. Selectively isolated 473HD⁺-precursor cells derived from E13 mouse cortices exhibited a threefold increased generation of nsphs in the clonal density assay supplemented with EGF and FGF 2 in comparison to the nonselected control cells (von Holst et al., 2006). Additionally, after interfering in clonal density assays with ChABC treatment or addition of mAb 473HD, a reduced generation of nsphs was observed (von Holst et al., 2006). These studies also indicate an involvement of a specific CS sulfation pattern in self-renewal property regulation during cortical development.

The CDA analysis differs from proliferation analysis with EdU incorporation in the restriction of included proliferating cell types. The CDA exclusively detects nsphs forming NSCs, whereas the EdU assay includes all cells, which undergo mitosis and incorporate the EdU during DNA replication. This cell pool is bigger and includes also more lineage restricted cell types as for example transit amplifying cells or neural precursor cells. The EdU assay did not reveal a significant difference in the amount of proliferating cells, which corresponds to the stable numbers of neural precursor cells (Nestin⁺) obtained in the differentiation assay as well as to the not altered amount of self-renewing NSCs in the CDA assay, leaving the w/o condition aside. Indicating that the single overexpression of Ust only offers, if any, a very small impact on NSC self-renewal and proliferation capacity *in vitro*, the complete CS-GAG digestion with ChABC exhibited a reduced number of BrdU-incorporating cells in the nsphs culture system derived from cortex and ganglionic eminence of E13 mice as well as a reduced amount of neural progenitor cells (Nestin⁺) (Sirko et al., 2007). The increase of CS-D units in the sulfation pattern of CSPGs is therefore not sufficient to confirm the general implication of CS-GAGs in NSC proliferation and self-renewal behaviour.

4.3.2 NSC SELF-RENEWAL AND PROLIFERATION *IN VIVO*

The analysis of the proliferation capacity *in vivo* revealed no difference after Ust overexpression in comparison to the control. It confirmed our EdU assay *in vitro* observations and also the constant neural progenitor (Nestin⁺) pool in the differentiation assay. Therefore, it can be rather excluded as a cause for the reduced CP thickness. The unchanged thickness of the VZ after Ust overexpression was expected because of the not altered proliferation and self-renewal capacities. Although, the small but significant effect on NSC self-renewal without supplemented GFs *in vitro* might explain the slightly increased amount of Pax6⁺ radial glia cells in the VZ after Ust overexpression. Additionally, the trend towards an increased GF responsiveness leads to the conclusion that Ust overexpression either promotes self-renewal of

RGCs or keeps RGCs in a self-renewal state and therefore longer detectable as Pax6⁺ RGCs. This is consistent with data that showed 473HD expression on NSCs and increased self-renewal capacity of 473HD⁺-selected NSCs (von Holst et al., 2006) and leads to the suggestion, that Ust overexpression increases the generation of the 473HD motif, therefore generating a bigger Pax6⁺-cell fraction, which in this case would correlate with the abundant NSCs, the Pax6⁺-RGCs. Either generating more of the Pax6⁺-RGCs in the VZ would be an explanation for the increased amount of Pax6⁺-RGCs or keeping them in the VZ, which would be in line with an obtained greater distance of BrdU-incorporating cells to the ventricular surface after ChABC treatment (Sirko et al., 2007), but still needs to be further analysed. The reduced amount of neurons and the increased number of Pax6⁺-RGCs might have been caused by a decreased cell cycle exit rate. The experiments to analyse the EdU⁺/Ki67⁻-cell fraction was unfortunately not reliable due to technical problems and is therefore excluded from the results. The detected amount of Ki67⁺-cells was at a very low level and not comparable to literature values at this developmental stage (Hartfuss et al., 2001, Woodhead et al., 2006, Yu et al., 2009).

These observations fit to the endogenous expression of FGF 2 during cerebral cortex development in the ventricular zones of the cortex and the midline in the examined developmental time window between E12 and E14 (Raballo et al., 2000, Iwata and Hevner, 2009), which would make an increased responsiveness of Pax6⁺ RGCs in the VZ to FGF 2 biologically reasonable. Moreover, it was shown that the removal of CS-GAGs via intracerebroventricular ChABC injection resulted in a decreased number of nsph forming NSCs in the presence of FGF 2 (Sirko et al., 2010). They also obtained decreased proliferation rates of FGF 2-sensitive NSCs after ChABC treatment in the presence of FGF 2. Thus, an alteration of the proliferation capacity would have been possible after Ust overexpression as well, although the obtained results show, that the single modification by Ust overexpression is not sufficient to change proliferation rates. Probably, the orchestration of the different Chsts is needed to generate the required sulfation pattern code to enable the FGF 2 signalling cascade.

Furthermore it was reported that 1 d after intracerebroventricular ChABC injection, less BrdU was incorporated into cortical cells at E14.5, concomitant with a greater distance to the ventricular surface (Sirko et al., 2007). Hence, NSC proliferation and also the localization of proliferating cells within the VZ are influenced by CS-GAGs, whereas modification of the sulfation pattern upon Ust overexpression was insufficient.

4.4 IMPLICATIONS OF THE SULFATION PATTERN ON NSC BEHAVIOUR AND POSSIBLE MECHANISMS

Only few studies deal with manipulation of Chst expression referring to NSC differentiation (Bian et al., 2011), mainly proliferation and migration are examined (Liu et al., 2006), or their involvement in CNS injury (Properzi et al., 2005) and cancer (Wade et al., 2013, Pantazaka and Papadimitriou, 2014, Silver and Silver, 2014). Especially rare are studies examining the impact of Ust on NSC behaviour (Ishii and Maeda, 2008a, Nikolovska et al., 2015).

The present study revealed an implication of an Ust modified sulfation pattern on NSC differentiation and self-renewal *in vitro* and *in vivo*. It is the first time that Ust is overexpressed in NSC *in vitro* and *in vivo*, whereas a knockdown was already examined (Ishii and Maeda, 2008a). However, the knockdown study reported sulfation pattern involvement during neuronal migration and was not dealing with differentiation during cortical development.

Therefore, analysis referring to NSC differentiation processes and more detailed analysis on NSC self-renewal upon Ust-related manipulation of the sulfation pattern need to be performed. The mechanisms behind the influence of a modified sulfation pattern on cellular behaviour are still in the process of being elucidated. The analyses of Chst 11 and Chst 14 deficient knockout mice exhibited a decreased neurogenesis, a diminished proliferation of NSCs concomitant with changes in the NSCs marker expression, and an upregulation of FGF 2 and EGF receptor expression for Chst 14 (Bian et al., 2011). In contrast, Chst 11 deficiency did not have the mentioned impact on NSC biology and unfolds the distinct roles of a specific sulfation pattern on NSC behaviour, here CS units modified by Chst 11 versus DS units sulfated by Chst 14. These findings support the importance of a specific sulfation code for presenting GFs e.g. FGF 2 or EGF to their receptors, which decreased FGF 2- and EGF-mediated proliferation of NSCs *in vitro* and proliferation rate in the adult NSC niches, dentate gyrus and subventricular zone (Bian et al., 2011). Moreover, Chst 14 deficiency also impaired neuronal differentiation *in vitro* and in the adult hippocampus, but not in NSCs obtained from the adult SVZ (Bian et al., 2011), referring to a spatially and temporally regulated impact of the sulfation pattern on NSC behaviour (Nurcombe et al., 1993, Ishii and Maeda, 2008b). The involvement of CSPGs in the regulation of proliferation and differentiation had been described for FGF 2-dependent signalling supporting NSC proliferation and maintaining neuron-generating properties (Ida et al., 2006, Sirko et al., 2010), leading to the suggestion that regulated CS structural changes during development correspond to the shift from FGF 2-dependent neurogenesis to delayed EGF-dependent gliogenesis (Maeda, 2010). Opposing effects on neurogenesis and astrocytogenesis after ChABC treatment have been reported as well (Gu et al., 2009), which were explained by different NSC origin. FGF 2 ligand binding to cell surface PG GAGs and its thereby enabled presentation to FGF receptors are well studied for heparan sulfates (Pellegrini L, 2000) and because of the structural similarities of HS to CS also transferable. So far, HS and CS demonstrate controversial effects concerning FGF signalling pathways, but they are with respect to structure and sulfation pattern variability of the PGs (core protein + GAGs) explainable (Deepa et al., 2004, Nikolovska et al., 2015). In addition to the immense structural complexity, the functionality is also dependent on the GAG bound factors, which can cause e.g. CS to operate as an attractant or repellent regulated by the sulfation pattern (Shipp and Hsieh-Wilson, 2007, Maeda, 2015). Anyway, the sulfation pattern of CSPGs exhibits an effect on NSC differentiation, migration, proliferation and neurite outgrowth.

The research focus is more concentrated on migration, plasticity and regeneration corresponding to CS sulfation alterations. Analysis of Ust-mediated 2-O-sulfation revealed FGF 2-induced neuronal migration through ERK1/2 activation (Nikolovska et al., 2015). Moreover, it was reported that the correct positioning of neurons during developmental migration in the cerebral cortex is regulated by CS-E and CS-D unit appearance (Ishii and Maeda, 2008a). Especially the binding capacities of distinct CS-units have been analysed. Exemplarily, CS-E exhibits a high binding affinity to axon guidance molecules, whereas CS-A shows only low binding capacities (Shipp and Hsieh-Wilson, 2007). A high binding affinity to several GFs (FGF, EGF, etc.) for CS-E has also been revealed (Rogers et al., 2011). Furthermore, increased binding of phosphacan, which exhibits an especially high amount of CS-D units, to pleiotrophin was observed (Maeda et al., 2003) and its implication on neurite outgrowth was

unfolded (Faissner et al., 1994, Clement et al., 1998, Bao et al., 2005). But, the sulfation motif influence on neurite outgrowth showed opposing effects depending on the neuronal lineage examined (Clement et al., 1998, Garwood et al., 1999), also referring to the specialized microenvironment influencing the sulfation pattern impact regulated by the distinct ECM composition and factors apparent in the respective surroundings.

CSPGs are involved in numerous processes, therefore CSPG implications in many diseases seems to be logical. It was revealed, that neurons with aggrecan containing PNNs are protected from tau-pathology in Alzheimer's disease (Burnside and Bradbury, 2014). CSPG expression is upregulated after CNS injury and limits regeneration (inhibits axon growth, restricts plasticity) (Bradbury et al., 2002, Silver and Miller, 2004, Lau et al., 2012, Silver and Silver, 2014). Another example of CSPG involvement is the decreased levels of tenascin and lecticans during active periods of multiple sclerosis, whereas inactive lesions exhibit normalized tenascin levels, but lecticans are chronically upregulated (Burnside and Bradbury, 2014). There are studies that associate PGs and PG-related genes to (mental) disorders in humans (Maeda, 2015), for example is one variant of *Ust* associated with job-related exhaustion (Sulkava et al., 2013) and phosphacan seems to be associated with schizophrenia (Buxbaum et al., 2008, Takahashi et al., 2011).

The implication of CSPGs by changing the sulfation pattern and thereby influencing various signalling pathways appears presumable, because I support with our findings once more the influence of a modified sulfation pattern on NSC behaviour. The negative charge along the GAG chains and its variability by *Chst* modification are under discussion to provide a regulation system for electrostatic interactions with binding factors (Ishii and Maeda, 2008a). Most interesting is the proposition of a HS sulfation pattern code hypothesis, which provides a communication platform within the extracellular matrix for its inherent cells (Habuchi et al., 2004, Bulow and Hobert, 2006). Because of the similar structure of chondroitin sulfate and its sulfation pattern, this hypothesis would be transferable and applicable in general for sulfated proteoglycan GAG chains.

Figure 24 shows a possible mechanism how modifying the sulfation pattern improves binding affinity for signalling molecules, here exemplarily depicted for growth factors. The increase in sulfation raises the negative charge of the GAGs as well as changes their 3D conformational state and thereby generating for example more binding sites for growth factors or other signalling molecules. The GFs can be stored within the ECM by secreted or transmembrane PGs and, when needed, sequestered by their GAGs into the ECM. Transmembrane PGs rather present the signalling molecules to their receptors on the cell surface or increase the activity of signalling cascades as it was already shown for HS (Pellegrini L, 2000, Schlessinger et al., 2000). Moreover, transmembrane PGs are capable of directly transducing signals through cell membranes (Alexopoulou et al., 2007) and additionally of releasing active GAG-containing ectodomains by shedding the transmembrane PG (Manon-Jensen et al., 2010). So far, several signalling pathways have been shown to be implicated in CSPG and CS-GAG functionality, for example the Rho/ROCK signalling pathway, ERK1/2 signalling, FAK and Src phosphorylation and integrin signalling (Wu et al., 2005, Gu et al., 2009, Brown et al., 2012, Dyck and Karimi-Abdolrezaee, 2015, Nikolovska et al., 2015). The functionality does not simply depend on the negative charge, but for example on the ratio of 4- to 6-sulfated CS, which terminates the

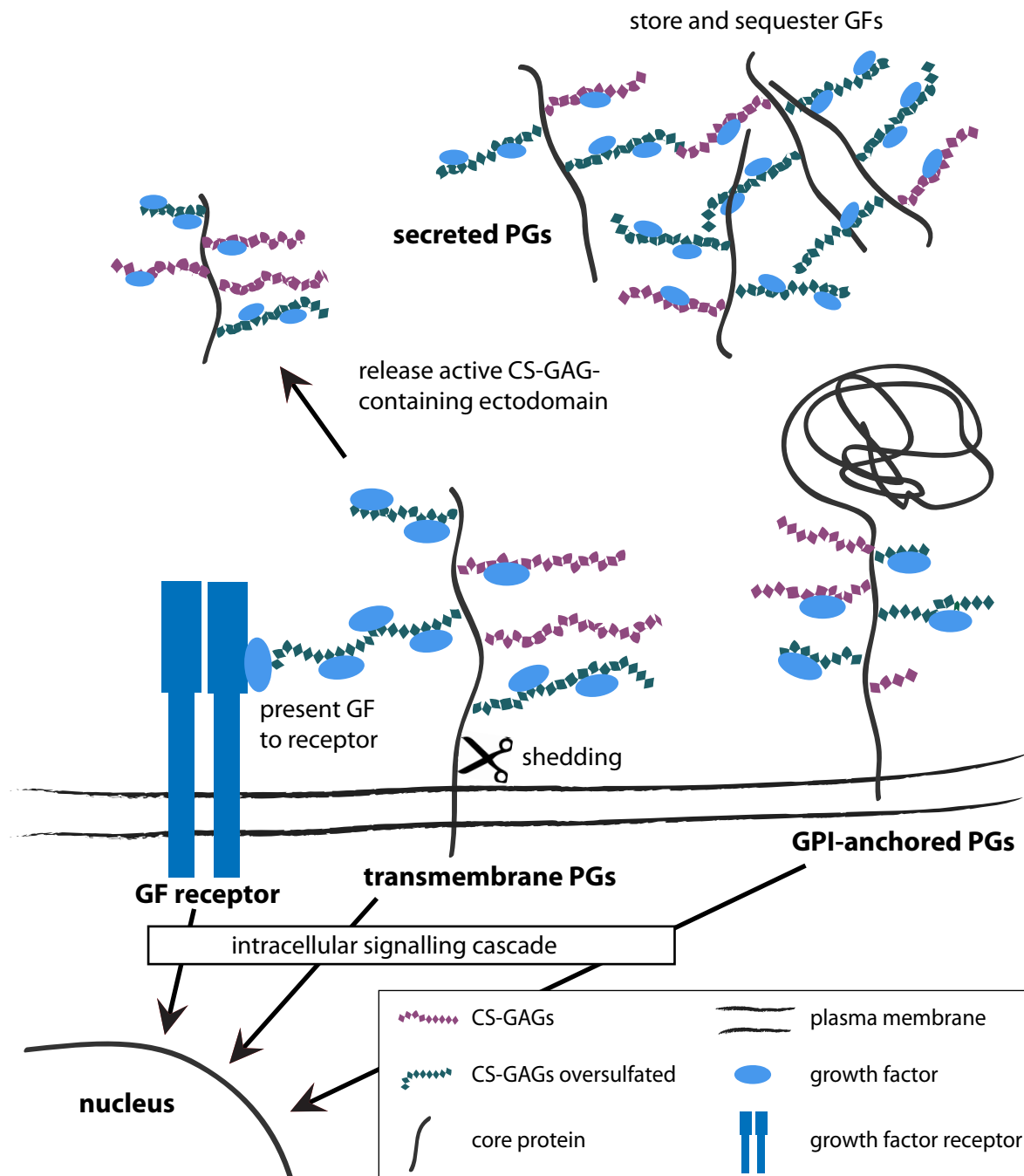


Figure 24 Important functions and possible mechanisms of CSPGs

There are three forms of CSPGs: secreted, transmembrane and GPI-anchored CSPGs. The shedding of transmembrane CSPGs releases an active CS-GAG-containing ectodomain into the ECM. There are several ways of CSPGs or PGs in general to influence signalling pathways. Here, the most probable and important interactions of CSPGs with a modified sulfation pattern referring to the influence on NSC behaviour are exemplarily depicted for GF signalling. CS-GAGs exhibit growth factor binding sites and after modifying the sulfation pattern, e.g. by overexpression of Ust, the number of binding sites present can be increased. With more GFs bound to the GAGs, the probability to present the GFs to its relevant receptor is higher and the activity of this signalling pathway is increased. Another function of CSPGs is to store and sequester GFs in the matrix. Thereby, they can regulate the relevant signalling pathways, enable the spatial and temporal regulation of the release and establish morphogen gradients. CSPG: chondroitin sulphate proteoglycan, PG: proteoglycan, CS-GAG: chondroitin sulphate glycosaminoglycan. GF: growth factor.

critical period for ocular dominance plasticity (Miyata et al., 2012), supporting the hypothesis of the GAG sulfation pattern sequence and architecture importance.

Generally, the sequence, the conformation and the electrostatic potential of PG-GAGs appear more important than the simple degree of sulfation (Mizumoto et al., 2013). There is evidence, that the GAG sulfation pattern becomes adapted to its needs of specific developmental time points (e.g. neurogenesis, gliogenesis) by the spatial and temporal regulation of PG and PG-related gene expression (Nurcombe et al., 1993, Akita et al., 2008, Ishii and Maeda, 2008b, Mizumoto et al., 2013). The functionality of PGs acts in a context-dependent manner by structural PG core and GAG diversity (Lindahl, 2014, Maeda, 2015). This means in conclusion, that the differentially regulated Chst and CSPG expression is essential for the mode of operation and because of their involvement in so many processes it is complicated and yet needed to unravel the basic mechanisms underlying the complex system of PG ECM interaction. Finally, it has to be further analysed, whether there is a sulfation code existing or if the GAG sulfation pattern functionality is due to a statistical process based on the stoichiometric availability of the different GAG units. One ECM component is only a small part of the big picture and its specific function is regulated by its temporal and spatial expression within its ECM molecule context as well as the additional possible combinatorial effects, which increase functional diversity and expand the possible influencing pathways. To throw light on the big picture these correlations remain to be better understood in the basic research and maybe allow some day to improve treatment potentials of relevant diseases or developmental disorders.

4.5 FUTURE ASPECTS

As Ust shRNA experiments using *in utero* electroporation revealed defects in neuronal migration as well as divergent neuron morphology (Ishii and Maeda, 2008a), opposite effects on migration and an increase in bipolar shaped neurons in comparison to multipolar shaped neurons in the control situation would be expected after Ust overexpression, although this still needs to be experimentally analysed and validated.

In utero electroporation is a suitable way to analyse implications of a modified CSPG sulfation pattern by overexpression or knockdown of distinct Chsts, because it bypasses possible compensatory mechanisms that usually appear with chronic manipulations (Rauch et al., 2005), especially with a number of 7 Chsts available to modify CS-GAGs. Additionally, to prevent functional compensation an inducible conditional knockout mouse line would be an excellent opportunity to examine sulfation pattern implication on e.g. NSC behaviour by specifically timed or restricted to specific cell types gene inactivation/deletion. Designing the Ust knockout strategy (see 2.11.3 Strategy) and starting the preparation of the Ust conditional knockout construct enable a fast generation of the transgenic mouse line and a promising analysis strategy for future experiments to directly examine the role of a missing Ust CS-GAG sulfation on differentiation, self-renewal, proliferation and migration during development at the desired time point and addressing the favoured cell types. This would also allow the analysis of later developmental time points as for example gliogenesis or long-term effects, which were not possible to analyse by using the *in utero* electroporation method. It would be interesting to see,

whether Ust deletion confirms the here already reported impacts on NSC neurogenesis and self-renewal and additionally whether it alters oligodendrocyte precursor cell development or astrocyte generation.

5 ACKNOWLEDGMENTS/DANKSAGUNG

Prof. Dr. Joachim Kirsch und PD Dr. Alexander von Holst danke ich dafür, dass sie mir die Arbeit in Heidelberg am Institut für Anatomie und Zellbiologie an diesem interessanten Thema ermöglicht haben.

Ich danke auch Dr. Gonzalo Alvarez-Bolado und Dr. Roberta Haddad-Tóvulli für die Möglichkeit die *in utero* Elektroporationsmethode zu erlernen und in ihren Räumlichkeiten mit ihren Geräten anzuwenden.

Außerdem möchte ich Prof. Dr. Thomas Kuner danken, der durch die Mitnutzung seines Equipments einen Großteil der Auswertung ermöglicht hat.

Dr. Francesca Ciccolini und ihrer Arbeitsgruppe danke ich für unseren Austausch in unseren Seminaren.

Die Nutzung des 4D Electroporators zur NSC Transfektion hat freundlicherweise Dr. Ulrike Müller ermöglicht, neben der zur Verfügungstellung des Plasmids für die Knockout-Mauslinie und die beratenden Gespräche mit Dr. Jakob Tschäpe.

Beate Quenzer danke ich herzlich für die Anfertigung und Färbung der schönen Cryoschnitte in meiner Arbeit.

Den Mitarbeitern des Instituts möchte ich für die herzliche Aufnahme und eine schöne gemeinsame Zeit danken, aber auch für die technische und persönliche Unterstützung während meiner Zeit in Heidelberg.

Liebe Sabrina, lieber Richard, mein besonderer Dank gilt euch, unserem 3-köpfigen Doktoranden-Team, ohne das vieles wohl anders gelaufen wäre. Ich danke euch so sehr für den starken Zusammenhalt, die gegenseitige Unterstützung in jeglicher Form und besonders auch für unseren offenen, ehrlichen Umgang mit viel Humor. Danke auch an unser ehemaliges Labormitglied Valentin.

Michi, du bist das Beste, was mir passiert ist. Ich danke dir für deine Unterstützung, fürs Dasein, für deine Liebe.

Besonderer Dank gilt meiner Familie für eure unermüdliche, liebevolle Unterstützung, schon mein Leben lang. Ich freue mich sehr über die herzliche Aufnahme in Michis Familie, ihr zählt für mich genauso dazu, also danke auch an euch.

Ein Hoch auf Freunde und Familie: BBQ am Neckar, Balkon/Terrassen-Spaghettieis, Atzentag, Sonntagsfrühstück, Kochsessions, Hängematten, Slacklinien, KinoMontag, Gammeln am See, Bierchen/Weinchen?!, Abspacken, Beachen, Kaffeepäuschen, FestivalFeeling, Eispäuschen, Lehrstuhlfrühstück/Filmabend, Wandern bis nach Neckarsteinach?!, InlinerTouren, Sushisessions, Lasertag, und noch so vieles mehr... Danke!

Ihr seid schlicht und einfach die Besten :)

5 REFERENCES

- Akita K, von Holst A, Furukawa Y, Mikami T, Sugahara K, Faissner A (2008) Expression of multiple chondroitin/dermatan sulfotransferases in the neurogenic regions of the embryonic and adult central nervous system implies that complex chondroitin sulfates have a role in neural stem cell maintenance. *Stem Cells* 26:798-809.
- Alexopoulou AN, Multhaupt HA, Couchman JR (2007) Syndecans in wound healing, inflammation and vascular biology. *Int J Biochem Cell Biol* 39:505-528.
- Bandtlow CE, Zimmermann DR (2000) Proteoglycans in the developing brain: new conceptual insights for old proteins. *Physiol Rev* 80:1267-1290.
- Bao X, Mikami T, Yamada S, Faissner A, Muramatsu T, Sugahara K (2005) Heparin-binding growth factor, pleiotrophin, mediates neuritogenic activity of embryonic pig brain-derived chondroitin sulfate/dermatan sulfate hybrid chains. *The Journal of biological chemistry* 280:9180-9191.
- Barry DS, Pakan JM, McDermott KW (2014) Radial glial cells: key organisers in CNS development. *Int J Biochem Cell Biol* 46:76-79.
- Bartus K, James ND, Bosch KD, Bradbury EJ (2012) Chondroitin sulphate proteoglycans: key modulators of spinal cord and brain plasticity. *Experimental neurology* 235:5-17.
- Bian S, Akyuz N, Bernreuther C, Loers G, Laczynska E, Jakovcevski I, Schachner M (2011) Dermatan sulfotransferase Chst14/D4st1, but not chondroitin sulfotransferase Chst11/C4st1, regulates proliferation and neurogenesis of neural progenitor cells. *J Cell Sci* 124:4051-4063.
- Bradbury EJ, Moon LD, Popat RJ, King VR, Bennett GS, Patel PN, Fawcett JW, McMahon SB (2002) Chondroitinase ABC promotes functional recovery after spinal cord injury. *Nature* 416:636-640.
- Brown JM, Xia J, Zhuang B, Cho KS, Rogers CJ, Gama CI, Rawat M, Tully SE, Uetani N, Mason DE, Tremblay ML, Peters EC, Habuchi O, Chen DF, Hsieh-Wilson LC (2012) A sulfated carbohydrate epitope inhibits axon regeneration after injury. *Proceedings of the National Academy of Sciences of the United States of America* 109:4768-4773.
- Bulow HE, Hobert O (2006) The molecular diversity of glycosaminoglycans shapes animal development. *Annu Rev Cell Dev Biol* 22:375-407.
- Burnside ER, Bradbury EJ (2014) Manipulating the extracellular matrix and its role in brain and spinal cord plasticity and repair. *Neuropathol Appl Neurobiol* 40:26-59.
- Buxbaum JD, Georgieva L, Young JJ, Plescia C, Kajiwara Y, Jiang Y, Moskvina V, Norton N, Peirce T, Williams H, Craddock NJ, Carroll L, Corfas G, Davis KL, Owen MJ, Harroch S, Sakurai T, O'Donovan MC (2008) Molecular dissection of NRG1-ERBB4 signaling implicates PTPRZ1 as a potential schizophrenia susceptibility gene. *Mol Psychiatry* 13:162-172.
- Calegari F, Haubensak W, Haffner C, Huttner WB (2005) Selective lengthening of the cell cycle in the neurogenic subpopulation of neural progenitor cells during mouse brain development. *J Neurosci* 25:6533-6538.
- Carey DJ (1997) Syndecans: multifunctional cell-surface co-receptors. *The Biochemical journal* 327 (Pt 1):1-16.
- Carulli D, Laabs T, Geller HM, Fawcett JW (2005) Chondroitin sulfate proteoglycans in neural development and regeneration. *Current opinion in neurobiology* 15:116-120.
- Carulli D, Pizzorusso T, Kwok JC, Putignano E, Poli A, Forostyak S, Andrews MR, Deepa SS, Glant TT, Fawcett JW (2010) Animals lacking link protein have attenuated perineuronal nets and persistent plasticity. *Brain : a journal of neurology* 133:2331-2347.
- Carulli D, Rhodes KE, Brown DJ, Bonnert TP, Pollack SJ, Oliver K, Strata P, Fawcett JW (2006) Composition of perineuronal nets in the adult rat cerebellum and the cellular origin of their components. *The Journal of comparative neurology* 494:559-577.
- Clement AM, Nandanaka S, Masayama K, Mandl C, Sugahara K, Faissner A (1998) The DSD-1 carbohydrate epitope depends on sulfation, correlates with chondroitin sulfate D motifs, and is sufficient to promote neurite outgrowth. *The Journal of biological chemistry* 273:28444-28453.
- Deepa SS, Carulli D, Galtrey C, Rhodes K, Fukuda J, Mikami T, Sugahara K, Fawcett JW (2006) Composition of perineuronal net extracellular matrix in rat brain: a different disaccharide composition for the net-associated proteoglycans. *The Journal of biological chemistry* 281:17789-17800.
- Deepa SS, Yamada S, Zako M, Goldberger O, Sugahara K (2004) Chondroitin sulfate chains on syndecan-1 and syndecan-4 from normal murine mammary gland epithelial cells are structurally and functionally distinct and cooperate with heparan sulfate chains to bind growth factors. A novel function to control binding of midkine, pleiotrophin, and basic fibroblast growth factor. *The Journal of biological chemistry* 279:37368-37376.
- Dimou L, Gotz M (2014) Glial cells as progenitors and stem cells: new roles in the healthy and diseased brain. *Physiol Rev* 94:709-737.

- Discher DE, Mooney DJ, Zandstra PW (2009) Growth factors, matrices, and forces combine and control stem cells. *Science* 324:1673-1677.
- Doetsch F (2003) A niche for adult neural stem cells. *Current Opinion in Genetics & Development* 13:543-550.
- Douet V, Arikawa-Hirasawa E, Mercier F (2012) Fractone-heparan sulfates mediate BMP-7 inhibition of cell proliferation in the adult subventricular zone. *Neuroscience letters* 528:120-125.
- Dyck SM, Karimi-Abdolrezaee S (2015) Chondroitin sulfate proteoglycans: Key modulators in the developing and pathologic central nervous system. *Experimental neurology* 269:169-187.
- Esko JD, Kimata K, Lindahl U (2009) Proteoglycans and Sulfated Glycosaminoglycans. In: *Essentials of Glycobiology* (Varki, A. et al., eds) Cold Spring Harbor (NY).
- Evers MR, Xia G, Kang HG, Schachner M, Baenziger JU (2001) Molecular cloning and characterization of a dermatan-specific N-acetylgalactosamine 4-O-sulfotransferase. *The Journal of biological chemistry* 276:36344-36353.
- Faissner A, Clement A, Lochter A, Streit A, Mandl C, Schachner M (1994) Isolation of a neural chondroitin sulfate proteoglycan with neurite outgrowth promoting properties. *The Journal of cell biology* 126:783-799.
- Faissner A, Pyka M, Geissler M, Sobik T, Frischknecht R, Gundelfinger ED, Seidenbecher C (2010) Contributions of astrocytes to synapse formation and maturation - Potential functions of the perisynaptic extracellular matrix. *Brain research reviews* 63:26-38.
- Filmus J, Capurro M (2014) The role of glypicans in Hedgehog signaling. *Matrix Biol* 35:248-252.
- Freeze HH (2009) Genetic Disorders of Glycan Degradation. In: *Essentials of Glycobiology* (Varki, A. et al., eds) Cold Spring Harbor (NY).
- Galtrey CM, Fawcett JW (2007) The role of chondroitin sulfate proteoglycans in regeneration and plasticity in the central nervous system. *Brain research reviews* 54:1-18.
- Garwood J, Schnadelbach O, Clement A, Schutte K, Bach A, Faissner A (1999) DSD-1-proteoglycan is the mouse homolog of phosphacan and displays opposing effects on neurite outgrowth dependent on neuronal lineage. *J Neurosci* 19:3888-3899.
- Gotz M, Huttner WB (2005) The cell biology of neurogenesis. *Nature reviews Molecular cell biology* 6:777-788.
- Gu WL, Fu SL, Wang YX, Li Y, Lu HZ, Xu XM, Lu PH (2009) Chondroitin sulfate proteoglycans regulate the growth, differentiation and migration of multipotent neural precursor cells through the integrin signaling pathway. *BMC neuroscience* 10:128.
- Habuchi H, Habuchi O, Kimata K (2004) Sulfation pattern in glycosaminoglycan: does it have a code? *Glycoconj J* 21:47-52.
- Habuchi O (2000) Diversity and functions of glycosaminoglycan sulfotransferases. *Biochim Biophys Acta*.
- Hacker U, Nybakken K, Perrimon N (2005) Heparan sulphate proteoglycans: the sweet side of development. *Nature reviews Molecular cell biology* 6:530-541.
- Harrach D (2010) Structure and Function of Chondroitin Sulfates in the Neural Stem Cell Niche.
- Hartfuss E, Galli R, Heins N, Gotz M (2001) Characterization of CNS precursor subtypes and radial glia. *Dev Biol* 229:15-30.
- Haupt LM, Murali S, Mun FK, Teplyuk N, Mei LF, Stein GS, van Wijnen AJ, Nurcombe V, Cool SM (2009) The heparan sulfate proteoglycan (HSPG) glypican-3 mediates commitment of MC3T3-E1 cells toward osteogenesis. *J Cell Physiol* 220:780-791.
- Herndon ME, Lander AD (1990) A diverse set of developmentally regulated proteoglycans is expressed in the rat central nervous system. *Neuron* 4:949-961.
- Hiraoka N, Nakagawa H, Ong E, Akama TO, Fukuda MN, Fukuda M (2000) Molecular cloning and expression of two distinct human chondroitin 4-O-sulfotransferases that belong to the HNK-1 sulfotransferase gene family. *The Journal of biological chemistry* 275:20188-20196.
- Hirose J, Kawashima H, Yoshie O, Tashiro K, Miyasaka M (2001) Versican interacts with chemokines and modulates cellular responses. *The Journal of biological chemistry* 276:5228-5234.
- Hopkins AM, DeSimone E, Chwalek K, Kaplan DL (2015) 3D in vitro modeling of the central nervous system. *Prog Neurobiol* 125:1-25.
- Huttner WB, Brand M (1997) Asymmetric division and polarity of neuroepithelial cells. *Current opinion in neurobiology* 7:29-39.
- Ida M, Shuo T, Hirano K, Tokita Y, Nakanishi K, Matsui F, Aono S, Fujita H, Fujiwara Y, Kaji T, Oohira A (2006) Identification and functions of chondroitin sulfate in the milieu of neural stem cells. *The Journal of biological chemistry* 281:5982-5991.
- Ihrle RA, Alvarez-Buylla A (2011) Lake-front property: a unique germinal niche by the lateral ventricles of the adult brain. *Neuron* 70:674-686.
- Iozzo RV, Karamanos N (2010) Proteoglycans in health and disease: emerging concepts and future directions. *FEBS J* 277:3863.

- Iozzo RV, Murdoch AD (1996) Proteoglycans of the extracellular environment: clues from the gene and protein side offer novel perspectives in molecular diversity and function. *FASEB J* 10:598-614.
- Ishii M, Maeda N (2008a) Oversulfated chondroitin sulfate plays critical roles in the neuronal migration in the cerebral cortex. *The Journal of biological chemistry* 283:32610-32620.
- Ishii M, Maeda N (2008b) Spatiotemporal expression of chondroitin sulfate sulfotransferases in the postnatal developing mouse cerebellum. *Glycobiology* 18:602-614.
- Ito Y, Hikino M, Yajima Y, Mikami T, Sirko S, von Holst A, Faissner A, Fukui S, Sugahara K (2005) Structural characterization of the epitopes of the monoclonal antibodies 473HD, CS-56, and MO-225 specific for chondroitin sulfate D-type using the oligosaccharide library. *Glycobiology* 15:593-603.
- Iwata T, Hevner RF (2009) Fibroblast growth factor signaling in development of the cerebral cortex. *Dev Growth Differ* 51:299-323.
- Johansson PA, Cappello S, Gotz M (2010) Stem cells niches during development--lessons from the cerebral cortex. *Current opinion in neurobiology* 20:400-407.
- Johansson PA, Irmeler M, Acampora D, Beckers J, Simeone A, Gotz M (2013) The transcription factor Otx2 regulates choroid plexus development and function. *Development* 140:1055-1066.
- Jossin Y, Cooper JA (2011) Reelin, Rap1 and N-cadherin orient the migration of multipolar neurons in the developing neocortex. *Nature neuroscience* 14:697-703.
- Kang W, Wong LC, Shi SH, Hebert JM (2009) The transition from radial glial to intermediate progenitor cell is inhibited by FGF signaling during corticogenesis. *J Neurosci* 29:14571-14580.
- Kerever A, Schnack J, Vellinga D, Ichikawa N, Moon C, Arikawa-Hirasawa E, Efrid JT, Mercier F (2007) Novel extracellular matrix structures in the neural stem cell niche capture the neurogenic factor fibroblast growth factor 2 from the extracellular milieu. *Stem Cells* 25:2146-2157.
- Kitagawa H, Fujita M, Ito N, Sugahara K (2000) Molecular cloning and expression of a novel chondroitin 6-O-sulfotransferase. *The Journal of biological chemistry* 275:21075-21080.
- Kitagawa H, Uyama T, Sugahara K (2001) Molecular cloning and expression of a human chondroitin synthase. *The Journal of biological chemistry* 276:38721-38726.
- Kobayashi M, Sugumaran G, Liu J, Shworak NW, Silbert JE, Rosenberg RD (1999) Molecular cloning and characterization of a human uronyl 2-sulfotransferase that sulfates iduronyl and glucuronyl residues in dermatan/chondroitin sulfate. *The Journal of biological chemistry* 274:10474-10480.
- Kreshuk A, Straehle CN, Sommer C, Koethe U, Cantoni M, Knott G, Hamprecht FA (2011) Automated detection and segmentation of synaptic contacts in nearly isotropic serial electron microscopy images. *PloS one* 6:e24899.
- Kriegstein A, Alvarez-Buylla A (2009) The glial nature of embryonic and adult neural stem cells. *Annual review of neuroscience* 32:149-184.
- Kusche-Gullberg M (2003) Sulfotransferases in glycosaminoglycan biosynthesis. *Current Opinion in Structural Biology* 13:605-611.
- Kwok JC, Dick G, Wang D, Fawcett JW (2011) Extracellular matrix and perineuronal nets in CNS repair. *Developmental neurobiology* 71:1073-1089.
- Kwok JC, Warren P, Fawcett JW (2012) Chondroitin sulfate: a key molecule in the brain matrix. *Int J Biochem Cell Biol* 44:582-586.
- LaMonica BE, Lui JH, Hansen DV, Kriegstein AR (2013) Mitotic spindle orientation predicts outer radial glial cell generation in human neocortex. *Nature communications* 4:1665.
- LaPierre DP, Lee DY, Li SZ, Xie YZ, Zhong L, Sheng W, Deng Z, Yang BB (2007) The ability of versican to simultaneously cause apoptotic resistance and sensitivity. *Cancer Res* 67:4742-4750.
- Lau LW, Cua R, Keough MB, Haylock-Jacobs S, Yong VW (2013) Pathophysiology of the brain extracellular matrix: a new target for remyelination. *Nature reviews Neuroscience* 14:722-729.
- Lau LW, Keough MB, Haylock-Jacobs S, Cua R, Doring A, Sloka S, Stirling DP, Rivest S, Yong VW (2012) Chondroitin sulfate proteoglycans in demyelinated lesions impair remyelination. *Ann Neurol* 72:419-432.
- Lehtinen MK, Zappaterra MW, Chen X, Yang YJ, Hill AD, Lun M, Maynard T, Gonzalez D, Kim S, Ye P, D'Ercole AJ, Wong ET, LaMantia AS, Walsh CA (2011) The cerebrospinal fluid provides a proliferative niche for neural progenitor cells. *Neuron* 69:893-905.
- Levy AD, Omar MH, Koleske AJ (2014) Extracellular matrix control of dendritic spine and synapse structure and plasticity in adulthood. *Front Neuroanat* 8:116.
- Lindahl U (2014) A personal voyage through the proteoglycan field. *Matrix Biol* 35:3-7.
- Liu J, Chau CH, Liu H, Jang BR, Li X, Chan YS, Shum DK (2006) Upregulation of chondroitin 6-sulphotransferase-1 facilitates Schwann cell migration during axonal growth. *J Cell Sci* 119:933-942.
- Loulier K, Lathia JD, Marthiens V, Relucio J, Mughal MR, Tang SC, Coksaygan T, Hall PE, Chigurupati S, Patton B, Colognato H, Rao MS, Mattson MP, Haydar TF, Ffrench-Constant C (2009) beta1 integrin maintains integrity of the embryonic neocortical stem cell niche. *PLoS Biol* 7:e1000176.

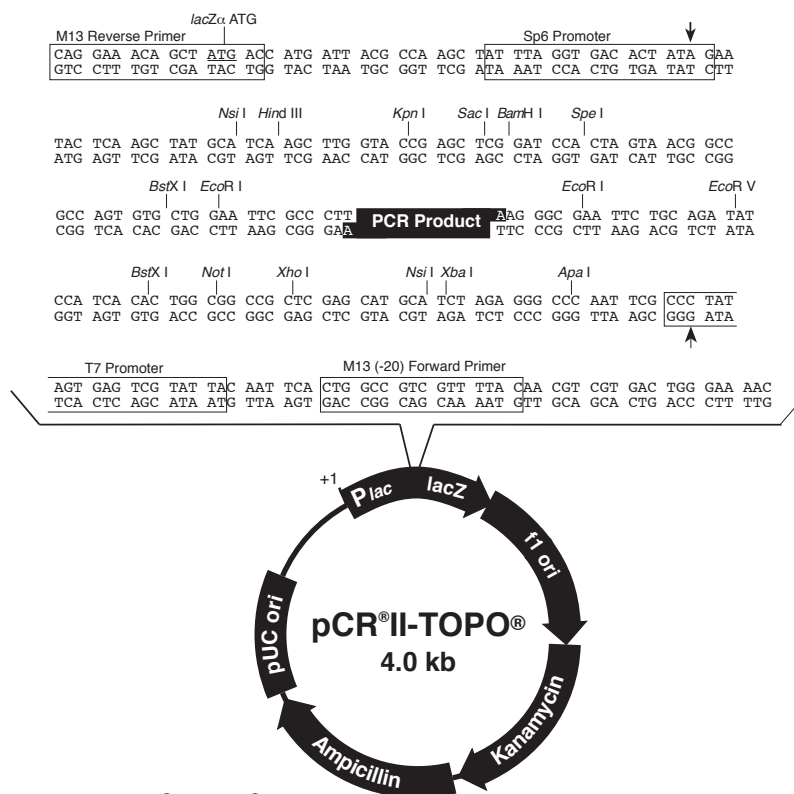
- Maeda N (2010) Structural Variation of Chondroitin Sulfate and its role in the Central nervous system. *Central Nervous System Agents in Medicinal Chemistry* 10:22-31.
- Maeda N (2015) Proteoglycans and neuronal migration in the cerebral cortex during development and disease. *Front Neurosci* 9:98.
- Maeda N, Hamanaka H, Shintani T, Nishiwaki T, Noda M (1994) Multiple receptor-like protein tyrosine phosphatases in the form of chondroitin sulfate proteoglycan. *FEBS Lett* 354:67-70.
- Maeda N, He J, Yajima Y, Mikami T, Sugahara K, Yabe T (2003) Heterogeneity of the chondroitin sulfate portion of phosphacan/6B4 proteoglycan regulates its binding affinity for pleiotrophin/heparin binding growth-associated molecule. *The Journal of biological chemistry* 278:35805-35811.
- Maeda N, Ishii M, Nishimura K, Kamimura K (2011) Functions of chondroitin sulfate and heparan sulfate in the developing brain. *Neurochemical research* 36:1228-1240.
- Manon-Jensen T, Itoh Y, Couchman JR (2010) Proteoglycans in health and disease: the multiple roles of syndecan shedding. *FEBS J* 277:3876-3889.
- Marin O, Rubenstein JL (2003) Cell migration in the forebrain. *Annual review of neuroscience* 26:441-483.
- Martynoga B, Drechsel D, Guillemot F (2012) Molecular control of neurogenesis: a view from the mammalian cerebral cortex. *Cold Spring Harb Perspect Biol* 4.
- Maurel P, Rauch U, Flad M, Margolis RK, Margolis RU (1994) Phosphacan, a chondroitin sulfate proteoglycan of brain that interacts with neurons and neural cell-adhesion molecules, is an extracellular variant of a receptor-type protein tyrosine phosphatase. *Proceedings of the National Academy of Sciences of the United States of America* 91:2512-2516.
- Mercier F, Kitasako JT, Hatton GI (2002) Anatomy of the brain neurogenic zones revisited: fractones and the fibroblast/macrophage network. *The Journal of comparative neurology* 451:170-188.
- Mikami T, Kitagawa H (2013) Biosynthesis and function of chondroitin sulfate. *Biochim Biophys Acta* 1830:4719-4733.
- Miyata S, Komatsu Y, Yoshimura Y, Taya C, Kitagawa H (2012) Persistent cortical plasticity by upregulation of chondroitin 6-sulfation. *Nature neuroscience* 15:414-422, S411-412.
- Mizumoto S, Fongmoon D, Sugahara K (2013) Interaction of chondroitin sulfate and dermatan sulfate from various biological sources with heparin-binding growth factors and cytokines. *Glycoconj J* 30:619-632.
- Morgenstern DA, Asher RA, Fawcett JW (2002) Chondroitin sulphate proteoglycans in the CNS injury response. *Prog Brain Res* 137:313-332.
- Muramatsu T (2014) Structure and function of midkine as the basis of its pharmacological effects. *Br J Pharmacol* 171:814-826.
- Nikolovska K, Spillmann D, Seidler DG (2015) Uronyl 2-O sulfotransferase potentiates Fgf2-induced cell migration. *J Cell Sci* 128:460-471.
- Ninkovic J, Gotz M (2014) A time and place for understanding neural stem cell specification. *Dev Cell* 30:114-115.
- Noctor SC, Martinez-Cerdeno V, Ivic L, Kriegstein AR (2004) Cortical neurons arise in symmetric and asymmetric division zones and migrate through specific phases. *Nature neuroscience* 7:136-144.
- Nurcombe V, Ford MD, Wildschut JA, Bartlett PF (1993) Developmental regulation of neural response to FGF-1 and FGF-2 by heparan sulfate proteoglycan. *Science* 260:103-106.
- Ogawa T, Hagihara K, Suzuki M, Yamaguchi Y (2001) Brevican in the developing hippocampal fimbria: differential expression in myelinating oligodendrocytes and adult astrocytes suggests a dual role for brevican in central nervous system fiber tract development. *The Journal of comparative neurology* 432:285-295.
- Ohtake S, Ito Y, Fukuta M, Habuchi O (2001) Human N-acetylgalactosamine 4-sulfate 6-O-sulfotransferase cDNA is related to human B cell recombination activating gene-associated gene. *The Journal of biological chemistry* 276:43894-43900.
- Osumi N, Shinohara H, Numayama-Tsuruta K, Maekawa M (2008) Concise review: Pax6 transcription factor contributes to both embryonic and adult neurogenesis as a multifunctional regulator. *Stem Cells* 26:1663-1672.
- Pantazaka E, Papadimitriou E (2014) Chondroitin sulfate-cell membrane effectors as regulators of growth factor-mediated vascular and cancer cell migration. *Biochim Biophys Acta* 1840:2643-2650.
- Paridaen JT, Huttner WB (2014) Neurogenesis during development of the vertebrate central nervous system. *EMBO reports* 15:351-364.
- Peles E, Schlessinger J, Grumet M (1998) Multi-ligand interactions with receptor-like protein tyrosine phosphatase beta: implications for intercellular signaling. *Trends Biochem Sci* 23:121-124.
- Pellegrini L BD, von Delft F, Mulloy B, Blundell TL (2000) Crystal structure of fibroblast growth factor receptor ectodomain bound to ligand and heparin. *Nature*.
- Perissinotto D, Iacopetti P, Bellina I, Doliana R, Colombatti A, Pettway Z, Bronner-Fraser M, Shinomura T, Kimata K, Morgelin M, Lofberg J, Perris R (2000) Avian neural crest cell migration is diversely regulated by the two major hyaluronan-binding proteoglycans PG-M/versican and aggrecan. *Development* 127:2823-2842.

- Pilz GA, Shitamukai A, Reillo I, Pacary E, Schwausch J, Stahl R, Ninkovic J, Snippert HJ, Clevers H, Godinho L, Guillemot F, Borrell V, Matsuzaki F, Gotz M (2013) Amplification of progenitors in the mammalian telencephalon includes a new radial glial cell type. *Nature communications* 4:2125.
- Properzi F, Carulli D, Asher RA, Muir E, Camargo LM, van Kuppevelt TH, ten Dam GB, Furukawa Y, Mikami T, Sugahara K, Toida T, Geller HM, Fawcett JW (2005) Chondroitin 6-sulphate synthesis is up-regulated in injured CNS, induced by injury-related cytokines and enhanced in axon-growth inhibitory glia. *The European journal of neuroscience* 21:378-390.
- Pyka M, Wetzel C, Aguado A, Geissler M, Hatt H, Faissner A (2011) Chondroitin sulfate proteoglycans regulate astrocyte-dependent synaptogenesis and modulate synaptic activity in primary embryonic hippocampal neurons. *The European journal of neuroscience* 33:2187-2202.
- Raballo R, Rhee J, Lyn-Cook R, Leckman JF, Schwartz ML, Vaccarino FM (2000) Basic fibroblast growth factor (Fgf2) is necessary for cell proliferation and neurogenesis in the developing cerebral cortex. *J Neurosci* 20:5012-5023.
- Rakic P (1972) Mode of cell migration to the superficial layers of fetal monkey neocortex. *The Journal of comparative neurology* 145:61-83.
- Rakic P (1995) A small step for the cell, a giant leap for mankind: a hypothesis of neocortical expansion during evolution. *Trends in neurosciences* 18:383-388.
- Rauch U, Zhou XH, Roos G (2005) Extracellular matrix alterations in brains lacking four of its components. *Biochemical and biophysical research communications* 328:608-617.
- Reynolds BA, Tetzlaff W, Weiss S (1992) A multipotent EGF-responsive striatal embryonic progenitor cell produces neurons and astrocytes. *J Neurosci* 12:4565-4574.
- Reynolds BA, Weiss S (1992) Generation of neurons and astrocytes from isolated cells of the adult mammalian central nervous system. *Science* 255:1707-1710.
- Rogers CJ, Clark PM, Tully SE, Abrol R, Garcia KC, Goddard WA, Hsieh-Wilson LC (2011) Elucidating glycosaminoglycan-protein-protein interactions using carbohydrate microarray and computational approaches. *Proceedings of the National Academy of Sciences of the United States of America* 108:9747-9752.
- Rowitch DH, Kriegstein AR (2010) Developmental genetics of vertebrate glial-cell specification. *Nature* 468:214-222.
- Rozario T, DeSimone DW (2010) The extracellular matrix in development and morphogenesis: a dynamic view. *Dev Biol* 341:126-140.
- Sahara S, O'Leary DD (2009) Fgf10 regulates transition period of cortical stem cell differentiation to radial glia controlling generation of neurons and basal progenitors. *Neuron* 63:48-62.
- Scadden DT (2006) The stem-cell niche as an entity of action. *Nature* 441:1075-1079.
- Schlessinger J, Plotnikov AN, Ibrahimi OA, Eliseenkova AV, Yeh BK, Yayon A, Linhardt RJ, Mohammadi M (2000) Crystal structure of a ternary FGF-FGFR-heparin complex reveals a dual role for heparin in FGFR binding and dimerization. *Mol Cell* 6:743-750.
- Schnepp A, Komp Lindgren P, Hulsmann H, Kroger S, Paulsson M, Hartmann U (2005) Mouse testican-2. Expression, glycosylation, and effects on neurite outgrowth. *The Journal of biological chemistry* 280:11274-11280.
- Shipp EL, Hsieh-Wilson LC (2007) Profiling the sulfation specificities of glycosaminoglycan interactions with growth factors and chemotactic proteins using microarrays. *Chem Biol* 14:195-208.
- Siegenthaler JA, Ashique AM, Zarbalis K, Patterson KP, Hecht JH, Kane MA, Folias AE, Choe Y, May SR, Kume T, Napoli JL, Peterson AS, Pleasure SJ (2009) Retinoic acid from the meninges regulates cortical neuron generation. *Cell* 139:597-609.
- Silbert JE, Sugumaran G (2002) Biosynthesis of chondroitin/dermatan sulfate. *IUBMB Life* 54:177-186.
- Silver DJ, Silver J (2014) Contributions of chondroitin sulfate proteoglycans to neurodevelopment, injury, and cancer. *Current opinion in neurobiology* 27:171-178.
- Silver J, Miller JH (2004) Regeneration beyond the glial scar. *Nature reviews Neuroscience* 5:146-156.
- Sirko S, von Holst A, Weber A, Wizenmann A, Theodoridis U, Gotz M, Faissner A (2010) Chondroitin sulfates are required for fibroblast growth factor-2-dependent proliferation and maintenance in neural stem cells and for epidermal growth factor-dependent migration of their progeny. *Stem Cells* 28:775-787.
- Sirko S, von Holst A, Wizenmann A, Gotz M, Faissner A (2007) Chondroitin sulfate glycosaminoglycans control proliferation, radial glia cell differentiation and neurogenesis in neural stem/progenitor cells. *Development* 134:2727-2738.
- Soleman S, Filippov MA, Dityatev A, Fawcett JW (2013) Targeting the neural extracellular matrix in neurological disorders. *Neuroscience* 253:194-213.
- Sommer I, Schachner M (1981) Monoclonal antibodies (O1 to O4) to oligodendrocyte cell surfaces: an immunocytological study in the central nervous system. *Dev Biol* 83:311-327.

- Sugahara K (2003) Recent advances in the structural biology of chondroitin sulfate and dermatan sulfate. *Curr Opin Struct Biol* 13:612-620.
- Sugahara K, Mikami T (2007) Chondroitin/dermatan sulfate in the central nervous system. *Curr Opin Struct Biol* 17:536-545.
- Sulkava S, Ollila HM, Ahola K, Partonen T, Viitasalo K, Kettunen J, Lappalainen M, Kivimaki M, Vahtera J, Lindstrom J, Harma M, Puttonen S, Salomaa V, Paunio T (2013) Genome-wide scan of job-related exhaustion with three replication studies implicate a susceptibility variant at the UST gene locus. *Hum Mol Genet* 22:3363-3372.
- Takahashi N, Sakurai T, Bozdagi-Gunal O, Dorr NP, Moy J, Krug L, Gama-Sosa M, Elder GA, Koch RJ, Walker RH, Hof PR, Davis KL, Buxbaum JD (2011) Increased expression of receptor phosphotyrosine phosphatase-beta/zeta is associated with molecular, cellular, behavioral and cognitive schizophrenia phenotypes. *Transl Psychiatry* 1:e8.
- Takahashi T, Nowakowski RS, Caviness VS, Jr. (1995) The cell cycle of the pseudostratified ventricular epithelium of the embryonic murine cerebral wall. *J Neurosci* 15:6046-6057.
- Taverna E, Gotz M, Huttner WB (2014) The cell biology of neurogenesis: toward an understanding of the development and evolution of the neocortex. *Annu Rev Cell Dev Biol* 30:465-502.
- Taverna E, Huttner WB (2010) Neural progenitor nuclei IN motion. *Neuron* 67:906-914.
- Theiler K (1989) *The House Mouse - Atlas of Embryonic Development*.
- Theocharidis U, Long K, French-Constant C, Faissner A (2014) Regulation of the neural stem cell compartment by extracellular matrix constituents. *Prog Brain Res* 214:3-28.
- Uchimura K, Kadomatsu K, Fan QW, Muramatsu H, Kurosawa N, Kaname T, Yamamura K, Fukuta M, Habuchi O, Muramatsu T (1998) Mouse chondroitin 6-sulfotransferase: molecular cloning, characterization and chromosomal mapping. *Glycobiology* 8:489-496.
- Uyama T, Ishida M, Izumikawa T, Trybala E, Tufaro F, Bergstrom T, Sugahara K, Kitagawa H (2006) Chondroitin 4-O-sulfotransferase-1 regulates E disaccharide expression of chondroitin sulfate required for herpes simplex virus infectivity. *The Journal of biological chemistry* 281:38668-38674.
- Vigetti D, Viola M, Karousou E, De Luca G, Passi A (2014) Metabolic control of hyaluronan synthases. *Matrix Biol* 35:8-13.
- von Holst A, Sirko S, Faissner A (2006) The unique 473HD-Chondroitinsulfate epitope is expressed by radial glia and involved in neural precursor cell proliferation. *J Neurosci* 26:4082-4094.
- Wade A, McKinney A, Phillips JJ (2014) Matrix regulators in neural stem cell functions. *Biochim Biophys Acta* 1840:2520-2525.
- Wade A, Robinson AE, Engler JR, Petritsch C, James CD, Phillips JJ (2013) Proteoglycans and their roles in brain cancer. *FEBS J* 280:2399-2417.
- Wang Q, Yang L, Alexander C, Temple S (2012) The niche factor syndecan-1 regulates the maintenance and proliferation of neural progenitor cells during mammalian cortical development. *PloS one* 7:e42883.
- Wight TN, Kinsella MG, Evanko SP, Potter-Perigo S, Merrilees MJ (2014) Versican and the regulation of cell phenotype in disease. *Biochim Biophys Acta* 1840:2441-2451.
- Woodhead GJ, Mutch CA, Olson EC, Chenn A (2006) Cell-autonomous beta-catenin signaling regulates cortical precursor proliferation. *J Neurosci* 26:12620-12630.
- Woodworth MB, Custo Greig L, Kriegstein AR, Macklis JD (2012) SnapShot: cortical development. *Cell* 151:918-918 e911.
- Wu YJ, La Pierre DP, Wu J, Yee AJ, Yang BB (2005) The interaction of versican with its binding partners. *Cell research* 15:483-494.
- Yamauchi S, Kurosu A, Hitosugi M, Nagai T, Oohira A, Tokudome S (2011) Differential gene expression of multiple chondroitin sulfate modification enzymes among neural stem cells, neurons and astrocytes. *Neuroscience letters* 493:107-111.
- Yamauchi S, Mita S, Matsubara T, Fukuta M, Habuchi H, Kimata K, Habuchi O (2000) Molecular cloning and expression of chondroitin 4-sulfotransferase. *The Journal of biological chemistry* 275:8975-8981.
- Yoon K, Nery S, Rutlin ML, Radtke F, Fishell G, Gaiano N (2004) Fibroblast growth factor receptor signaling promotes radial glial identity and interacts with Notch1 signaling in telencephalic progenitors. *J Neurosci* 24:9497-9506.
- Yu W, Wang Y, McDonnell K, Stephen D, Bai CB (2009) Patterning of ventral telencephalon requires positive function of Gli transcription factors. *Dev Biol* 334:264-275.
- Zappaterra MW, Lehtinen MK (2012) The cerebrospinal fluid: regulator of neurogenesis, behavior, and beyond. *Cell Mol Life Sci* 69:2863-2878.
- Zimmermann DR, Dours-Zimmermann MT (2008) Extracellular matrix of the central nervous system: from neglect to challenge. *Histochem Cell Biol* 130:635-653.

6 APPENDIX

Plasmid maps



Comments for pCR[®]II-TOPO[®]
3973 nucleotides

LacZ gene: bases 1-589
 M13 Reverse priming site: bases 205-221
 Sp6 promoter: bases 239-256
 Multiple Cloning Site: bases 269-383
 T7 promoter: bases 406-425
 M13 (-20) Forward priming site: bases 433-448
 f1 origin: bases 590-1027
 Kanamycin resistance ORF: bases 1361-2155
 Ampicillin resistance ORF: bases 2173-3033
 pUC origin: bases 3178-3851

